Chesapeake Bay Land Subsidence and Sea Level Change

An Evaluation of Past and Present Trends and Future Outlook

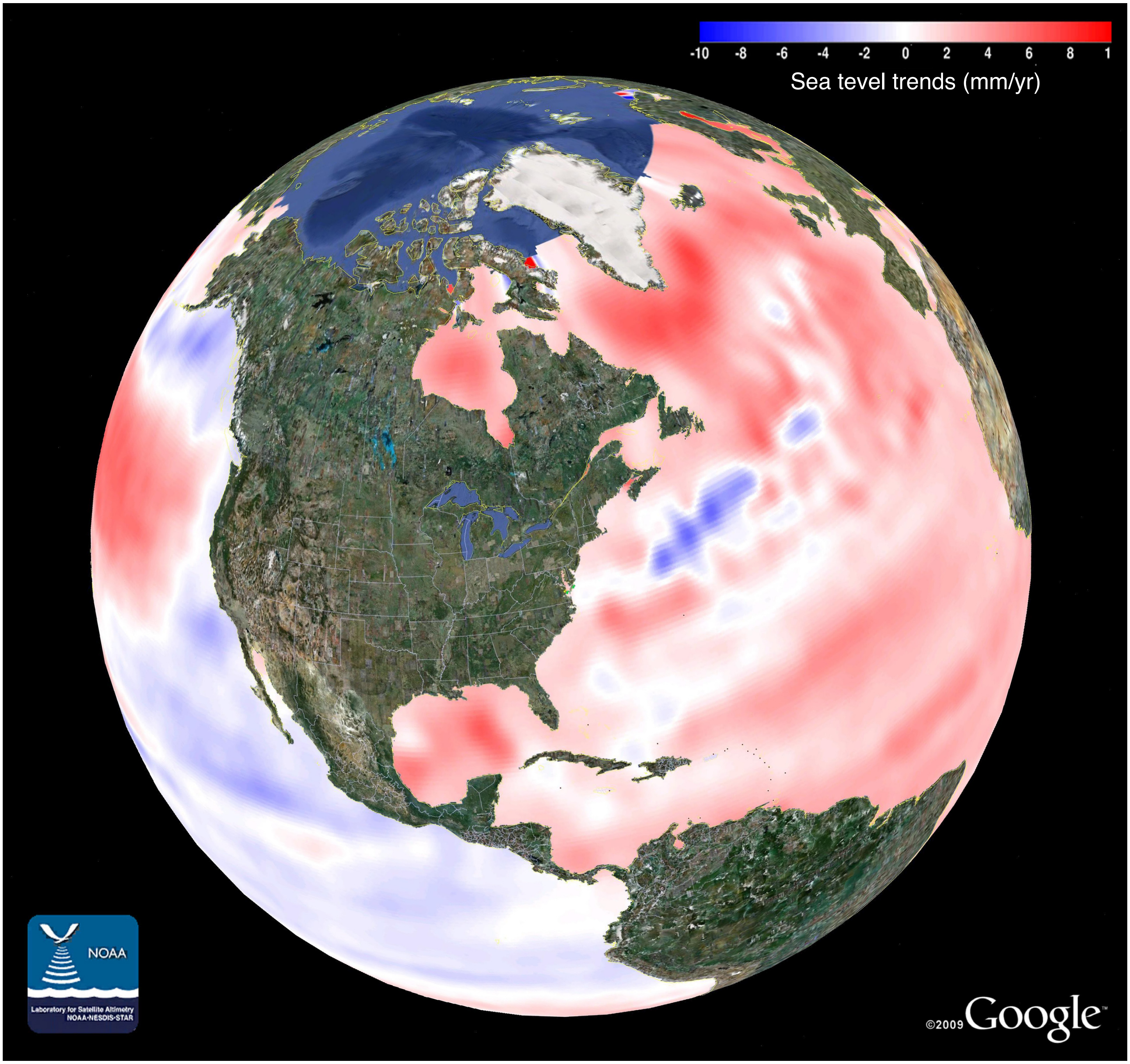

John D. Boon
John M. Brubaker
David R. Forrest

A report to the
U.S. Army Corps of Engineers
Norfolk District

William & Mary
VIMS
Virginia Institute of Marine Science
School of Marine Science

Virginia Institute of Marine Science
Special Report No. 425 in Applied Marine
Science and Ocean Engineering
November 2010

Cover graphic shows a map of local sea level rise in mm/year from TOPEX, Jason-1, and Jason-2 data provided by the NOAA Laboratory for Satellite Altimetry, downloaded as a Google Earth kml file from http://ibis.grdl.noaa.gov/SAT/slr/LSA_SLR_maps.php.

Cover design by Margaret Pizer, Virginia Sea Grant Communicator

CHESAPEAKE BAY LAND SUBSIDENCE AND SEA LEVEL CHANGE:

AN EVALUATION OF PAST AND PRESENT TRENDS AND FUTURE OUTLOOK

John D. Boon
John M. Brubaker
David R. Forrest

A Report to the

U.S. Army Corps of Engineers
Norfolk District
803 Front Street
Norfolk, VA 23510-1096

Special Report No. 425 in
Applied Marine Science and Ocean Engineering

Virginia Institute of Marine Science
Gloucester Point, Virginia 23062

John T. Wells
Director

November 2010

TABLE OF CONTENTS

LIST OF FIGURES

LIST OF TABLES

LIST OF ACRONYMS

ASL	Absolute Sea Level
ASLR	Absolute Sea Level Rise
CO-OPS	Center for Operational Oceanographic Products and Services
CORS	Continuously Operating Reference Station
DSE	Decadal Signal Extraction
GIA	Glacial Isostatic Adjustment
LIDAR	Light Detection and Ranging
MSL	Mean Sea Level
mmsl	monthly mean sea level
NGS	National Geodetic Survey
NOAA	National Oceanic and Atmospheric Administration
NOS	National Ocean Service
NRC	National Research Council
NWLON	National Water Level Observation Network
RSL	Relative Sea Level
RSLR	Relative Sea Level Rise
USACE	U.S. Army Corps of Engineers

EXECUTIVE SUMMARY

Ten Chesapeake Bay water level stations presently have a combined total of 647 years of water level measurements with record lengths varying between 35 years (1975-2009) at the Chesapeake Bay Bridge Tunnel, VA, and 107 years (1903-2009) at Baltimore, MD. All ten stations, with the exception of Gloucester Point, VA, are active stations in the National Water Level Observation Network of water level stations maintained by the U.S. National Oceanic and Atmospheric Administration, Center for Operational Oceanographic Products and Services.

New technologies such as sea surface range measurements from earth-orbiting satellites now provide a global assessment of absolute sea level (ASL) trends relative to the center of a reference ellipsoid rather than fixed points on the earth's surface to which relative sea level (RSL) measurements refer. New methodologies have also been applied to derive spatial averages of ASL trends over large regions with greater accuracy. *Notwithstanding these advances, there is still no substitute for an accurate time series of water level measurements obtained locally, preferably one spanning several decades, when assessing RSL trends that will affect a specific community or township in the coming decades.* RSL trends will determine local inundation risk whether due to vertical land movement (emergence or subsidence) or the ASL trend found as the sum of RSL trend and land movement when both are measured positive upward. In Chesapeake Bay, RSL trends are consistently positive (rising) while land movement is negative (subsiding).

By choosing a common time span for the ten bay stations evaluated in this report, we are able to compare differences in RSL rise rates with approximately the same degree of confidence at each station. Uncertainty has been reduced by extracting the decadal signal present at all ten stations before using linear regression to obtain new RSL rise rates with smaller than usual confidence intervals, permitting both temporal and spatial comparisons to be made.

Temporal comparisons at five bay stations over two periods, 1944-1975 and 1976-2007, suggest that, while RSL continues to rise at some of the highest rates found along the U.S. Atlantic coast, there is presently no evidence of a statistically significant increase marking an acceleration in RSL rise at any of the five bay stations. Small but steady increases in RSL rise rate with time are still a possibility as RSL trend confidence intervals remain too large for statistical inference.

Spatial comparisons at ten stations for the 1976-2007 period provide new evidence on spatial variability of RSL rise rates within Chesapeake Bay. Global positioning system (GPS) data from ground stations further define the pattern of spatial variability and permit new estimates of ASL rise rates in the region, all of which are significantly less than the global ASL rise rate of 3.1 mm/yr over 1993 to 2003 reported in the IPCC Fourth Assessment Report. Present evidence suggests an ASL rise rate of about 1.8 mm/yr in Chesapeake Bay over the 1976-2007 period. Applying this rate uniformly throughout the bay, subsidence rates ranging from about -1.3 mm/yr to -4.0 mm/yr are found, leading to the general conclusion that about 53% of the RSL rise measured at bay water level stations is, on average, due to local subsidence.

<u>Outlook</u>: Land subsidence in Chesapeake Bay is likely to continue at or near present rates. Future ASL rise in the bay region remains uncertain owing to diverse and possibly changing trends world-wide (see report cover). Their combination strongly suggests a need for future monitoring.

NOTICE

The findings and/or recommendations contained herein do not constitute Corps of Engineers approval of any project(s) or eliminate the need to follow normal regulatory permitting processes.

I. INTRODUCTION

The Chesapeake Bay is the largest estuary in the United States. From its open boundary with the Atlantic Ocean in Virginia to its northern limits in Maryland, the bay is approximately 200 miles (320 km) long and, including its tributaries, has a reported 11,684 miles (18,808 km) of shoreline length. Most of this boundary between land and water is low-lying and much of it is subject to inundation during tropical and extratropical storms. These natural hazards represent an especially challenging problem for communities large and small in the coastal regions of Virginia and Maryland.

As population densities continue to increase in the coastal regions, the flood hazard unfortunately is increasing as well due to locally high rates of land subsidence in the mid-Atlantic region of the U.S. east coast combined with global sea level rise. The combination – global sea level rise and coastal subsidence – is doubly significant even in locations where the occurrence of major hurricanes is relatively rare compared to other regions of the country. In the Chesapeake Bay region in particular, extratropical cyclones or “nor’easters” that have not caused significant flooding in the past will begin to do so - and with greater frequency - as sea level continues to rise *relative* to the land. This threat calls for smarter coastal planning and development looking toward the future but also underscores the present need for emergency planning and effective response measures when coastal inundation is imminent. Flood hazard mitigation at a minimum requires an understanding of the land and bay-ocean processes that contribute to it in complex and often unpredictable ways.

II. SEA LEVEL DYNAMICS

The following sections contain an introduction to water level processes that affect flood risk in the Chesapeake Bay and what is presently known about them. Much of the information has been provided by the National Oceanic and Atmospheric Administration (NOAA), an organization within the U.S. Department of Commerce.

Global Sea Level Rise - Global or absolute sea level (ASL) at the present time is rising in most locations due to the overall increase in volume and water mass of the world's oceans and seas. An increase in volume is happening now because of warming and thermal expansion of the ocean water column. An increase in water mass and volume is occurring as ice on land continues to melt and discharge into the ocean. Eustatic sea level rise is another term that has been used to describe this change but in the context of a uniform, average rise worldwide.

ASL in the geologic past has both fallen and risen as the Earth experienced glacial and interglacial periods, respectively. During a glacial period, part of the ocean's water mass is transferred to ice sheets and continental glaciers on land via the atmosphere and the reverse occurs through melting and stream flow into the ocean during interglacial periods. The present interglacial period that began approximately 12,000 years ago is still continuing (Kearney, 2001). Several kinds of evidence now show that the term 'rise' is justified when speaking of the sea level change expected for the Earth as a whole in the 21st century and perhaps beyond.

One type of evidence of rise comes in the form of long-term water level records at tide stations. These records depict water level change measured locally relative to the land, going back nearly 100 years or more at a few stations in North America and longer at some stations in Europe (Woodworth, 1990). Relative sea level (RSL) measured at tide stations must be corrected for local vertical land movement in order to provide useful information on ASL change.

More recent evidence of global sea level rise comes from space-based measurements. Earth-orbiting satellites have measured their altitude and range to the ocean's surface from known positions in space since 1993; *satellite altimetry* now provides world-wide estimates of sea level relative to a reference ellipsoid surrounding the Earth. This is an obvious advantage over tide stations which can provide only local estimates. One key finding from satellite altimetry is that the rate of global sea level change is not uniform (or even positive everywhere) but varies from one region of the world's oceans to another as shown in Fig. 1 from NOAA's Laboratory for Satellite Altimetry (http://ibis.grdl.noaa.gov/SAT/slr/).

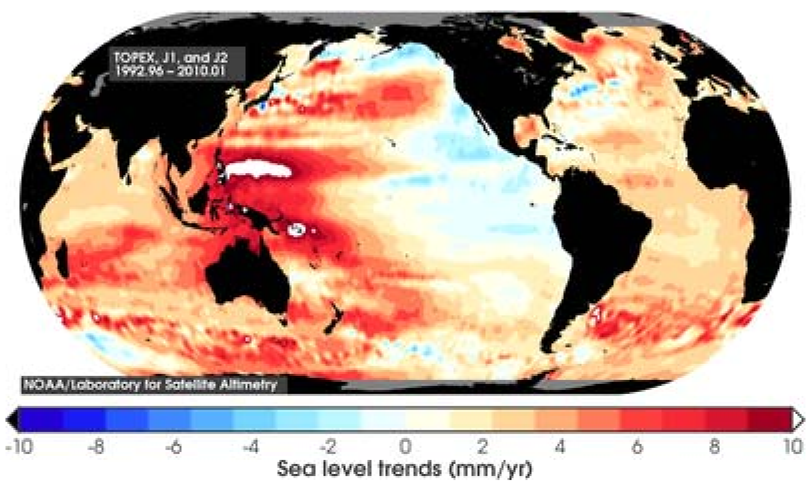

Figure 1. Global mean sea level determined from satellite altimetry. Data in this figure are provided by the NOAA Laboratory for Satellite Altimetry.

The term *sea level trend* is used in Fig.1, and by NOAA generally, because sea levels in some areas of the globe have fallen slightly during the period of satellite observations (1993-2010). Other areas have sea levels rising much faster than the global average trend of 3.0 ± 0.4 mm/yr for this period. A number of explanations exist for the diversity observed in ASL trends including global variations in heat and momentum exchange between the atmosphere and the ocean and the continuing addition of meltwater and crustal adjustment in certain regions (e.g., Greenland and Antarctica), changes not evenly distributed to produce a globally uniform rate of sea level rise (Conrad and Hager, 1997; Mitrovica et al., 2001; Douglas, 2008). Recent satellite measurements of the Earth's gravity field (http://www.csr.utexas.edu/grace/) provide further information on the time-varying change in the global distribution of ocean water mass.

Relative Sea Level, Subsidence and Emergence - Relative sea level (RSL) refers to sea level relative to the land as measured by a tide gauge. In land areas undergoing *subsidence* or sinking relative to the center of the earth, RSL is rising faster than ASL; where uplift or *emergence* of the land is taking place, RSL is reduced compared to ASL. Speaking globally, RSL change over time is best referred to as the RSL *trend* rather than RSL rise since there are a number of areas where the linear trend is near zero or negative. The RSL trend at Skagway, AK, for example, is approximately -17.12 mm/yr (Zervas, 2009). There are several reasons for this. In addition to the slightly negative global trend in the Gulf of Alaska (light blue area, top of Fig. 1), Skagway is located in a tectonically active region of convergence between the North American Plate and the Pacific Plate, as well as in a region undergoing postglacial uplift.

Removal of the massive overburden of continental ice sheets results not only in a gradual rise of the land underneath that will continue for thousands of years but the gravitational influence of the shrinking ice mass will relax its hold on ocean waters locally, allowing them to move away from the region. To balance these effects, there is an accompanying subsidence and sea level change in other regions farther away as both the Earth's crust and the ocean continue to adjust (Mitrovica et al. 2001; Church et al., 2004; Snay et al., 2007; Fiedler and Conrad, 2010). Almost every coastal region is thus undergoing some degree of glacial isostatic adjustment (GIA) and corrections to RSL trends have been devised that allow estimates of ASL trends to be derived locally (Peltier, 1996; 2001). The question may be asked why this is necessary – why not rely on satellite altimetry entirely rather than tide gauge records? The answer is that satellite altimetry records still have a relatively short duration compared to tide gauge records and satellite ranging itself requires calibration using tide gauge data to achieve its accuracy.

Estimates of globally-averaged ASL trends for the twentieth century, based on tide station records (RSL adjusted for GIA), have been made by numerous authors. Much of this work has been assimilated in the Contribution of Working Group I to the Fourth Assessment Report, Intergovernmental Panel on Climate Change (IPCC Summary for Policymakers, 2007). The following statements are made on p. 5 of the WG I summary:

> "Global average sea level rose at an average rate of 1.8 [1.3 to 2.3] mm per year over 1961 to 2003. The rate was faster over 1993 to 2003, about 3.1 [2.4 to 3.8] mm per year. Whether the faster rate for 1993 to 2003 reflects decadal variability or an increase in the longer-term trend is unclear."

The above statement introduces two matters of central importance in the present study – faster or *accelerated rates* of sea level rise and *decadal variability*. An ASL rise rate of 1.7 to 1.8 mm/yr is considered by most authorities to be the average global rate for the 20th century which need only be compared with the global rate of rise obtained from satellite altimetry, 3.0 mm/yr over 1993-2010, to infer an acceleration. Climate models predict an acceleration on this order and Church and White (2006) claimed to have evidence of an acceleration based on a quadratic fit to their reconstructed global sea level data from 1870 to 2004. However, Woodworth et al. (2009) in reviewing the evidence for accelerated sea level rise in the 20th century, concluded that the largest acceleration signals appear as trend changes or 'inflexions' in water level time series, noting an acceleration in 1920-1930 and a slight deceleration (in some but not all regions) in 1960. Holgate (2007) further describes these as decadal rates of sea level change which he observed at carefully selected stations with high quality data, further challenging the notion of an enduring, exponential-like increase in the long-term trend based on tide gauge records available at present. An example of what that increase might look like can be found in a simulated time series by Woodworth (1990, Fig. 2). The same author used a least squares quadratic fit to show that no significant accelerations, positive or negative, were discernable in European tide gauge records for the period 1870-1986, speculating, however, that evidence of an acceleration should become observable in a long-term record at Newlyn (U.K.) by 2010.

Low-frequency Sea Level Change - Periodicity found in water level records exists for motions witnessed over a wide range of time scales in many areas including Chesapeake Bay. These can be divided according to source, type and period into the following five categories:

1. surface gravity waves (wind-driven), periods measured in seconds
2. astronomic tide (diurnal, semidiurnal cycles), periods measured in hours
3. subtidal variability (recurring weather systems), periods measured in days
4. seasonal variability (annual, semiannual cycles), periods measured in months
5. decadal variability (ocean-atmosphere exchange), periods measured in years

Storm surge is not included in the above list because it occurs as a transient, mostly *aperiodic* change in water level, although it can be argued that it is part of the subtidal variability distinguished only by the level of amplitude shown during a weather event. Note also that the astronomic tide represents only one category of motion, hence the term 'tide level' is not an appropriate descriptor of the raw output from a tide gauge.

Low-frequency (long-period) sea level change exists mainly within categories 4 and 5 listed above and averaging (filtering) is commonly used to separate it from motions occurring at higher frequencies. Tide stations use a mechanical filter (stilling well) to remove surface gravity waves and monthly averaging effectively removes both the astronomic tide and the subtidal variability. At this point the term 'sea level' – as in *monthly mean sea level (mmsl)* - is usually adopted in place of 'water level' to signify the transition to longer period variations.

Seasonal Cycle - Averaging over each calendar month in the year for a series of years (5-19 years typically) produces the *seasonal cycle*, an average oscillation that is represented in NOAA tide predictions by the solar annual (Sa) and solar semiannual (Ssa) tidal constituents which have fixed periods of 12 months and 6 months, respectively. Alternatively, Sa, Ssa amplitude and phase can be determined from least squares harmonic analysis of mmsl time series (Boon, 2007). Although solar tide-producing forces contribute some change at these periods, it is minor compared to meteorological forcing in the form of thermal expansion/contraction of the ocean water column due to seasonal heating and cooling. A recent study by Sweet et al. (2009) suggests that the seasonal cycle in the southern half of the U.S. east coast region, including lower Chesapeake Bay, is also influenced by seasonal variability in the strength of the Florida Current in response to oceanic forcing. This particular variability favors an increase in Ssa amplitude, leading to secondary highs and lows in seasonal water level during an average year (see Fig. 2a).

Decadal Variability - Although the seasonal cycle represented by tidal constituents Sa, Ssa is essential for making tidal predictions, it is removed from mmsl series before determining the RSL trend at a tide station. The reason for this will be explained in Section III but it should be noted here that no one year is truly average when viewing the seasonal cycle. In any given year, it is normal for observed mmsl to deviate, often substantially, from mmsl predicted for the seasonal cycle in one or more calendar months. Figure 2a,b presents two examples using mmsl for the last seven years at Hampton Roads (Sewells Point), VA and Baltimore, MD. The seasonal cycle (blue circles, Fig. 2a,b) was extracted through least squares harmonic analysis of the mmsl series available in complete years; the RSL trend (red line) was obtained by a least squares linear fit to the reduced data. The observed deviations from the seasonal cycle are not a sign of faulty prediction but a reminder that seasonal variability consists of more than just the seasonal cycle. *Interannual variability* appears as near-random change from one year to the next, but in addition there is evidence of quasi-periodic variability at much longer periods – the *decadal variability*.

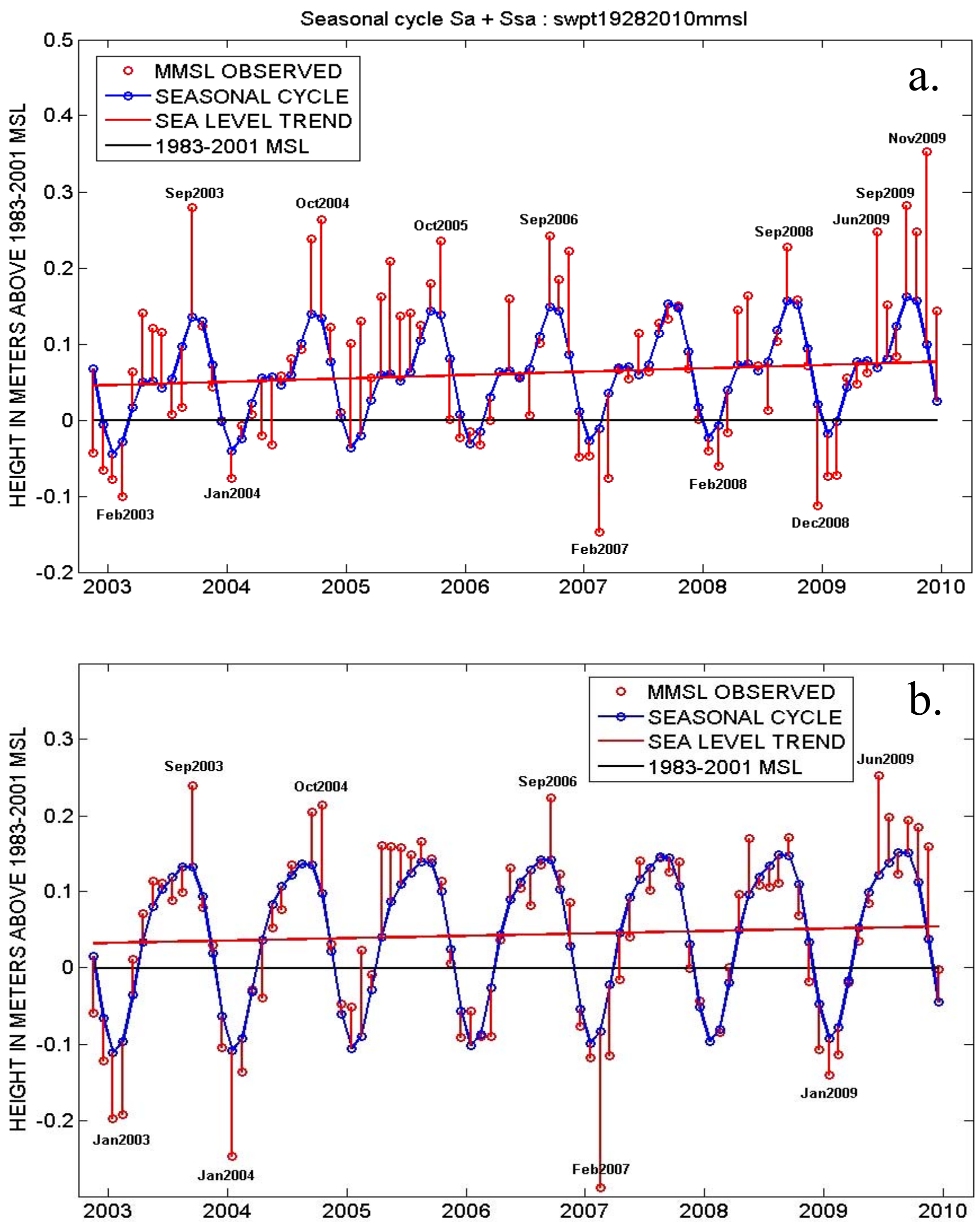

Figure 2. Observed mmsl, seasonal cycle and sea level trend at a) Sewells Point, VA, b) Baltimore, MD. Observations from the NOAA Center for Operational Oceanographic Products and Services (CO-OPS) http://www.tidesandcurrents.noaa.gov/. For locations see Fig.3. MSL 1983-2001 refers to mean sea level for the U.S. National Tidal Datum Epoch which currently includes the years 1983 through 2001.

III. CHESAPEAKE BAY SEA LEVEL TRENDS

At the end of 2009, NOAA's National Water Level Observation Network (NWLON) had near-continuous records going back to the beginning of 1975 at a total of ten active water level stations in Chesapeake Bay and its tributaries, including Washington DC on the Potomac River (Fig. 3). The ten mmsl time series available over a common time span, each 35 years in length, represents a unique data set for comparing sea level trends, both RSL and ASL, in the bay. RSL trends are obtainable using linear regression and linear filtering techniques; ASL estimates are derived through other methods described in Section IV.

Relative Sea Level (RSL) Trends - The longest water level record in Chesapeake Bay comes from the NWLON station at Baltimore, MD (BALT) at the location shown in Fig. 3. A plot of the raw mmsl time series for years 1903 through 2009 at this station is shown in Fig. 4. Although a rising trend is visually apparent in this plot, including a hint of an acceleration in rise after 1930, a high level of variance in the mmsl series is apparent as well. Some of the variance in Fig. 4 can be eliminated by removing the seasonal cycle obtained with the same least squares procedure used to extract the seasonal cycle in Fig. 2 (blue line with blue circles). After subtracting the seasonal cycle from the raw series at Baltimore, a new mmsl series appears with reduced variance as shown in Fig. 5.

The rising trend noted in Fig. 4 is also present in Fig. 5 but the mmsl series variance is considerably reduced. This is highly desirable because it reduces the amount of mmsl variance that must be explained by a regression model of y (mmsl) on x (serial years).

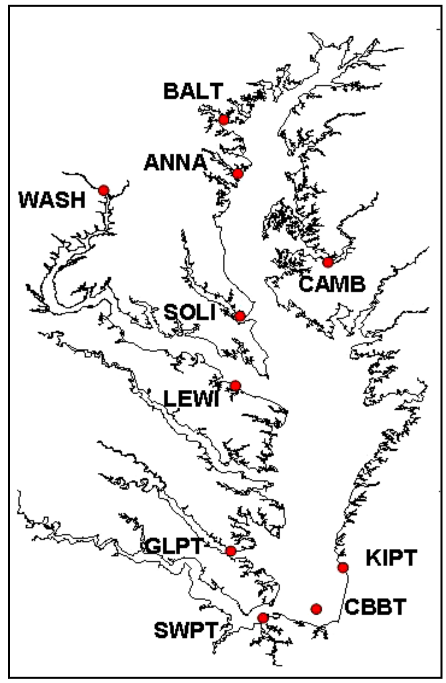

Figure 3. NWLON station location map. Station abbreviation key:
BALT (Baltimore, MD);
ANNA (Annapolis, MD);
WASH (Washington, DC);
CAMB (Cambridge, MD);
SOLI (Solomons Island, MD);
LEWI (Lewisetta, VA);
GLPT (Gloucester Point, VA);
KIPT (Kiptopeke, VA);
CBBT (Ches. Bay Bridge Tunnel);
SWPT (Sewells Point, VA);

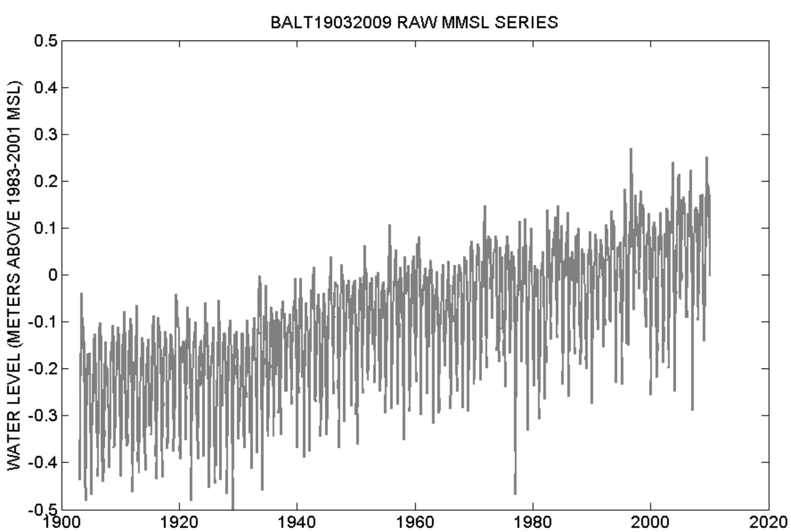

Figure 4. Raw mmsl series from 1903 through 2009, Baltimore, MD.

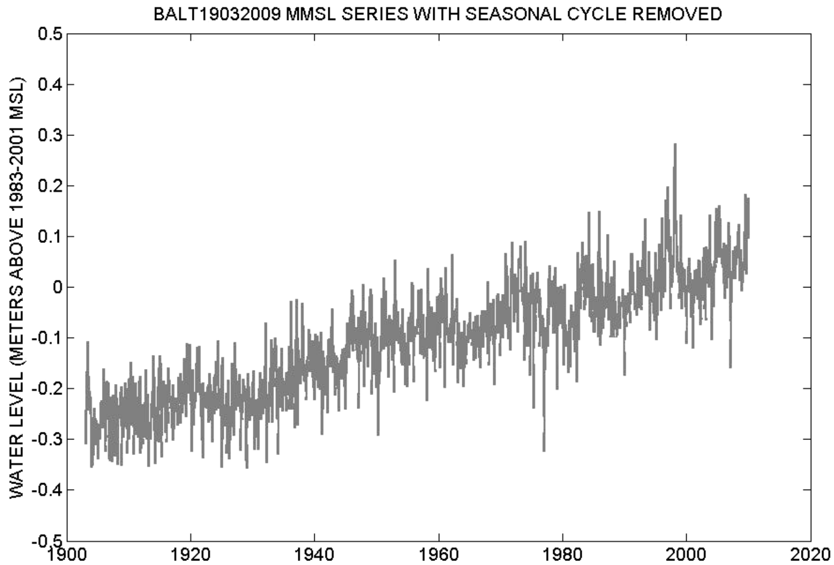

Figure 5. 1903-2009 mmsl series, seasonal cycle removed, Baltimore, MD.

A simple regression model is used below to estimate the linear trend representing the rate of sea level rise from reduced mmsl data; curvilinear regression is also used to evaluate the significance of an added quadratic term representing possible acceleration or deceleration in sea level trend.

Linear Regression – Simple linear regression is performed using the model

$$y = b_1 x + b_0 + \varepsilon \qquad (1)$$

where y is the dependent variable (mmsl), x is the independent variable (time in years), b_1,b_0 are regression coefficients and ε is an error term. If $\hat{y} = b_1x + b_0$ is the regression estimate of y, then $y-\hat{y} = \varepsilon$ is the residual error with zero mean and variance σ^2. Least squares methods obtain the b_1,b_0 values that yield the minimum residual error for a bivariate (paired x,y) data sample of size n. The method for obtaining the minimum error for simple linear regression is as follows:

Method - After computing the bivariate means, $\bar{x} = \Sigma x/n$ and $\bar{y} = \Sigma y/n$, the data are then put in deviate form as $X = x - \bar{x}$ and $Y = y - \bar{y}$. The linear regression coefficient b_1 (the slope of the fitted line) and b_0 (the y-axis intercept) are then computed as

$$b_1 = \Sigma XY / \Sigma X^2 \qquad (2)$$

and

$$b_0 = \bar{y} - b_1 \bar{x} \qquad (3)$$

Confidence intervals about b_1 are obtained by computing the deviation sum of squares from regression,

$$\Sigma d^2 = \Sigma Y^2 - (\Sigma XY)^2 / \Sigma X^2 \qquad (4)$$

the mean square deviation from regression,

$$s^2 = \Sigma d^2 / (n-2) \tag{5}$$

and the sample standard error of the regression coefficient,

$$s_m = s / \sqrt{\Sigma X^2} \tag{6}$$

The linear trend and 95% confidence interval are

$$b_1 \pm s_m t_{.05} \tag{7}$$

where $t_{.05}$ is the *t*-statistic with 0.05 probability of a larger value[1], degrees of freedom $n-2$. For the regression to be significant at the 95% level of confidence, the interval $\pm s_m t_{.05}$ must not include zero; otherwise the null hypothesis H_o: $b_1=0$ cannot be rejected at this level.

It is clear from inspection of Figs. 4-5 that the removal of the seasonal cycle reduces the mean square deviation from regression and the standard error of regression (Eqs. 5-6), thus narrowing the confidence intervals about b_1, the RSL trend at Baltimore in this case (see Fig. 6a).

There is another reason for removing the seasonal cycle due to its presence in the data as a simple cosine wave (Sa) combined with its first harmonic (Ssa). While this cycle is present, serial correlation will likely exist between successive values of the residual, y-$\hat{y}$, which in turn violates an assumption of the regression model – the assumption that the residual errors are random normally distributed. Tests for serial correlation are described later in this section.

Curvilinear Regression – A regression can also be performed using the quadratic model

$$y = b_2 x^2 + b_1 x + b_0 + \varepsilon \tag{8}$$

with b_2 as the quadratic coefficient. Assuming Eq. 8 is the correct model for regressing y (mmsl) on x (serial time in years), the acceleration (deceleration) in sea level would be given by $2b_2$. The MATLAB® function polyfit obtains the required parameters in Eq. 8 and an analysis of variance can be used to determine if the contribution of the quadratic term $b_2 x^2$ is statistically significant. Figure 6a contains the results of a quadratic model test for 1903-2009 mmsl at Baltimore in which the quadratic term is found not to be significant; however, if the Baltimore series were only as long as the next longest series in the bay (1928-2009 at Sewells Point, VA), Fig. 6b shows that a *negative* quadratic term would be significant at the 99% level of confidence (i.e., the null hypothesis H_o: $b_2=0$ is rejected at this level). This result is consistent with Houston and Dean (in press) whose quadratic analysis of 1930-2009 records at 26 U.S. water level stations found deceleration at 19 locations and acceleration at only 7.

---

[1] For large sample sizes (n>500), $t_{.05} \approx 1.97$.

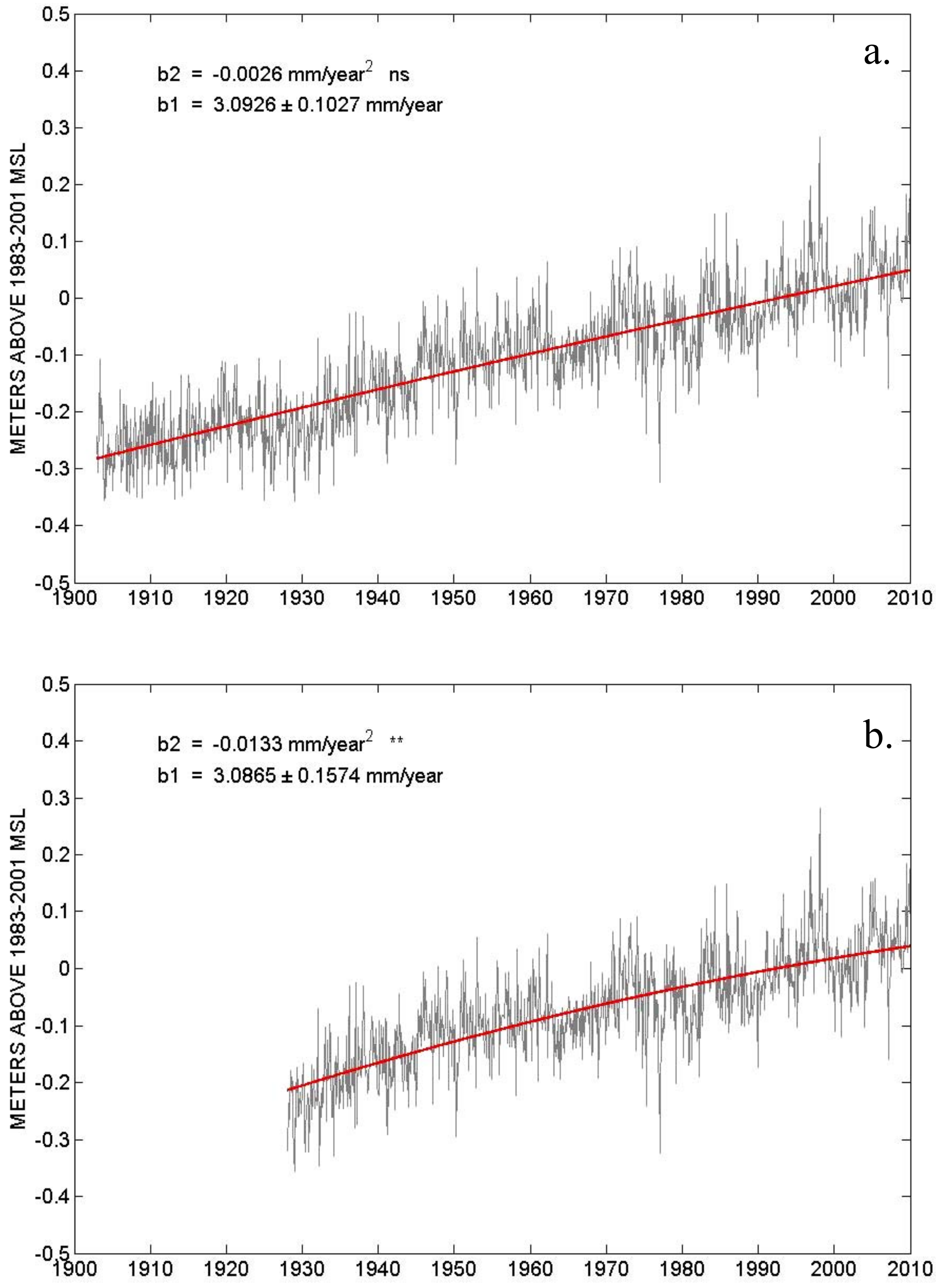

Figure 6. Observed mmsl at Baltimore, MD, and curvilinear regression (red lines) for a) 1903-2009 mmsl, b) 1928-2009 mmsl. The quadratic term, *b*2, is negative for both series; however, its contribution to regression in a) is not significant (ns) in an analysis of variance (ANOVA) while its contribution in b) is significant at the 99% level of confidence (**).

The alternative to Eq. 8 in the search for signs of an acceleration in sea level rise rates is to apply linear regression to different segments of the available record - ideally segments constrained to join at an 'inflexion' point for which 1929-1930 has been cited as an example that precedes an acceleration (Woodworth, 1990; 2009; Church and White, 2006; Miller and Douglas, 2007; Douglas, 2008). The year 1930 may well mark such a point in the Baltimore record but unfortunately the pre-1930 mmsl record is very short and unlikely, even at Baltimore, to be of any use in this regard. Some of the above authors also refer to a deceleration of sea level rise beginning in 1960. Douglas (2008) observes a leveling off at that time at tide stations at Boston, Portland and Halifax in the northern region of the U.S. east coast, but not at New York City and Atlantic City south of that region. As will be shown later in this section, there is no indication of a 1960 deceleration at any of the Chesapeake Bay NWLON stations once the decadal variability is accounted for.

Sea Level Trend Comparisons in Chesapeake Bay – In order to make comparisons at the ten NWLON stations shown in Fig. 3, it is desirable to do so over a common span of time. The minimum span in this instance is set by the 35-year record available at the Chesapeake Bay Bridge Tunnel (CBBT in Fig. 3). A very useful guide has been provided by Zervas (2009) based on trend confidence interval estimates derived from water level records at stations in the Atlantic, Pacific and Gulf of Mexico regions, as well as the Caribbean region and Bermuda. Figure 7 (Fig. 30 from Zervas) shows that a 35-year record may be expected to produce a linear trend with a 95% confidence interval (CI) between ± 1.0 and ± 1.5 mm/yr. We would prefer to compare trends with a 95% CI at least half as large: on the order of ± 0.5 mm/yr. According to Fig. 7, this would require a record span of at least 60 years but only five bay stations meet this requirement. The goal of comparing ten stations in recent time thus requires other means of reducing the CI. Accounting for the decadal variability in mmsl records provides an approach.

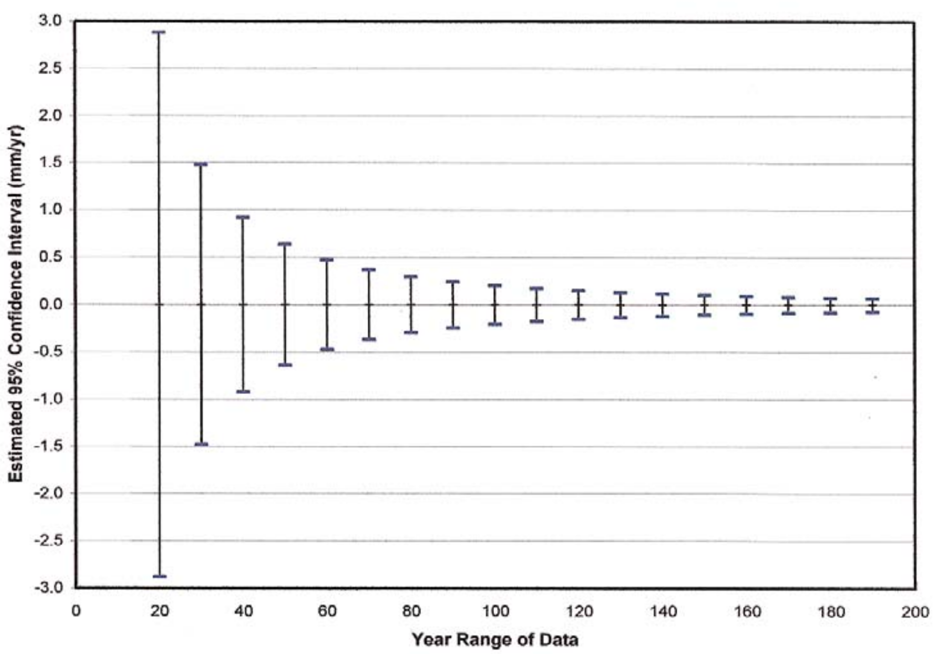

Figure 7. Estimated sea level trend confidence intervals at the 95% level of confidence as a function of data span in years. Figure 30 from Zervas (2009), NOAA/NOS Center for Operational Oceanographic Products and Services (CO-OPS).

Decadal Variability in Chesapeake Bay – Decadal variability, in contrast to the seasonal cycle, does not consist of water level motion at any fixed frequency. One of the more concise and simply stated descriptions of decadal variability comes from Hong et al. (2000):

> "When we examine sea level records on the east coasts of continents, we see surprisingly large variations at periods on the order of 100 months or longer."

The authors go on to describe 10-15 cm fluctuations at periods of a decade, more or less, caused in the case of the U.S. east coast by wind stress curl over the North Atlantic. They attribute the restriction to the east coast of continents to Rossby waves of very long period that travel from east to west. Related to this is the east coast winter storm climatology and an enhanced storm track, storm productivity mode during El Niño (Hirsch et al., 2001; Eichler and Higgins, 2006).

Although decadal variability has little predictability compared with the seasonal cycle, it is not difficult to extract its history as a quasi-periodic signal from water level records using a numerical filter. When this is done at water level stations in Chesapeake Bay, the result is a set of highly coherent signals from one station to the next. Rather than a simple moving average, we have used a general linear filter developed by Bloomfield (2000), taking advantage of his least squares approach to design a finite impulse response (FIR) filter with specific response characteristics. The one used here is a low-pass filter with a cutoff period of 24 months and filter width of 24 months, producing a full response for motions present at periods of 100 months and longer. The design and rationale for choosing this particular filter for decadal signal extraction (DSE) in Chesapeake Bay are given in Appendix A. Trend derivation is called DSE analysis.

Figure 8 provides an example of the decadal signal superposed on the mmsl series at Baltimore, after removal of the seasonal cycle. The linear trend (red line) is derived using Eq. 1. Decadal variability, as seen in the magenta curve in Fig. 8, explains why quadratic curve fitting to sea level data becomes problematic when it is present. Results depend very much on the serial times wherein the fitted series begin and end, as Fig. 6a,b demonstrates.

Figure 9a,b illustrates that the decadal signal is well correlated even as the tidal characteristics vary widely among the ten Chesapeake Bay stations. But as noted below, serial correlation in the residual errors is highly significant as a result.

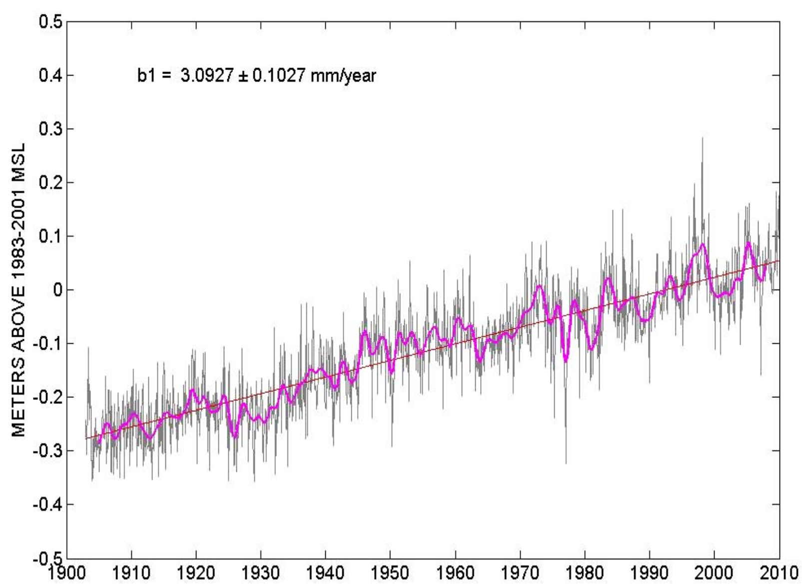

Figure 8. 1903-2009 mmsl series, seasonal cycle removed, Baltimore, MD. Magenta curve is the decadal signal, red line is the best fit linear trend.

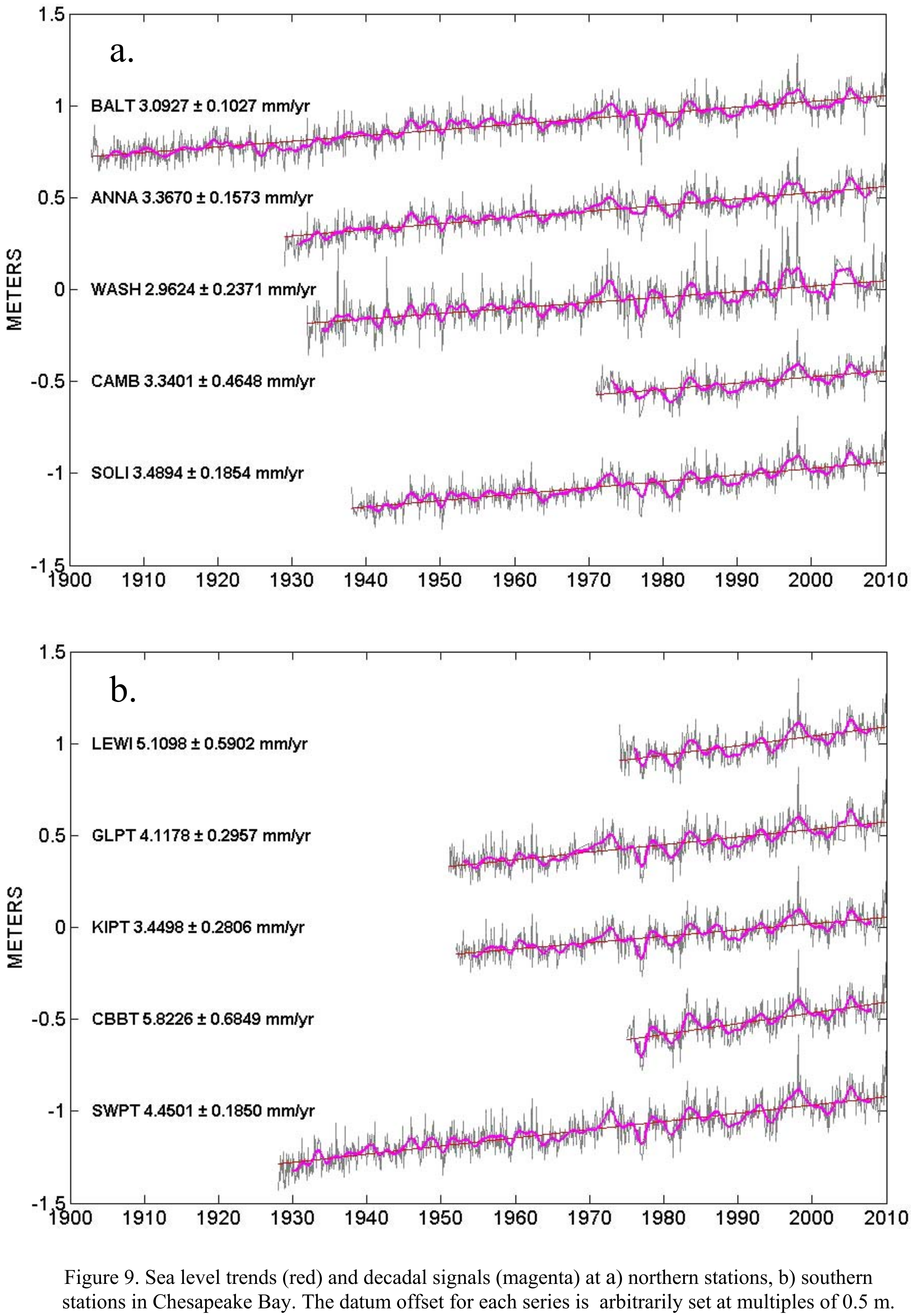

Figure 9. Sea level trends (red) and decadal signals (magenta) at a) northern stations, b) southern stations in Chesapeake Bay. The datum offset for each series is arbitrarily set at multiples of 0.5 m. Serial correlation for each mmsl series shown is significant at the 99% level of confidence.

Serial Correlation: Durbin-Watson Test – Residuals obtained from least squares regression using Eq. 1 are serial errors assumed to be independent of one another. If instead each residual is correlated with the one before and after it, then the slope coefficient and CI obtained from the regression model are questionable. Tests for serial correlation may be found in Draper and Smith (1998) and von Storch and Zwiers (1999). The Durbin-Watson test described in Draper and Smith (1998, p.69) is employed here based on the Durbin-Watson statistic

$$d = \sum_{i=2}^{n} (e_i - e_{i-1})^2 / \sum_{i=1}^{n} e_i^2 \tag{9}$$

where

$e_i = (y_i - \hat{y}) = i^{\text{th}}$ residual

n = series length

The distribution of d is symmetric about 2 and has range $0 \le d \le 4$. If d is near zero, positive serial correlation is indicated and if near 4, a negative serial correlation may exist. The test is applied by comparing d, or 4-d if this value is closer to zero, with critical values d_L and d_U for a given significance point (see Table 2.6 in Draper and Smith). The null condition is that no serial correlation exists and non-significance is indicated by $d > d_U$ or $(4-d) > d_U$. If $d < d_L$ or $(4-d) < d_L$ the null condition is rejected at the specified significance point, but if $d_L < d < d_U$ or $d_L < (4-d) < d_U$ the test is inconclusive.

Segmented Series Comparison – Comparison of all ten Chesapeake Bay water level time series over a common time span dictates selection of the shortest series in Fig. 9a,b; namely the 35-year series from 1975 through 2009 at CBBT (Chesapeake Bay Bridge Tunnel). In addition to the seasonal cycle previously removed, we also remove the decadal signal to evaluate the potential for further CI reduction about sea level trend slopes and to eliminate serial correlation as described above. The decadal signal, as previously noted, is obtained using a low-pass filter with 24-month filter width (see Appendix A). Employing a filter of this type is done at a cost of two years at either end of the original series. This action sets the upper limit of the reduced series at the end of 2007. Applying the filter to the full length of each series in Fig. 9a,b, the lower limit can be set at the beginning of 1975 for all but two stations: CBBT and LEWI (Lewisetta, VA, 1974-2009). We set the lower limit at the beginning of 1976 which gives a 32-year span at every station but CBBT where the 12-months of the beginning year were obtained by extrapolation from adjacent stations. The 32-year span allowed a single comparison of all ten stations over 1976-2007, a two-segment comparison (1944-1975, 1976-2007) at five stations and a three-segment comparison (1912-1943, 1944-1975, 1976-2007) at Baltimore.

Figure 10a,b and 11a,b illustrate the 1976-2007 mmsl segment for Sewells Point and Baltimore with the decadal signal present (Fig.10a, Fig.11a) and removed (Fig.10b, Fig.11b). The seasonal cycle has been previously removed in each case. Results for other stations and other segments may be found in Appendix B. These examples underscore the importance of removing not only the seasonal cycle but the decadal signal in short (32-year) segments at Chesapeake Bay stations. The linear trend estimating the RSL rate of rise clearly differs as does the 95% CI depending on whether the decadal signal is removed or not removed. **Most notably, serial correlation is significant at the 99% level in every case where the decadal signal is not removed and is significant at the 95% level in only one case (WASH) where it is removed.**

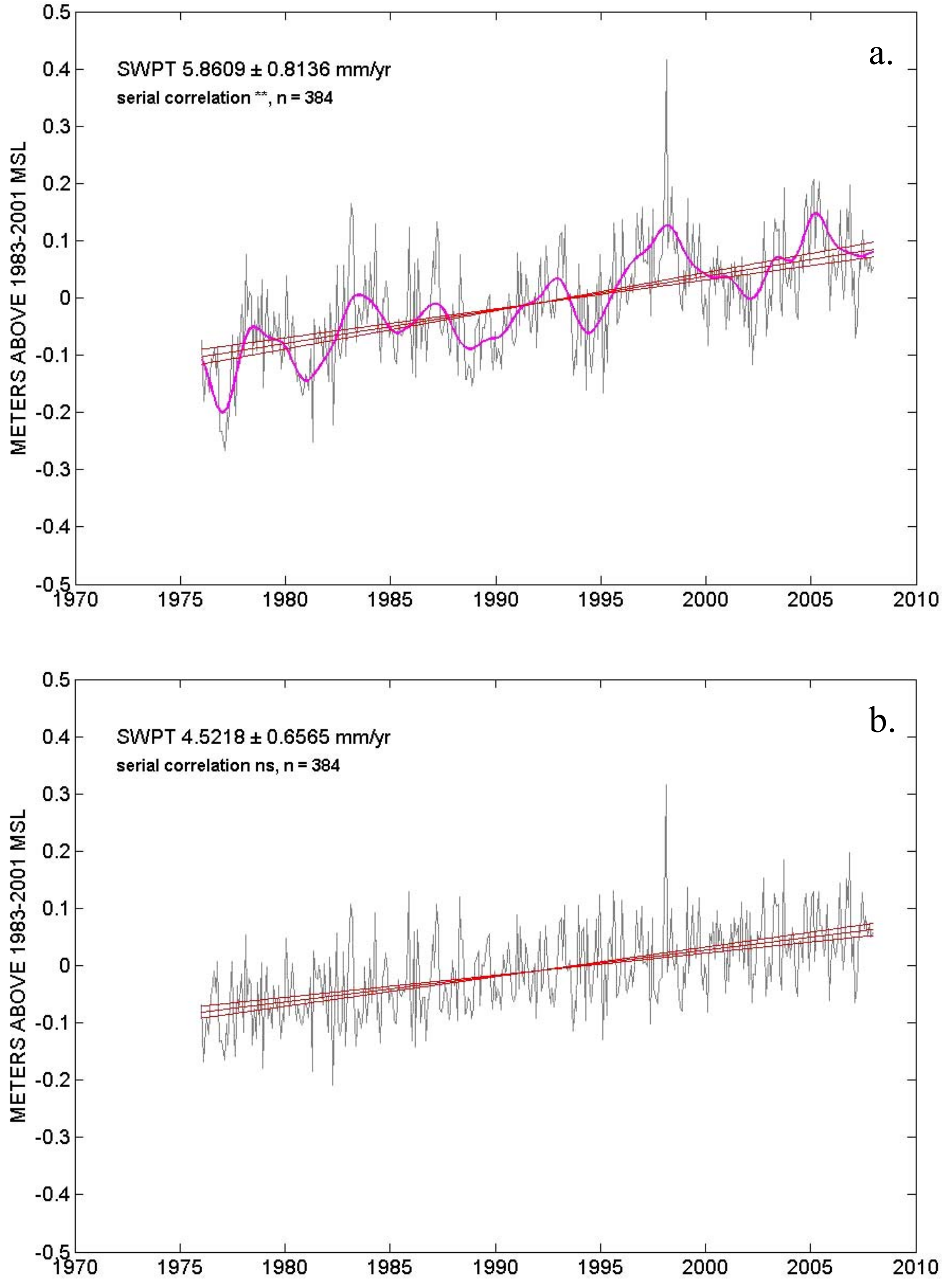

Figure 10. 1976-2007 mmsl segment at Sewells Point, VA (SWPT) where a) decadal signal is shown superposed but is not removed and b) decadal signal is removed. Serial correlation is significant at the 99% level in a) but is not significant in b). Note difference in estimate of linear trend and 95% CI between a) and b). Trend, CI values shown are un-rounded metadata.

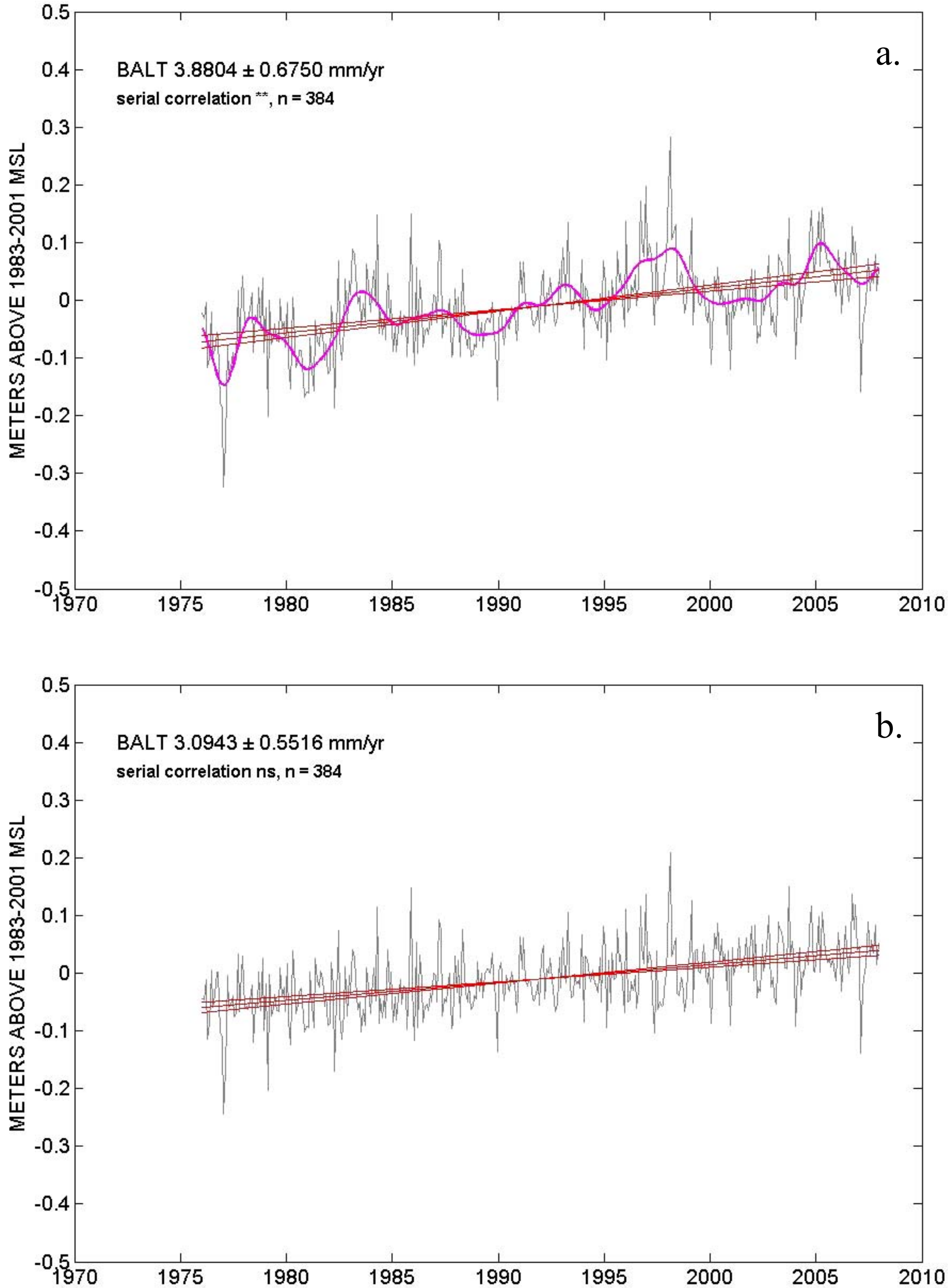

Figure 11. 1975-2007 mmsl segment at Baltimore, MD (BALT) where a) the decadal signal is shown superposed but is not removed and b) decadal signal is removed. Serial correlation is significant at the 99% level in a) but is not significant in b). Note difference in estimate of linear trend and 95% CI between a) and b), the latter by DSE analysis. Trend, 95% CI values shown are un-rounded metadata. Final values to three significant digits presented in Table 3 .

Sensitivity to RSL Rise Acceleration – Removal of the decadal signal and seasonal cycle are necessary steps for eliminating serial correlation in Chesapeake Bay mmsl series as the above analyses show. It is not known if the same is true elsewhere but application of Durbin-Watson or a similar test is advisable in every case. However, while serial correlation itself may not be significant, the question remains whether the use of a low-pass filter to perform DSE analysis may in fact remove or modify the long-term mmsl change, thus lowering the sensitivity of a short-segment, DSE-derived trend in detecting an RSL acceleration should one exist. One way of evaluating sensitivity in this instance is to add a hypothetical quadratic component (b_2x^2 term in Eq. 8) to the raw mmsl series and compare results. An engineering example is given below.

Three eustatic sea level rise scenarios based on updated 1987 National Research Council (NRC) equations have been introduced by the U.S. Army Corps of Engineers (USACE Circular No. 1165-2-211) as shown in Fig. 12. Modified quadratic equations were developed for planning purposes that produce a sea level rise by the year 2100 of 0.5 m, 1.0 m, and 1.5 m starting from zero in 1986. The quadratic coefficients required to produce the curves labeled Modified NRC-I, Modified NRC-II and Modified NRC-III in Fig. 12 are b_2 = 0.0000236, 0.0000620, and 0.0001005 mm/yr^2, respectively, with b_1 = 1.7 mm/yr.

Sensitivity testing was accomplished for each of the three NCR scenarios by adding a quadratic component to the raw mmsl time series for Sewells Point (SWPT) beginning January 1986. The added component was computed as b_2t^2 using the NCR scenario values listed above for b_2 and the value of t in serial years starting with t = 1/24 as the serial time for mid-January 1986, incrementing t by 1/12 for subsequent months. Each test series thus consists of observed mmsl at SWPT to which a hypothetical acceleration has been added. The three modified series were then processed for the 1976-2007 period using DSE analysis identical to that previously applied to the unmodified series at SWPT.

The results shown in Fig. 13 suggest that RSL trends from DSE analysis are highly sensitive to accelerations posited by Modified NRC scenarios NRC-I, NRC-II and NRC-III, the three having produced linear trends of 4.60, 4.74, and 4.88 mm/yr, respectively, as compared to 4.52 mm/yr with no modification (Fig. 10b). Equally supportive is the fact that the accelerations detected cover only the first 22 years of the three scenarios (from 1986 to 2007) shown in Fig. 12. Trend uncertainty (95% CI) and non-significant serial correlation is unchanged, pointing to near-random interannual change as the factor limiting reduction of trend confidence intervals and with it the ability to detect statistically significant differences in RSL trend between consecutive mmsl series segments.

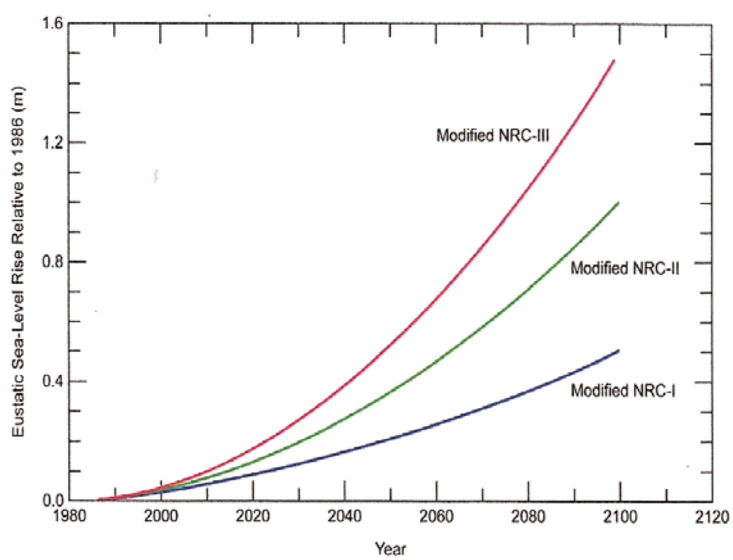

Figure 12. Three USACE/NRC scenarios for eustatic sea level rise.

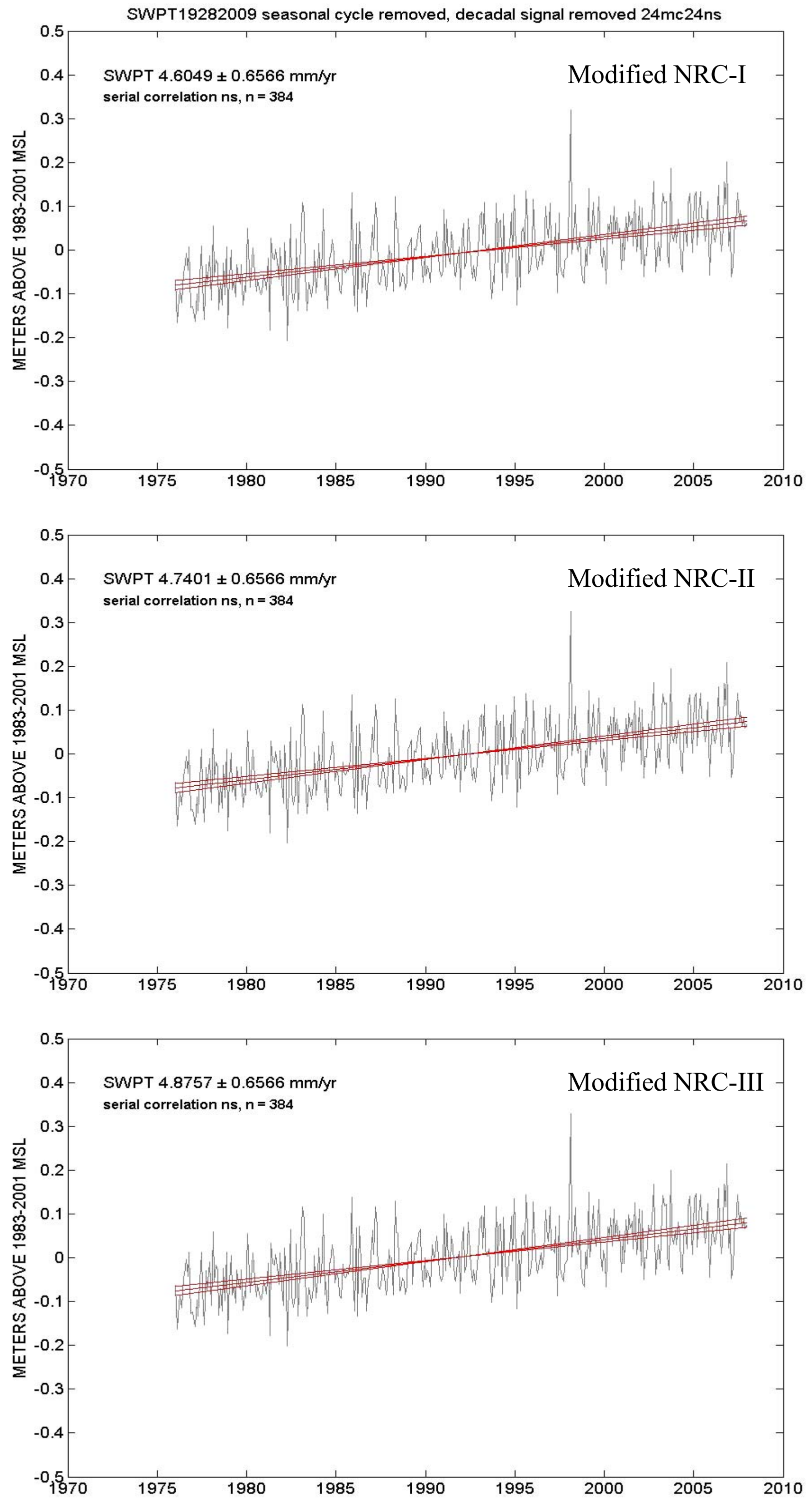

Figure 13. Linear RSL trends for 1976-2007 period after adding quadratic term from Modified NRC-I (upper), Modified NRC-II (middle), Modified NRC-III (lower). The corresponding trend over 1976-2007 increases from 4.60 mm/yr (upper) to 4.74 mm/yr (middle) to 4.88 mm/yr (lower). The linear RSL trend without quadratic term is 4.52 mm/yr as shown in Fig. 10b; 95% CI is constant.

IV. SUBSIDENCE IN CHESAPEAKE BAY

Subsidence, or the downward movement of the earth's crust relative to the earth's center, is particularly evident in the mid-Atlantic section of the U.S. east coast. Engelhart et al. (2009) used a geological database of late Holocene sea level indices to estimate subsidence rates of <0.8 mm/yr in Maine increasing to 1.7 mm/yr in Delaware before returning to rates <0.9 mm/yr in the Carolinas. If ASL rise rates are reasonably uniform across this region, as satellite altimetry suggests (see report cover), then their results are consistent with RSL trends observed at NWLON stations with some of the longest record lengths along the U.S. Atlantic Coast (Fig. 14). Further narrowing of the field of inquiry to the Chesapeake Bay region first requires a look at the factors most likely responsible for subsidence at both regional and local scales.

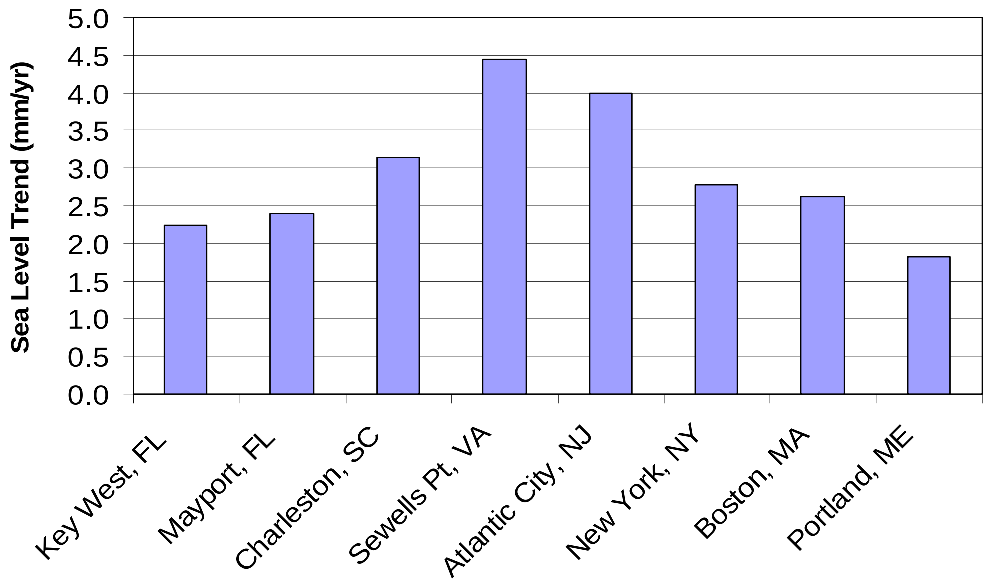

Figure 14. Linear RSL trends at eight NWLON stations along the U.S. east coast based on total record length available at each station. Record lengths vary between 1928-2006 at Mayport, FL and 1856-2006 at New York, NY. Data from Zervas (2009) who accounts for serial correlation using an autoregression technique.

<u>Regional Subsidence</u> – The zone separating Chesapeake Bay from the Atlantic Ocean, U.S. mid-Atlantic coastal region, consists of three broadly-defined geographic areas: the Atlantic Coast of the Delmarva Peninsula, the mouth of Chesapeake Bay and the mainland shore of southeastern Virginia (Fig. 15). Unlike Chesapeake Bay situated on its western shore, long-term water level measurements are lacking on the eastern shore of the Delmarva Peninsula. Consequently, there is little evidence of either subsidence or emergence from this source. Only two tide stations are found on the Atlantic side with suitable records for sea level trend analysis: Ocean City, MD (5.48 ± 1.67 mm/yr) and Lewes, DE (3.20 ± 0.28 mm/yr). The analysis for Ocean City is based on the years 1975-2006 while Lewes is based on the years 1919-2006 (Zervas, 2009).

New geodetic and geologic evidence is available that has allowed past stands of sea level to be determined and inferences to be made about subsidence in North America and the Virginia coastal zone (Sella et al., 2007; Engelhart, 2009; Hobbs et al., submitted). Glacial and inter-glacial episodes during the Pleistocene Epoch have led not only to a vertical rise and fall of sea level by more than 100 m but to multiple horizontal transgressions and regressions of the shoreline across the mid-Atlantic coastal region, leaving scarps and ridges to mark high stands of sea level in the geologic past. Given an ocean volume history derived from oxygen-isotope marine dating methods in combination with land deposits dated by other methods, land surface elevations can be accurately placed within recent glacial-interglacial sequences. Inferences can then be made concerning regional patterns of uplift and subsidence as well as their cause. For example, at the beginning of the Sangamonian interglacial period approximately 120,000 years before present, land surfaces were found to be anomalously high in the mid-Atlantic compared to other regions. Hobbs et al. (submitted) attribute this to the presence of a glacial forebulge adjacent to an ice mass to the north that existed during the earlier Illinoian glacial period. Glacial isostatic adjustment subsequently led to post-glacial rebound in the north and forebulge collapse in the south - collapse and land subsidence that was most prominent in the mid-Atlantic region (Fig.16). The adjustment occurring in the Sangamonian period is an analog for adjustments in the present interglacial period following the last glaciation (Laurentide).

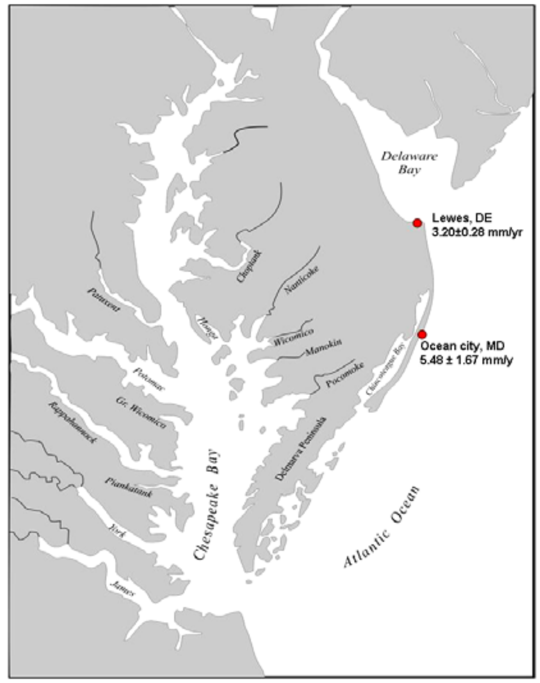

Figure 15. Ocean tide stations, Delmarva Peninsula.

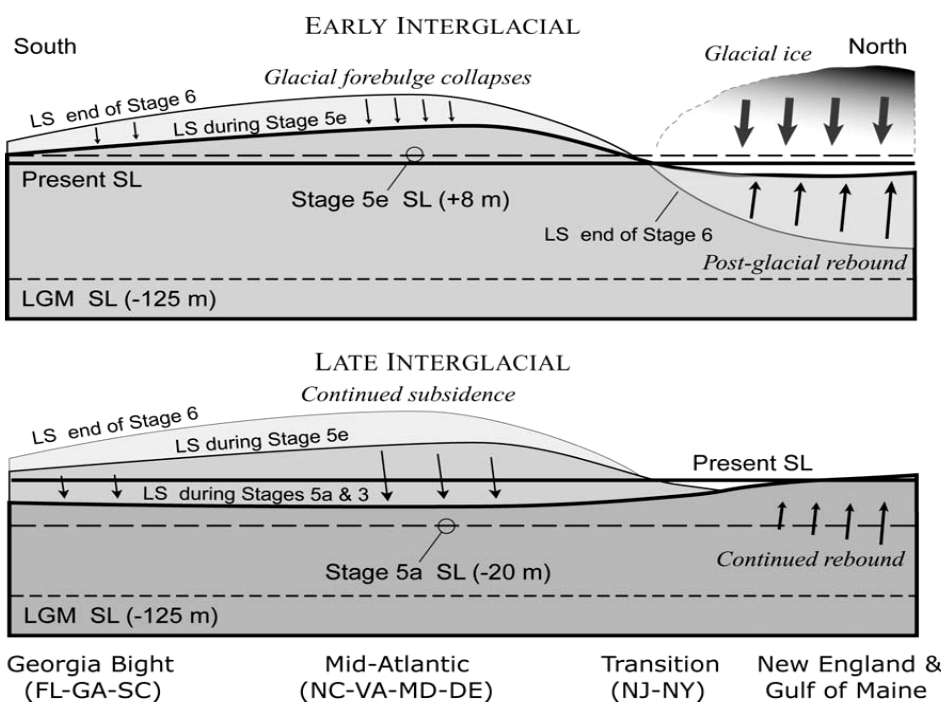

Figure 16. Regional isostatic response of the Atlantic coast after Illinoian glacial period (marine stage 6). LS, land surface; SL, sea level; LGM, last glacial maximum (Fig. 12 from Hobbs et al., with permission).

Local Subsidence – Subsidence can occur locally within a region due to several causes. Among these are settlement due to compaction of subsurface sedimentary layers aided by groundwater or hydrocarbon removal, sinkholes in the earth's surface caused by karst processes and faulting/consolidation associated with filled structures.

A prominent fill structure has only recently been discovered beneath the lower Chesapeake Bay and surrounding area (Fig. 17). This structure, the Chesapeake Bay Impact Crater (CBIC), was formed as a large comet or meteor struck the earth approximately 35 million years ago near Cape Charles, VA (Poag et al., 1992; Powars and Bruce, 1999; Powars, 2000). The outer rim, annular trough and peak ring surrounding the center of the crater are common features of impact structures and mark zones of profound change in the subsurface geology, including block-faulting of sedimentary layers along the outer rim and raised crystalline basement rocks along the peak ring (Fig. 18). Four of the ten NWLON stations used in our RSL trend investigations lie within the CBIC. Those located on or very near the outer rim (SWPT, CBBT, GLPT) are positioned above a disruption boundary created at impact, a boundary likely to be associated with megablock faulting and subsidence just inside the crater (Fig. 18). This is consistent with high RSL trends at these stations (see Fig. 9). In contrast, the fourth station, KIPT, is positioned along the peak ring where lower subsidence would be consistent with lower RSL trend at KIPT.

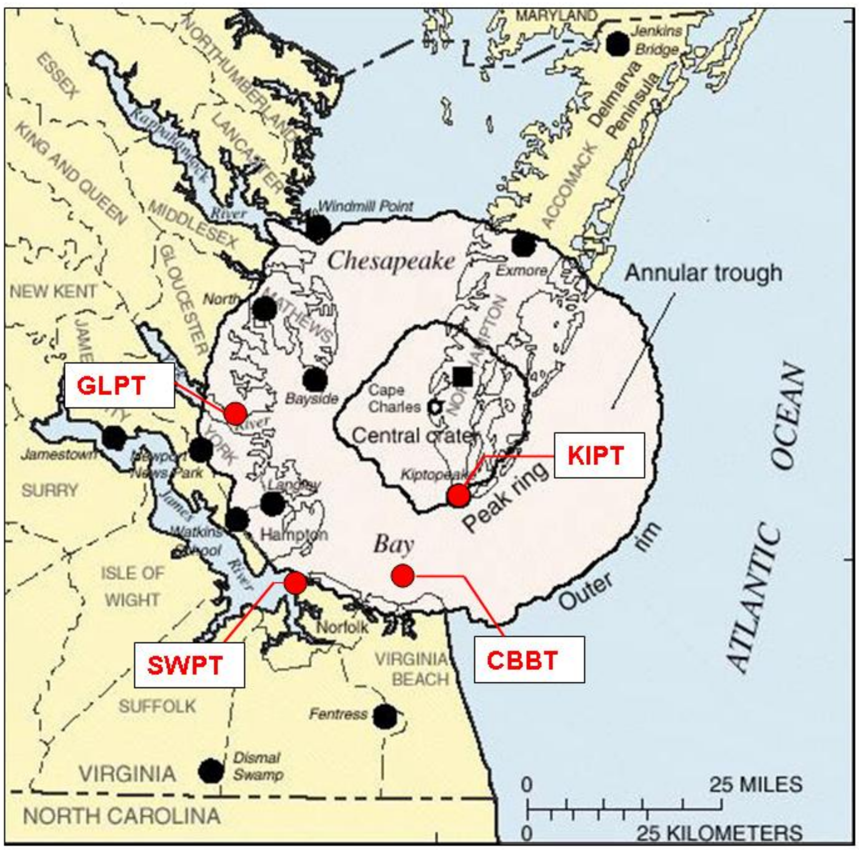

Figure 17. Map showing subsurface extent of the Chesapeake Bay Impact Crater. NWLON stations at Sewells Point (SWPT), Chesapeake Bay Bridge Tunnel (CBBT), Kiptopeke (KIPT) and Gloucester Point (GLPT) are shown by red dots. Black dots are core sampling stations used in studies of the subsurface geology.

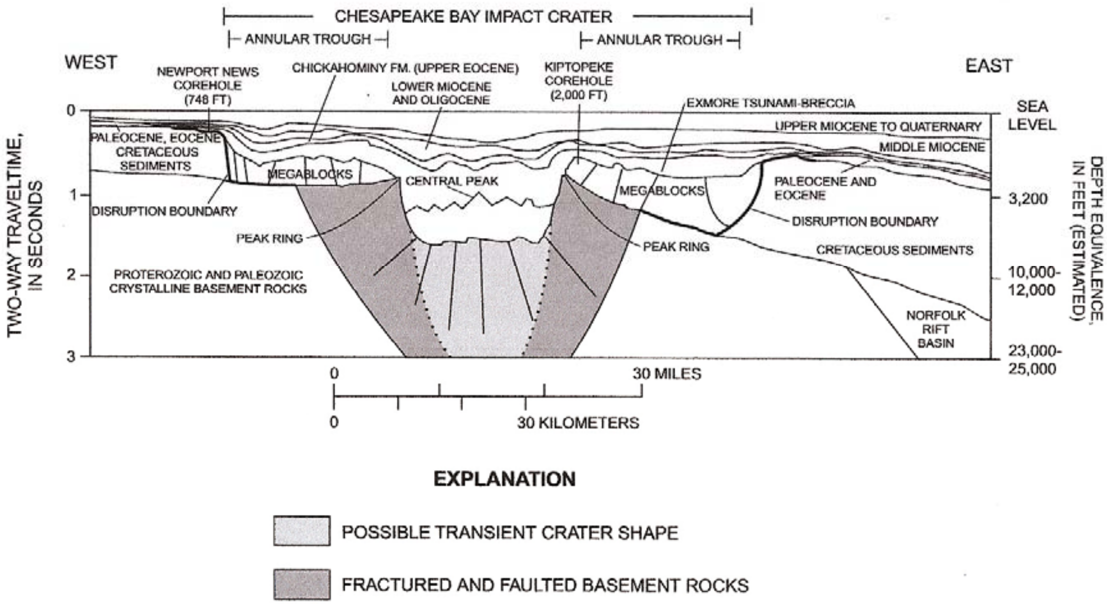

Figure 18. Generalized geologic section of Chesapeake Bay Impact Crater (Powars, 2000).

Direct Measurement via GPS Satellites – NOAA's National Geodetic Survey (NGS) operates the Continuously Operating Reference Station (CORS) network (http://www.ngs.noaa.gov/CORS/) that now provides direct measurement of vertical land movements at the surface of the earth's crust referenced to the ITRF2000 ellipsoid. CORS consists of a network of fixed sensors on land that continuously record their horizontal and vertical position using signals from global positioning system (GPS) satellites. Information on long-term vertical trends is still sparse and a high level of expertise is required to use CORS data effectively for that purpose. Similar to the uncorrected water level series previously examined, GPS time series observations exhibit serial correlation that requires the use of complex statistical procedures to determine standard error estimates associated with vertical crustal velocities (Snay et al., 2007).

Snay et al. (2007) analyzed GPS data for 550 CORS and some 140 other globally-distributed GPS base stations to derive time series of vertical crustal velocities in the continental U.S. and abroad. From this set, they selected a subset of 37 CORS stations subject to the restriction that each be located within 40 km of an NWLON station with RSL information. This restriction allowed ASL trend estimates to be made as the sum of RSL trends and CORS estimates of crustal velocity (negative for subsidence), thus bypassing the need for GIA corrections to RSL. CORS estimates were derived as an average of six independent GPS solutions within a span of 3 to 11 years. In addition, crustal velocities were assumed to be constant over multi-decadal time spans allowing their average value to be subtracted from RSL trends based on a much longer mmsl series. A sample consisting of 30 sites in the continental U.S. yielded an average ASL rate of 1.80 ± 0.18 mm/yr in the 1900-1999 period. At individual sites, uncertainty was characterized by a weighted RMS value of ± 0.85 mm/yr.

Of the abovementioned 37 stations, 15 sites along the U.S. east coast were designated by Snay et al. (2007) as the 'Atlantic Group'. The stations in this group are of particular interest here as five of them are located within Chesapeake Bay. Table 1 below contains RSL, ASL and CORS subsidence trends along with standard error estimates for these five stations excerpted from Snay et al. (2007).

It should be noted that uncertainties throughout Snay et al. (2007) are reported as one standard error unless otherwise stated, presumably including RSL trend estimates obtained from Zervas (2001) as cited in Table 1 below. Eq. 6 is used in this report to calculate the standard error for a linear trend. However, to obtain a confidence interval about a linear trend, standard error must be multiplied by the *t*-statistic at a specified level of confidence as in Eq. 7. A later report by Zervas specifies the 95% level of confidence on trend estimates for the same five stations (Table 2). Zervas (2009) used autocorrelation and a variance inflation factor to correct for serial correlation where the latter exists in the mmsl time series being analyzed - after the seasonal cycle has been removed. Keeping these nuances in mind, appropriate caution is required especially in circumstances where one sea level trend is said to be significantly different from another. Caution is also needed when evaluating RSL trends at stations specifying a long time span but with no indication of missing data. We have used only the 1971-2009 mmsl series at Cambridge, MD, because data from 1952 to 1971 are missing at that station.

Table 1. Relative, Absolute Sea Level Trend and Standard Error Estimates from Snay et al. (2007).

Station	RSL[a] (mm/yr)	time span	CORS (mm/yr)	time span	ASL[b] (mm/yr)	ASLD[c]
Cambridge, MD	3.52±0.24	1943-1999	0.24±1.16	1999-2005	3.76±1.18	1.96
Annapolis, MD	3.53±0.13	1928-1999	-3.05±1.74	2001-2005	0.48±1.74	-1.32
Solomons Is., MD	3.29±0.17	1937-1999	-2.19±1.16	1999-2005	1.10±.117	-0.70
Washington, DC	3.13±0.21	1931-1999	-1.72±1.39	2000-2005	1.41±1.41	-0.39
Gloucester Pt., VA	3.95±0.27	1950-1999	-2.58±1.16	1999-2005	1.37±1.19	-0.43

[a] Data from Zervas (2001). [b] ASL=RSL+CORS (mm/yr) with weighted standard error.
[c] Deviation of ASL trend estimate from 1.8 mm/yr 20th century average.

Table 2. Relative Sea Level Trend and 95% Confidence Interval Estimates from Zervas (2009).

Station	RSL (mm/yr)	time Span	range
Cambridge, MD	3.48±0.39	1943-2006	64 years
Annapolis, MD	3.44±0.23	1928-2006	79 years
Solomons Is., MD	3.41±0.29	1937-2006	70 years
Washington, DC	3.16±0.35	1924-2006	83 years
Gloucester Pt., VA	3.81±0.47	1950-2003	54 years

As evident from the data presented in Table 1, spatial variability is high among ASL trend estimates derived from CORS data applied at individual stations, a fact that explains why spatial averaging is necessary to derive ASL trends with a reasonable degree of certainty. Where both geological and water level measurement records are available in abundance, as on the U.S. Atlantic coast, distinct ASL spatial trends may be found in addition to an overall estimate. Although Engelhart et al. (2009) obtained a 20th century average ASL rise rate of 1.8 ± 0.2 mm/yr for this region, similar to the global average, they also inferred positive ASL rise rates increasing in a distinct spatial trend southward from Maine to South Carolina which they suggest may be related to wasting of the Greenland ice sheet and/or ocean steric effects.

V. DISCUSSION

Douglas (1991, 1992) has argued that water level records at least 60 years in length, preferably longer, are needed to precisely determine RSL trends at tide stations in the absence of other concerns such as location near a geologic fault. Many authors have since commented on the question of how many years are enough, pointing to low-frequency (interannual, decadal) change as the chief problem. Even with long records, results can differ depending on the starting and ending points, not to mention statistical problems introduced by serial correlation. Douglas (2001) was aware of serial correlation as he described interannual and longer-period sea level variations in Chesapeake Bay and the nearby Atlantic Ocean, remarking on the strong spatial correlation between low-pass filtered series at Baltimore and Annapolis, MD, and Atlantic City, NJ – correlation in spite of the inherent differences in estuarine and ocean environments.

We are aware of these and other concerns that dictate caution when analyzing water level data to determine RSL trends. In this report we depart, with due care, from the 60-year standard by recognizing that known geophysical processes provide most of the forcing that drives observed decadal variability – variability in sea level that is prominent on the western side of oceans (Hong et al., 2000; Sturges and Hong, 2001) and linked to ocean-atmosphere exchange of heat, vorticity and momentum. Changes in atmospheric circulation forced by teleconnections from the equatorial Pacific are far-reaching and most likely account for correlations we observe between decadal highs in Chesapeake Bay water level and El Niño events in the Pacific (see Fig. A-3, Appendix A). Likewise of interest is the observation by Trenberth et al. (2002) that a climate shift occurred around 1976/1977, reversing the east/west area of origin and direction of warm water movement in the Pacific equatorial region during ENSO events. Again, there is a degree of association between this shift and a perceptible change in decadal signal amplitude at approximately this time (see Fig. 9a,b). We assume these quasi-periodic processes are different and can be distinguished from the ones driving global sea level rise at a steady or an accelerating rate. Of foremost concern are signs of an acceleration in recent decades that is more exponential than cyclical in form – signs that Woodworth (1990) has said should be observable by 2010.

In the discussion that follows, we will refer to RSL *rise* rather than *trend* in discussing results for Chesapeake Bay.

<u>Relative Sea Level Rise (RSLR)</u> – RSLR and 95% confidence intervals about RSLR for the 1944-1975 and 1976-2007 periods adopted for this study are given in Table 3. Five stations have the necessary data for both periods while five cover 1976-2007 only; BALT covers three 32-year periods. None of the stations exhibit a significant RSLR difference over the 32-year interval although BALT, SOLI and SWPT are each quite consistent. The largest RSL change, 0.23 mm/yr at ANNA, is of interest because it coincides with a high CORS subsidence rate reported for that station (Table 1,4). WASH, on

Table 3. RSLR at Chesapeake Bay Stations

Station	1944-1975	1976-2007	RSLR Diff.
BALT[a]	3.08 ± 0.52	3.09 ± 0.55	0.01 mm/yr
ANNA	3.45 ± 0.51	3.68 ± 0.58	0.23 mm/yr
WASH	2.99 ± 0.66	2.91 ± 0.82[b]	-0.08 mm/yr
CAMB	no data	3.44 ± 0.49	-------------
SOLI	3.55 ± 0.50	3.61 ± 0.54	0.06 mm/yr
LEWI	no data	5.15 ± 0.55	-------------
GLPT	no data	4.30 ± 0.62	-------------
KIPT	no data	3.51 ± 0.58	-------------
CBBT	no data	5.80 ± 0.62	-------------
SWPT	4.47 ± 0.61	4.52 ± 0.66	0.05 mm/yr

[a] BALT 1912-1943 3.09 ± 0.52 mm/yr

[b] Serial correlation significant at 95% level of confidence

the other hand, is the only station to demonstrate serial correlation in either period after removal of the decadal signal (serial correlation significant at the 95% level of confidence, 1976-2007). WASH (Washington, DC) lies close to the fall line in the upper Potomac River where high river inflows may explain the unusual number of mmsl 'spikes' or interannual highs that appear in the 1976-2007 period (Appendix B, Fig. B-8) although, curiously, not as often in the 1944-1975 period (Appendix B, Fig. B-7). Notwithstanding the apparent riverine influence at WASH, the decadal signal clearly reaches the upper Potomac in the form seen at other stations (Fig.9).

Absolute Sea Level Rise (ASLR) Estimates - Addition of the 1976-2007 RSLR rates at Chesapeake Bay stations to the corresponding five CORS vertical velocity estimates by Snay et al. (2007) yields a set of ASLR estimates (Table 4) recalling that a negative CORS velocity indicates land subsidence. Of the two measurements, CORS velocities clearly have the greatest amount of uncertainty when comparing individual stations and the wide variation in ASLR rates listed in Table 4 should come as no surprise. Comparing the data in Tables 3 and 4, however, the results for ANNA, WASH and CAMB are perhaps the least expected in terms of key metrics ranging from serial correlation to anomalous land subsidence and emergence. The remaining two of the five stations with CORS data, SOLI and GLPT, hint at the global average rate of rise for the 20th century: 1.8 mm/yr.

Table 4. Absolute Sea Level Rise (ASLR) Estimates

Station	RSLR 1976-2007[a]	CORS velocity [b]	ASLR [c]
BALT	3.09 ± 0.55	no data	------------
ANNA	3.68 ± 0.58	-3.05 ± 1.74	0.63 mm/yr
WASH	2.91 ± 0.82	-1.72 ± 1.39	1.19 mm/yr
CAMB	3.44 ± 0.49	0.24 ± 1.16	3.68 mm/yr
SOLI	3.61 ± 0.54	-2.19 ± 1.16	1.42 mm/yr
LEWI	5.15 ± 0.55	no data	-------------
GLPT	4.30 ± 0.62	-2.58 ± 1.16	1.72 mm/yr
KIPT	3.51 ± 0.58	no data	-------------
CBBT	5.80 ± 0.62	no data	-------------
SWPT	4.52 ± 0.66	no data	-------------

[a] uncertainty expressed by 95% confidence interval about RSLR
[b] uncertainty expressed by standard error of regression
[c] ASLR = RSLR + CORS

Chesapeake Bay Subsidence Estimates – Subsidence in the Chesapeake Bay area is an ongoing process characterized by spatially varying rates. This view is supported by the available evidence and the factors likely contributing to subsidence in the region as described in Section IV. What is not expected to vary to any significant degree across the Chesapeake Bay sub-region is the actual ASLR which we do not know but can assume is close to the 1.8 mm/yr average given by IPCC AR4 for 1961-2003. The 1976-2007 Chesapeake Bay data in Table 4 do not disagree with this average nor does the global mean sea level trend near the entrance to Chesapeake Bay as shown on the satellite altimetry map in Fig. 1 and the report cover page. Table 5 contains the subsidence rate estimates based on the assumption of a constant ASLR of 1.8 mm/yr throughout the Chesapeake Bay.

Table 5. Chesapeake Bay Subsidence Rate Estimates

Station	RSLR 1976-2007[a]	Subsidence [b]	Percentage [c]
BALT	3.09 ± 0.55	-1.29 mm/yr	42
ANNA	3.68 ± 0.58	-1.88 mm/yr	51
WASH	2.91 ± 0.82	-1.11 mm/yr	38
CAMB	3.44 ± 0.49	-1.64 mm/yr	48
SOLI	3.61 ± 0.54	-1.81 mm/yr	50
LEWI	5.15 ± 0.55	-3.35 mm/yr	65
GLPT	4.30 ± 0.62	-2.50 mm/yr	58
KIPT	3.51 ± 0.58	-1.71 mm/yr	49
CBBT	5.80 ± 0.62	-4.00 mm/yr	69
SWPT	4.52 ± 0.66	-2.72 mm/yr	60

[a] uncertainty expressed by 95% confidence interval about RSLR
[b] subsidence = ASLR – RSLR ≈ 1.8 mm/yr – RSLR
[c] average subsidence is 53 % of average RSLR 1976-2007

VI. CONCLUSIONS AND FUTURE OUTLOOK

Linear trend analysis of monthly mean sea level (mmsl) data from ten Chesapeake Bay water level stations with a common time span have provided insight into temporal and spatial differences in relative sea level rise (RSLR) with approximately the same confidence interval at each station after decadal signal extraction (DSE). Time-segment comparisons indicate small increases in RSLR at four of five Chesapeake Bay stations with data arranged in two periods of equal, non-overlapping spans: 1944-1975 and 1976-2007. Although none of the increases are statistically significant, the methodology used here (DSE analysis) is still sensitive to recent changes on the order of ±0.05 mm/yr. Excluding Washington, DC (WASH), which has significant serial correlation for this period, 1976-2007 RSLR rates at nine stations show an average increase of 0.10 mm/yr compared to NOAA RSLR rates for the same nine stations as reported in Zervas (2009). The 1976-2007 RSLR rate at Sewells Point (SWPT) as determined in this study, for example, is 4.52 ± 0.66 mm/yr (Table 5) compared to 4.44 ± 0.27 mm/yr reported by Zervas (2009) for the 1927-2006 period at SWPT, an increase of 0.08 mm/yr above the NOAA rate.

Temporal Comparisons – Reducing confidence interval on trend dictates use of the longest series available in RSL trend analysis. In Chesapeake Bay and elsewhere, both interannual and decadal variability contribute to trend uncertainty and these factors together make it necessary to obtain record lengths on the order of 100 years before reaching a confidence interval as low as ± 0.15 mm/yr. Thus, if an absolute sea level (ASL) rate increase of 0.10 mm/yr were to be added in the next decade, its detection as a significant change would be unlikely even if decadal variability were accounted for. An increase on the order of 0.5 mm/yr may be required for a statistical significant acceleration to be confirmed in the years ahead. Meanwhile, time-segment comparisons that account for decadal variability are very likely to witness the smaller changes leading up to it, if indeed an acceleration does develop at this scale.

Having said the above, it is by no means certain that an RSLR acceleration will occur in Chesapeake Bay on the scale suggested by any of the USACE/NRC scenarios illustrated in Fig. 12. It must be kept in mind that the ASL trend estimate of 3.1 mm/yr over the 1993-2003 period, as given in the IPCC Fourth Assessment Report, was derived as a global average. Looking again at Fig. 1 and the image on the report cover, it is the considerable spatial variability among ASL trends from satellite altimetry that stands out, not to mention the fact that this 'snapshot' of world-wide trends is still evolving. And whereas spatial averaging of many local estimates can lead to reduced uncertainty for a global trend estimate, this process does not work in reverse. The uncertainty at a given point on the globe, such as the Chesapeake Bay, remains high.

Future Outlook – The take-home message is to keep bay tide gauges operational. Best prospects for RSLR monitoring going forward are the water level stations at Baltimore, MD, Solomons Island, MD, and Hampton Roads (Sewells Point), VA. These three long-term stations are strategically positioned at the head, mid-section and mouth of Chesapeake Bay and their data quality is excellent. Their value would increase substantially in terms of climate change monitoring if Continuously Operating Reference Stations (CORS) at Baltimore and Sewells Point were given priority in addition to Solomons Island.

Spatial Comparisons – RSLR rates at all ten bay stations for the 1976-2007 period underscore variability in subsidence rates assuming that the present ASL rise is uniform throughout the Chesapeake Bay area. Given the most likely ASLR rate of 1.8 mm/yr for what may be termed late 20^{th}/early 21^{st} century, inferred subsidence rates vary from -4.00 mm/yr at the Chesapeake Bay Bridge Tunnel, VA, to -1.29 mm/yr at Baltimore, MD (omitting Washington, DC, because of significant serial correlation over 1976-2007). In between these extremes, subsidence rates account for 50-60% of the measured RSLR at water level stations. These findings are in agreement with those of coastal geologists who report evidence of structural faults not only within the Chesapeake Bay Impact Crater in the lower bay but in areas further north in the mid-section of the bay (R. Berquist, pers. comm.). High RSLR at Lewisetta, VA, is likely due to additional subsidence induced through local faulting.

Future Outlook – Subsidence will clearly remain a problem as it will continue to add to high RSLR rates locally and heighten the risk of flooding from storm tides in the lower Chesapeake Bay as time goes on. Low-lying areas in communities such as Norfolk, Virginia Beach, Portsmouth, Chesapeake, Hampton and Poquoson are comprised of a patchwork of local areas that are not only vulnerable to storm tides but are experiencing varying rates of subsidence, meaning that some areas within these communities may be facing greater risk than others from global sea level rise going forward. In addition to CORS, other technologies such as airborne LIDAR (Light Detection and Ranging) will be needed to perform repeated mapping of ground topography to track changes in flood elevation contours with time.

VII. ACKNOWLEDGEMENTS

This project was supported by Federal Contract No. W91236-10-P-0122 under a cost-sharing agreement between the Norfolk District U.S. Army Corps of Engineers, 803 Front Street, Norfolk, VA 23510 and the Virginia Institute of Marine Science, Rt. 1208-Greate Road, Gloucester Point, VA 23062. This report is a summary of findings from the research completed for Tasks I through IV of the above-referenced contract.

We are indebted to Carl H. Hobbs of the Virginia Institute of Marine Science, Department of Physical Sciences, and C.R. Berquist of the Department of Geology, College of William and Mary for their critical review of the report manuscript and many helpful suggestions regarding the issue of subsidence in Chesapeake Bay.

Appreciation is also expressed to Jeffrey Halka, Director of the Maryland Geological Survey, for his comments on the report and to Chris Zervas and William Sweet of NOAA, National Ocean Service, Center for Operational Oceanographic Products and Services (CO-OPS) for their comments and suggestions.

VIII. REFERENCES

Boon, J.D., 2007. *Secrets of the Tide: Tide and Tidal Current Analysis and Applications, Storm Surges and Sea Level Rise*. Chichester (U.K.): Horwood Publishing, 2004, 2007.

Bloomfield, P., 2000. *Fourier Analysis of Time Series: An Introduction*. John Wiley & Sons, 1976, 2000.

Church, J.A., N.J. White, R. Coleman, K. Lambeck, and J.X. Mitrovica, 2004. Estimates of the Regional Distribution of Sea Level Rise over the 1950–2000 Period. *J. Climate,* 17: 2609-2625.

Church, J.A. and N.J. White (2006), A 20th century acceleration in global sea-level rise, *Geophys. Res. Lett.*, 33: L01602, doi:10.1029/2005GL024826.

Conrad, C.P., and B.H. Hager, 1997. Spatial variations in the rate of sea level rise caused by the present-day melting of glaciers and ice sheets. *Geophys. Res. Lett.*, 24: 1503-1506.

Douglas, B.C., 1991. Global sea level rise. *J. Geophys. Res.,* 96(C4): 6981–6992.

Douglas, B.C., 1992. Global sea level acceleration. *J. Geophys. Res.,* 97**:** 12 699–12 706.

Douglas B.C. 2001. Sea Level Change in the Era of the Recording Tide Gauge. In: *Sea Level Rise: History and Consequences*, Douglas B.C., Kearney M.S., Leatherman S.P. (eds). Academic Press: San Diego, CA; 37–64.

Douglas, B.C., 2008. Concerning evidence for fingerprints of glacial melting. *J. Coastal Research*, 24(2B): 218-227, DOI:10. 2112/06-0748.

Draper, N.R., and H. Smith, 1998. *Applied Regression Analysis*. 3rd Ed. John Wiley & Sons.

Eichler, T., and W. Higgins, 2006. Climatology and ENSO-related variability of North American extratropical cyclone activity. *Int. J. Climatol*. 19: 2076-2093.

Engelhart, S.E., B.P. Horton, B.C. Douglas, W.R. Peltier, and T.E. Törnqvist, 2009. Spatial variability of late Holocene and 20th century sea-level rise along the Atlantic coast of the United States. *Geology*, 37: 1115-1118; doi: 10.1130/G30360A.1.

Fiedler, J.W., and Conrad, C.P., 2010. Spatial variability of sea level rise due to water impoundment behind dams. *Geophys. Res. Lett.*, 37: L12603, doi:10.1029/2010GL043462.

Hirsch, M.E., A.T. DeGaetano, and S.J. Colucci, 2001. An east coast winter storm climatology. *Int. J. Climatol*. 14: 882-899.

Hobbs, C.H. III, D.E. Krantz, G.L. Wikel (submitted 2010). Coastal Processes and Offshore Geology. In: C. Bailey (ed.), The Geology of Virginia.

Holgate, S.J., 2007. On the decadal rates of sea level change during the twentieth century. *Geophys. Res. Lett.*, 34: L01602, doi:10.1029/2006GL028492.

Hong, B.G., W. Sturges, and A.J. Clarke 2000. Sea level on the U.S. east coast: Decadal variability caused by open ocean wind-curl forcing. *J. Physical Oceanography*, 30: 2088-2098.

Houston, J.R., and R.G. Dean, (in press). Is the rate of sea level rise increasing? An analysis based on U.S. tide gauges. In: Sea Level Rise and Coastal Infrastructure: Predictions, Risks and Solutions. B.M. Ayyub, M.S. Kearney (eds.), ASCE Monograph.

IPCC, 2007: Summary for Policymakers. In: Climate Change 2007: The Physical Science Basis. Contribution of Working Group I to the Fourth Assessment Report of the Intergovernmental Panel on Climate Change [Solomon, S., D. Qin, M. Manning, Z. Chen, M. Marquis, K.B. Averyt, M.Tignor and H.L. Miller (eds.)]. Cambridge University Press, Cambridge, United Kingdom and New York, NY, USA.

Kearney, M.S., 2001. Late Holocene Sea Level Variation. In: *Sea Level Rise: History and Consequences*, Douglas B.C., Kearney M.S., Leatherman S.P. (eds). Academic Press: San Diego, CA; 13–36.

Miller, L., and B.C. Douglas, 2007. Gyre-scale atmospheric pressure variations and their relation to 19th and 20th century sea level rise. *Geophys. Res. Lett., 34*, L16602, doi:10.1029/2007 GL03062.

Mitrovica, J.X., M.E. Tamisiea, and J.L. Davis, 2001. Recent mass balance of polar ice sheets inferred from patterns of global sea-level change. *Nature*, 409: 1026-1029.

Peltier, W.R., 1996. Global sea level rise and glacial isostatic adjustment: An analysis of data from the east coast of North America. *Geophys. Res. Lett.*, 23: 717-720.

Peltier, W.R., 2001. Global Glacial Isostatic Adjustment and Modern Instrumental Records of Relative Sea Level History. In: *Sea Level Rise: History and Consequences*, Douglas B.C., Kearney M.S., Leatherman S.P. (eds). Academic Press: San Diego, CA; 65–95.

Poag, C.W., Powars, D.S., Poppe, L.J., Mixon, R.B., Edwards, L.E., Folger, D.W., and Bruce, S., 1992. Deep Sea Drilling Project Site 612 bolide event—new evidence of a late Eocene impact-wave deposit and a possible impact site, U.S. east coast: *Geology*, 20: 771-774.

Powars, D.S., 2000. The effects of the Chesapeake Bay Impact Crater on the geologic framework and the correlation of hydrogeologic units of southeastern Virginia, south of the James River. U.S. Geologic Survey Professional Paper 1622 prepared in cooperation with the Hampton Roads Planning District Commission, 47 p., 2 Appendixes.

Powars, D.S., and Bruce, T.S., 1999. The effects of the Chesapeake Bay impact crater on the geological framework and correlation of hydrogeologic units of the lower York-James Peninsula, Virginia: U.S. Geological Survey Professional Paper 1612, 82 p., 7 pl.

Sella, G.F., S. Stein, T.H. Dixon, M. Craymer, T.S. James, S Mazzotti and R.K. Dokka, 2007. Observation of glacial isostatic adjustment in "stable" North America with GPS. *Geophys. Res. Lett.*, 34: L02306, doi:10.1029/2006GL027081.

Snay, R., M. Cline, W. Dillinger, R. Foote, S. Hilla, W. Kass, J. Ray, J. Rohde, G. Sella, and T. Soler, 2007. Using global positioning system-derived crustal velocities to estimate rates of absolute sea level change from North American tide gauge records. *J. Geophys. Research*, 112: B04409, doi:10.1029/2006JB004606.

Sturges, W. and B.G. Hong, 2001. Decadal Variability of Sea Level. In: *Sea Level Rise: History and Consequences*, Douglas B.C., Kearney M.S., Leatherman S.P. (eds). Academic Press: San Diego, CA; 165–180.

Sweet, W., C. Zervas, and S. Gill, 2009. Elevated east coast sea levels anomaly: July-June 2009. NOAA Tech. Rpt. NOS CO-OPS 051, 28 p., NOAA National Ocean Service, Silver Spring, MD.

Trenberth, K.E., J.M. Caron, D.P. Stepaniak, and S. Worley, 2002. Evolution of El Niño-Southern Oscillation and global atmospheric surface temperatures. *J. Geophys. Research*, 107: D8, 4065, 10.1029/2000JD000298.

von Storch, H., and F.W. Zwiers, 1999: *Statistical Analysis in Climate Research.* Cambridge University Press.

Woodworth, P.L., 1990. A search for accelerations in records of European mean sea level. *Int. J. Climatol*. 10: 129-143.

Woodworth, P.L., N.J. White, S. Jevrejeva, S.J. Holgate, J.A. Church and W.R. Gehrels, 2009. Evidence for the accelerations of sea level on multi-decade and century time scales. *Int. J. Climatol.* 29: 777-789.

Zervas, C., 2001. Sea Level Variations of the United States 1854-1999. NOAA Tech. Rpt. NOS CO-OPS 36, 186p., NOAA National Ocean Service, Silver Spring, MD.

Zervas, C., 2009. Sea Level Variations of the United States 1854-2006. NOAA Tech. Rpt. NOS CO-OPS 053, 78p. plus appendices, NOAA National Ocean Service, Silver Spring, MD.

IX. GLOSSARY OF TERMS

absolute sea level (ASL)
Sea level measured relative to the geographic center of the Earth or to the center of a reference ellipsoid approximating the size and shape of the earth. See eustatic sea level.

astronomic tide
The periodic rise and fall of the water resulting from gravitational interactions between the Sun, Moon, and Earth. Through the use of tidal harmonic constituents with known astronomic frequencies, the astronomic tide can be accurately predicted years in advance for water level stations at which tidal harmonic constants have been determined through harmonic analysis. Predictions made relative to the land require that astronomic tides be referenced to a tidal datum, usually mean sea level (MSL) for the current National Tidal Datum Epoch (NTDE). Predictions are made relative to other defined tidal datums such as mean lower low water (MLLW) by means of an offset from MSL. See tidal datum.

Continuously Operating Reference Station (CORS)
The National Geodetic Survey (NGS), an office of NOAA's National Ocean Service, manages a network of Continuously Operating Reference Stations (CORS) that provide Global Navigation Satellite System (GNSS) data in real time supporting three dimensional positioning, meteorology, space weather, and geophysical applications throughout the United States, its territories, and a few foreign countries. CORS time series data are now being used to develop local estimates of vertical crustal velocity.

decadal variability
A low-frequency change in water level at variable periods longer than about 100 months due to global ocean-atmosphere exchange that results in low-frequency waves (Rossby waves) propagating from east to west across oceans; e.g., the Atlantic Ocean. Decadal variability therefore appears primarily in long-term water level records at stations on the west side of the Atlantic; e.g., the east coast of the United States.

decadal signal extraction (DSE)
Extraction or removal of the low-frequency signal representing decadal variability from a water level record. Extraction by low-pass filtering or other means may be accomplished in coastal regions where decadal variability is pronounced, provided water level records of sufficient length are available.

El Niño, Southern Oscillation (ENSO)
El Niño refers to periods of anomalously warm water which alternate with periods of anomalously cold water (La Niña) in the Equatorial region of the Pacific Ocean. The Southern Oscillation refers to periodic variations in the sea level pressure difference between Darwin, Australia, and the island of Tahiti in the Central Pacific. Both are part of a large scale, ocean-atmosphere interaction involving heat and momentum transfers that have far-reaching effects on global weather.

equatorial tides

Tides occurring semimonthly as a result of the Moon being over the equator at zero declination in its orbit around the earth. At these times there is minimal tendency for a difference to appear in the heights of successive high waters and/or the heights of successive low waters, a difference referred to as a diurnal inequality. See tropic tides.

eustatic sea level

The distribution of absolute sea level worldwide. As shown by satellite altimetry, the distribution is non-uniform across the earth's oceans and seas. Same as global sea level.

extratidal water level

Water level that extends above highest predicted tide or below lowest predicted tide at a location. See highest astronomic tide, lowest astronomic tide.

Geodesy

The branch of geophysical science that deals with the size and shape of the earth.

Global Positioning System (GPS)

A space-based satellite system that provides location and time information to ground-based receivers having line of sight to four or more GPS satellites. It is maintained by the United States government and is freely accessible by anyone with a GPS receiver

Gravity Recovery and Climate Experiment (GRACE)

The GRACE mission with its unique design of twin-satellites flying in formation is expected to lead to an improvement of several orders of magnitude in spaced-based gravity measurements and allow much improved resolution of the broad to finer-scale features of Earth's gravitational field over both land and sea. Among other benefits, GRACE measurements are providing new information about the movement and redistribution of water mass in the world's oceans. See steric sea level.

highest astronomic tide (HAT)

The highest predicted level of the astronomic tide at a location. As a predicted water level, it represents the maximum height of the astronomic tide referred to the tidal datum of mean sea level (MSL) for the current National Tidal Datum Epoch (NTDE).

interannual variability

The near-random change in monthly mean sea level between years.

Light Detection and Ranging (LIDAR)

An optical remote sensing technology that measures properties of scattered light to find range between sensor and a target using laser pulses. A combination of aircraft-based LIDAR and GPS are now used to produce extremely accurate ground elevation maps.

lowest astronomic tide (LAT)

The lowest predicted level of the astronomic tide at a location. As a predicted water level, it represents the minimum height of the astronomic tide referred to the tidal datum of mean sea level (MSL) for the current National Tidal Datum Epoch (NTDE).

monthly mean sea level

The average of the hourly heights measured at a tide station over a calendar month.

National Tidal Datum Epoch (NTDE)

The specific l9-year period adopted by the National Ocean Service as the official time segment over which tide observations are taken and reduced to obtain mean values (e.g., mean lower low water, etc.) for tidal datums. The present National Tidal Datum Epoch is 1983 through 2001. It is reviewed annually for possible revision and must be actively considered for revision every 25 years. In regions undergoing exception rates of subsidence, revision is considered every 5 years.

National Water Level Observation Network (NWLON)

The network of tide and water level stations operated by the National Ocean Service along the marine and Great Lakes coasts and islands of the United States. The network is composed of the primary and secondary control tide stations of the National Ocean Service. Distributed along the coasts of the United States, this network provides the basic tidal datums for coastal and marine boundaries and for chart datum of the United States.

relative sea level (RSL)

Sea level measured relative to the land or, more specifically, to a set of tidal bench marks installed in the solid earth or a permanent structure next to a tide station. A primary bench mark at the station is designated as the permanent reference to which all subsequent water level measurements and tidal datums are referred. The stability of the reference is maintained and verified over time through mark preservation and periodic leveling between marks.

satellite altimetry

Satellite altimeter radar measurements combined with precisely known spacecraft orbits measure sea level on a global basis with unprecedented accuracy. A series of satellite missions that started with TOPEX/Poseidon (T/P) in 1992 and continued with Jason-1 (2001) and Jason-2 (2008) estimate global mean sea level every 10 days with an uncertainty of 3–4 mm. This climate record has continued with Jason-2 beginning in mid-2008 as a joint effort between NOAA, the National Aeronautics and Space Administration, France's Centre National d'Etudes Spatiales (CNES) and the European Organisation for the Exploitation of Meteorological Satellites (EUMETSAT).

seasonal cycle

As used by NOAA/NOS, tidal constituents Sa and Ssa together furnish predictions of the seasonal variation in water level usually derived as an average cycle at NWLON stations based on monthly mean sea level computations over many years. However, in any given year, the monthly mean sea level actually observed during a given calendar month may show considerable departure from the predicted seasonal value. This is an indication of the presence of additional water level components varying at lower than seasonal frequencies. See sea level anomaly.

sea level anomaly
A measure of low-frequency water level variation occurring on a time scale of months and years in response to global ocean-atmosphere exchange. The anomaly can be obtained as the difference between short-term mean sea level (e.g., monthly mean sea level) and epochal mean sea level (MSL for the current NTDE). The sea level anomaly accounts for differences between observed and predicted water level noticeable at times when subtidal variations and/or storm surge are minimal or absent. It consists of both interannual and decadal variability in sea level together with the relative sea level trend at a location. See interannual variability, relative sea level, storm tide, subtidal variability.

sea level trend
The rate of change in absolute or relative sea level with time. A relative sea level trend is usually derived as a linear trend by least squares fitting of a straight line to a time series of monthly mean sea level observations at a tide station. An absolute sea level trend may be obtained locally as the sum of the relative trend and the crustal velocity, if known, at or near a tide station. A positive trend indicates rising sea level and a negative trend indicates falling sea level. Positive crustal velocity indicates land emergence and negative crustal velocity indicates land subsidence.

steric sea level
Sea level determined by the density (mass per unit volume) of the ocean water column. Density change due to variations in water temperature and salinity cause water columns to rise (higher temperature, lower salinity) or fall (lower temperature, higher salinity). The Gravity Recovery and Climate Experiment (GRACE) was designed to detect the movement and redistribution of water mass by measuring time variable gravity.

storm surge
A transient, mostly aperiodic change in water level forced by surface wind stress and atmospheric pressure change during a storm of a certain intensity whose duration is typically measured in hours. In practice, storm surge can be difficult to distinguish from the subtidal variability which also occurs in response to meteorological forcing from locally recurring weather systems on a time scale of days.

storm tide
The combination of storm surge and astronomic tide. These components may be further augmented by the subtidal variation and the sea level anomaly, all of which can occur in an apparent random combination of amplitude and phase. A combination by chance of one or more components of similar phase can result in an unusually large storm tide. See sea level anomaly, subtidal variation.

subsidence
The vertical movement of the earth's crust in the downward (negative) direction, as opposed to emergence, the vertical movement of the earth's crust in the upward (positive) direction. Both

movements occur as the earth adjusts to tectonic forces regionally and to surface load adjustments more globally, the latter due to ice sheet removal in recent geologic time, a process known as glacial isostatic adjustment (GIA). Global and regional subsidence may be distinguished from local subsidence that includes *settlement* due to compaction of subsurface sedimentary layers aided by ground water and/or hydrocarbon removal, *sinkholes* at the earth's surface caused by karst processes, and geologic faults resulting from local crustal adjustments including adjustments associated with *filled structures* (e.g., the Chesapeake Bay Impact Crater).

subtidal variation

A quasi-periodic change in water level produced by recurring coastal weather systems. Subtidal variations and storm surge typically occur superposed in a single water level time series, the former appearing as irregular oscillations with periods measured in days, the latter appearing as a transient event of characteristically greater amplitude whose duration is measured in hours.

tidal constants

Tidal harmonic values that remain practically constant for any particular locality. Tidal constants consist of the amplitudes and epochs (phase) of the harmonic constituents and are derived from harmonic analysis of water level time series.

tidal datum

A vertical reference for water levels in tidal waterways. In the United States, tidal datums are derived by averaging recorded water levels at tide stations over the 19-year period of the National Tidal Datum Epoch, currently the years 1983 through 2001. The principal tidal datums include mean sea level (MSL) derived as the average of recorded hourly heights, mean higher high water (MHHW) derived as the average of the higher high waters recorded during each tidal day, and mean lower low water (MLLW) derived as the average of the lower low waters recorded during each tidal day. Other datums include mean high water (MHW) computed as the average of both high waters and mean low water (MLW) computed as the average of both low waters during each tidal day. See National Tidal Datum Epoch, tidal day.

tidal day

The time of the rotation of the earth with respect to the moon, approximately 24 hours and 50 minutes. Same as lunar day.

tidal harmonic analysis

A mathematical procedure used to analyze time series observations of water level, or water current, to extract the harmonic constants for tidal constituents representing the astronomic tide, or tidal current, at a particular location. Each tidal harmonic constituent accounts for the variance present at a known astronomic frequency due to a specific celestial motion. See astronomic tide.

tropic tides

Tides occurring semimonthly when the effect of the Moon's maximum declination is greatest. At these times there is a tendency for a difference to appear in the heights of successive high waters and/or the heights of successive low waters. The difference, when it occurs, is referred to as a diurnal inequality. See equatorial tides.

X. REVIEWER COMMENTS AND AUTHORS RESPONSE

Comments received and the authors response are included in the pages that follow.

MARYLAND
DEPARTMENT OF
NATURAL RESOURCES

Martin O'Malley, Governor
Anthony G. Brown, Lt. Governor
John R. Griffin, Secretary
Joseph P. Gill, Deputy Secretary

1 November, 2010

To Whom It May Concern:

Re: CHESAPEAKE BAY LAND SUBSIDENCE AND SEA LEVEL CHANGE:
AN EVALUATION OF PAST AND PRESENT TRENDS AND FUTURE OUTLOOK
By John Boon, John Brubaker and David Forrest

I have reviewed the subject document identified above and find it to be a comprehensive and well thought out assessment of sea level change in the Chesapeake Bay region based on the available evidence. Of particular value is the identification of serial correlations within the tide gage records and the removal of the decadal period signals from these records to obtain consistent relative sea level rise trends. The examination of local subsidence and the thorough discussion of the recent advances in direct measurements via GPS satellites is a significant addition to the discussion of sea level trends in the region. Overall I find the report to be thorough and with credible conclusions.

By way of background, I have been employed at the Maryland Geological Survey for 35 years with most of my work efforts centered on shore erosion and sediment transport and deposition in the Chesapeake Bay. I have chaired the Chesapeake Bay Program, Sediment Workgroup since 2003 providing important information on sediment issues in the Chesapeake for achieving the Bay Program's restoration goals. Since 2007, I have acted as Director of the Maryland Geological Survey and was appointed State Geologist in 2010.

Sincerely,

Jeffrey Halka, Director
Maryland Geological Survey

Maryland Geological Survey • 2300 St. Paul Street • Baltimore, Maryland 21218 • (410) 554-5500
www.mgs.md.gov • www.dnr.maryland.gov •

Review of

CHESAPEAKE BAY LAND SUBSIDENCE AND SEA LEVEL CHANGE:
AN EVALUATION OF PAST AND PRESENT TRENDS AND FUTURE OUTLOOK

John D. Boon
John M. Brubaker
David R. Forrest

By Chris Zervas and William Sweet
NOAA/National Ocean Service/CO-OPS

This comprehensive report is a regionally-focused analysis of the long-term sea level measurements from Chesapeake Bay. A common time span for ten bay stations is evaluated to compare spatial differences in relative sea level (RSL) rates with approximately the same degree of confidence at each station. After extracting the decadal variation, linear regression is used to obtain new RSL rise rates with smaller confidence intervals. Comparison of two, 32-yr period trends suggests that, while RSL continues to rise at some of the highest rates found along the U.S. Atlantic coast, there is presently no evidence of a statistically significant increase indicating an acceleration at any of the five stations with the longest records. Removing an absolute sea level rise of 1.8 mm/yr uniformly throughout the bay, subsidence rates of roughly the same magnitude are found. It is concluded that approximately 50% of the RSL rise measured at the bay stations is due to local subsidence.

We generally agree with the results of these analyses and the authors' conclusions. There is an issue needing some clarification or additional consideration. In the attempt to reduce the trend confidence interval for the stations with relatively short periods, the decadal signal extraction (DSE) method is used. The problem is that each station's correction for decadal variability is inherently dependent upon its calculated trend whether it comes from a less accurate short-term or a more accurate long-term series. For instance, when the same 32-yr data set is used to compute the trends at Sewells Point and CBBT, the initially calculated trends are quite close. However, after the DSE method is applied, the rate at Sewells Point adjusts much closer to its long-term value, while the rate at CBBT remains nearly the same. We would recommend calculating the decadal correction from a multi-station mean or from a selected station with the longest record.

Authors Response

We greatly appreciate the comments received above and the kindness of their authors in allowing us to include them in this report. Our response is given below.

Jeffrey Halka - We are grateful for the endorsement of Dr. Halka.

Chris Zervas and William Sweet – The comments from Drs. Zervas and Sweet are also much appreciated. As they have drawn attention to an issue central to our methodology, we are responding directly to three of their comments (in quotes) as follows:

"… each station's correction for decadal variability is inherently dependent upon its calculated trend whether it comes from a less accurate short-term or a more accurate long-term series. "

Response – Removal of a periodic component, the seasonal cycle, is routinely done by CO-OPS personnel prior to sea level trend analysis with the implicit assumption that a linear trend neither influences that component nor is influenced by it in turn. Least squares harmonic analysis of monthly mean sea level time series indeed requires removal of the trend prior to the analysis that yields the seasonal cycle. This has been the practice whether or not the seasonal cycle consists of a whole number of cycles and regardless of the fact that a partial cycle will impart some trend to the seasonal cycle obtained, however minor. Thus, we use a whole number of years to extract the seasonal cycle. This yields the mmsl series we show in gray color in Fig. 9, for example. From this series we again remove the trend with the data put in deviate form by removing the series mean and only then do we use a linear filter to extract the decadal signal which is quasi-periodic and not obtainable by least squares methods that we are aware of. To be clear about our methods, the last paragraph on page A-3 of Appendix A has been modified.

"… after the DSE method is applied, the rate at Sewells Point adjusts much closer to its long-term value, while the rate at CBBT remains nearly the same."

Response – We would argue that leaving the decadal signal in a short series prior to trend analysis introduces far more trend uncertainty than removing it. We would not put much weight on a comparison made against a short series of 32 years that still contains the decadal signal. Our paired graphics presented in Appendix B are meant to demonstrate that point.

"We would recommend calculating the decadal correction from a multi-station mean or from a selected station with the longest record."

Response – We compared decadal signals for the 1976-2007 period obtained at Baltimore (BALT), Sewells Point (SWPT), and the Chesapeake Bay Bridge Tunnel (CBBT). The first two stations have the longest records in Chesapeake Bay, CBBT the shortest. As shown in the two graphs on the next page, decadal amplitudes differ between stations although the signal phase is nearly identical. Following these plots are two additional mmsl plots suggesting that the amplitude patterns are unique to each location. For example, if the SWPT decadal signal is used to replace the decadal signal at CBBT, significant quadratic model regression appears at CBBT even though the addition of the quadratic term itself is not significant.

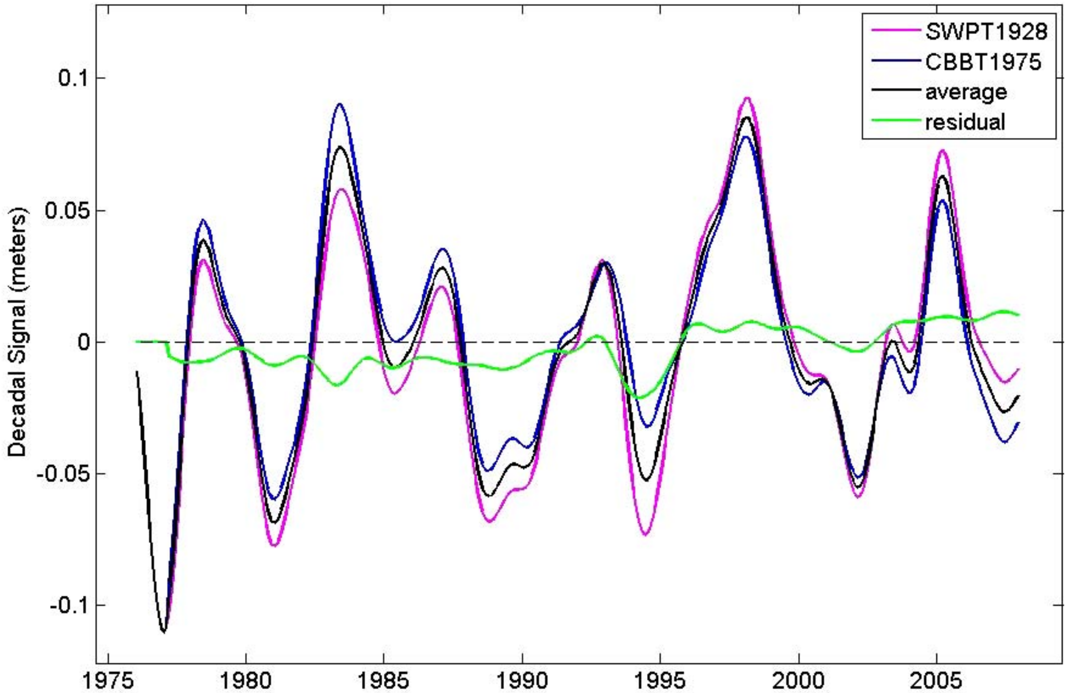

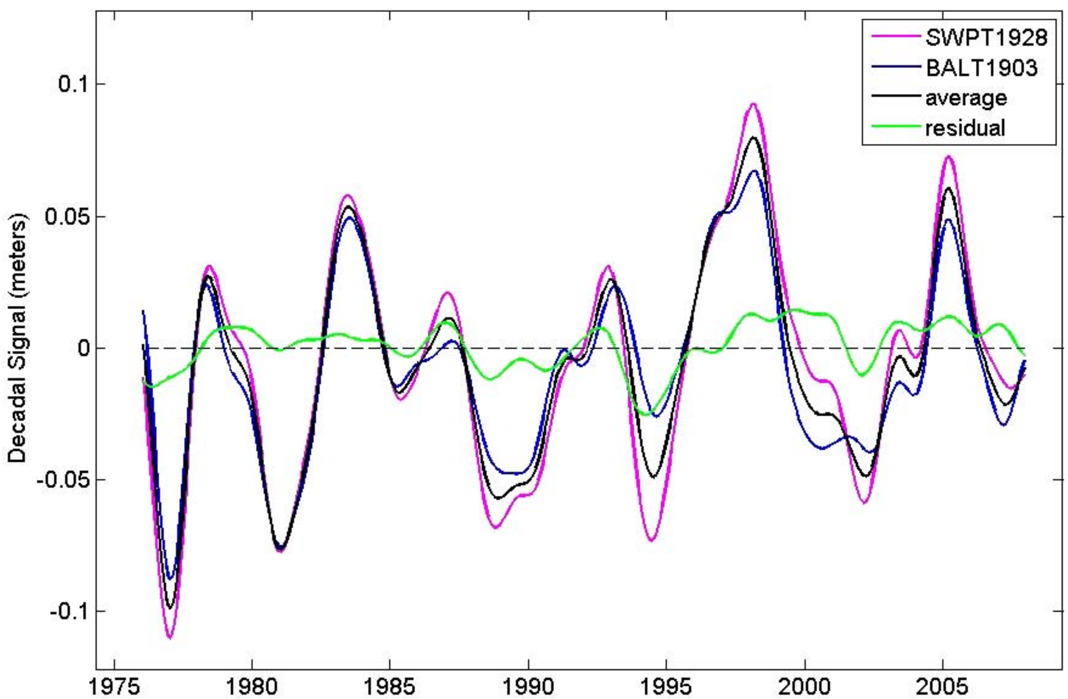

Fig. R1. Decadal signal overlays for stations SWPT and CBBT (upper), SWPT and BALT (lower). The mean of each signal pair is shown by a black line between the blue and magenta lines. The residual difference between stations is shown by the green curve. Note that the vertical range of the decadal signal at SWPT is nearly 20 cm or approximately the same vertical range as the seasonal cycle at this station (see Fig. 2a).

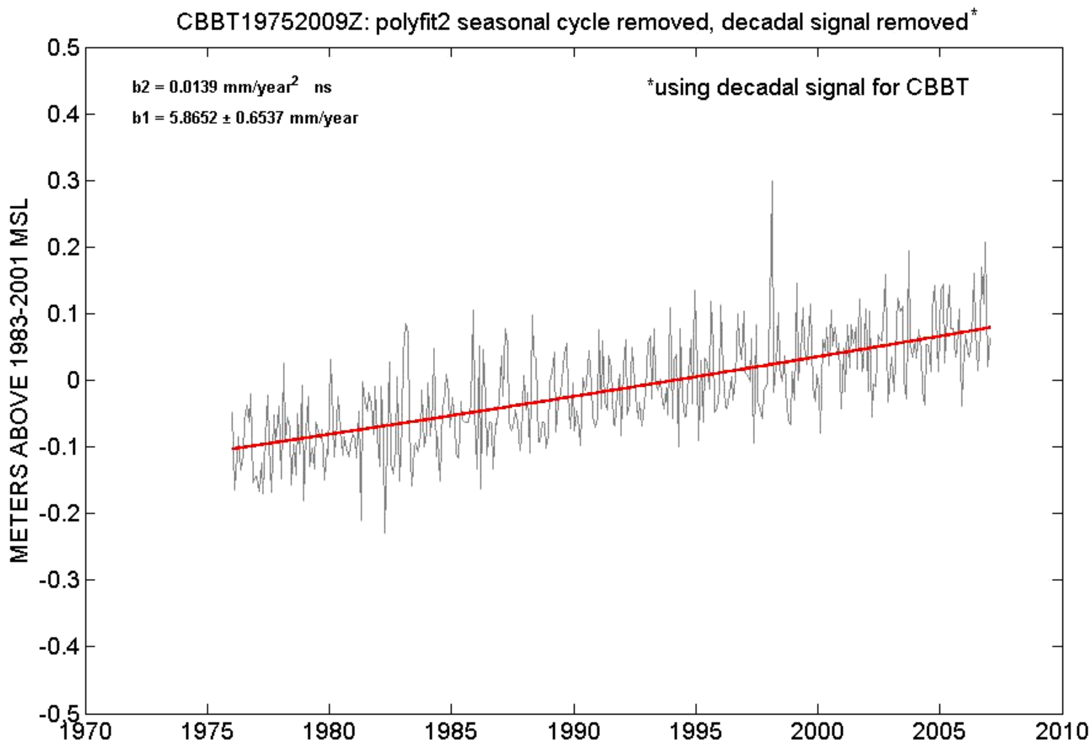

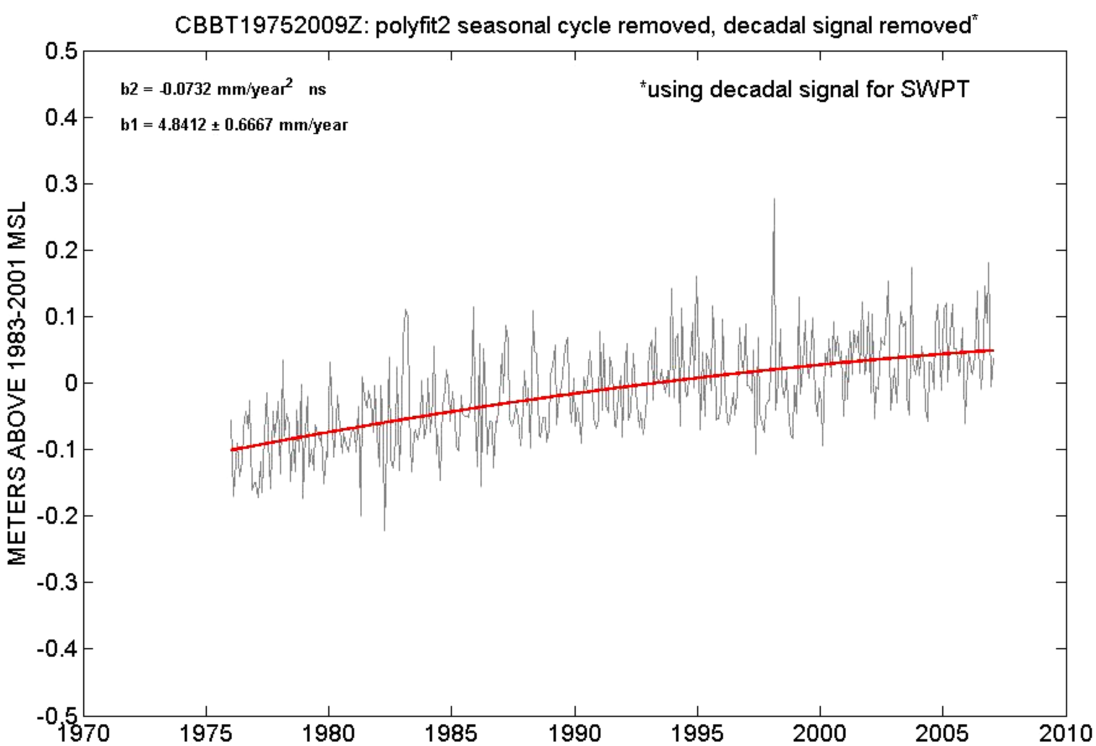

Fig. R2. Quadratic fit to mmsl series at station CBBT with CBBT decadal signal removed (upper) and quadratic fit to same station with decadal signal from nearby SWPT station removed (lower). The F value for the quadratic term in the lower plot is 3.03 compared to the critical value of 3.84.

APPENDIX A

DECADAL SIGNAL EXTRACTION BY LOW-PASS FILTERING

DECADAL SIGNAL EXTRACTION BY LOW-PASS FILTERING

I-A. GENERAL LINEAR FILTER

A general linear filter of the symmetric type consists of a set of 2*ns*+1 weights

$$\{g_{-ns}, g_{-ns+1}, \cdots, g_0, \cdots, g_{ns-1}, g_{ns}\}$$

that, when applied to an *input* time series y_t, of length N (t = 1,N), yields a filtered *output* series of length N-2*ns*

$$z_t = \sum_{u=-ns}^{ns} g_u y_{t+u} \qquad (1)$$

Note that when the filter is symmetric, $g_{-u} = g_u$. For example, a simple three-point moving average at time t would be computed as

$$\begin{aligned} z_t &= g_{-1}y_{t-1} + g_0 y_t + g_1 y_{t+1} \\ &= \tfrac{1}{3}y_{t-1} + \tfrac{1}{3}y_t + \tfrac{1}{3}y_{t+1} \end{aligned}$$

Filters based on Eq. (1) whose weights are *not* all equal but sum to one offer certain advantages in determining a filter's output through their ability to shape its *transfer function*. Associated with each symmetrical general linear filter is a transfer function or *frequency response function* for frequencies $0 < f < sr/2$ where $sr =$ sampling rate (1 sample per month for mmsl data with f in cycles per month). The equation for the transfer function,

$$G(\omega) = g_0 + 2\sum_{u>0} g_u \cos(\omega \cdot u) \qquad (2)$$

offers the key to what a given filter actually does when applied to input data. A value of *one* for G(ω) in Eq. (2) indicates a full response (the signal amplitude at frequency ω is passed) whereas a value of *zero* means no response (the signal amplitude at frequency ω is eliminated).

II-A. LEAST SQUARES DESIGN OF AN OPTIMUM FILTER

A number of methods are available for designing filters. An ideal filter is one that transitions from no response to full response at a single "cutoff" frequency. In reality, the transition occurs over a range of frequencies: the *transition band*. The width of this band depends on the filter width, *ns*. A procedure developed by Bloomfield (2000) obtains the closest approximation of the ideal filter in the least squares sense after the user has specified a cutoff period, Tc (inverse of cutoff frequency) and filter width, *ns*.

Filter Criteria - Based on the general assessment of Hong et al. (2000) that decadal variability on the U.S. east coast occurs at periods longer than 100 months (frequency of 0.01 cpm) a number of filter designs were explored. The optimum sought was a filter producing full response for $f \leq 0.01$ cpm and minimal response for $f \geq 0.05$ cpm. This criterion was approximately met by a filter with cutoff at Tc = 24 months and width *ns* = 24 months. Preference for working with mmsl in whole-year increments dictated an alternative of *ns* = 36 months, placing the filtered series upper limit at the end of 2006 at which point the data loss for trend determination is judged to be excessive. The response curve for the filter selected is shown in Fig. A-1 and a graph of the filter weights is presented in Fig. A-2.

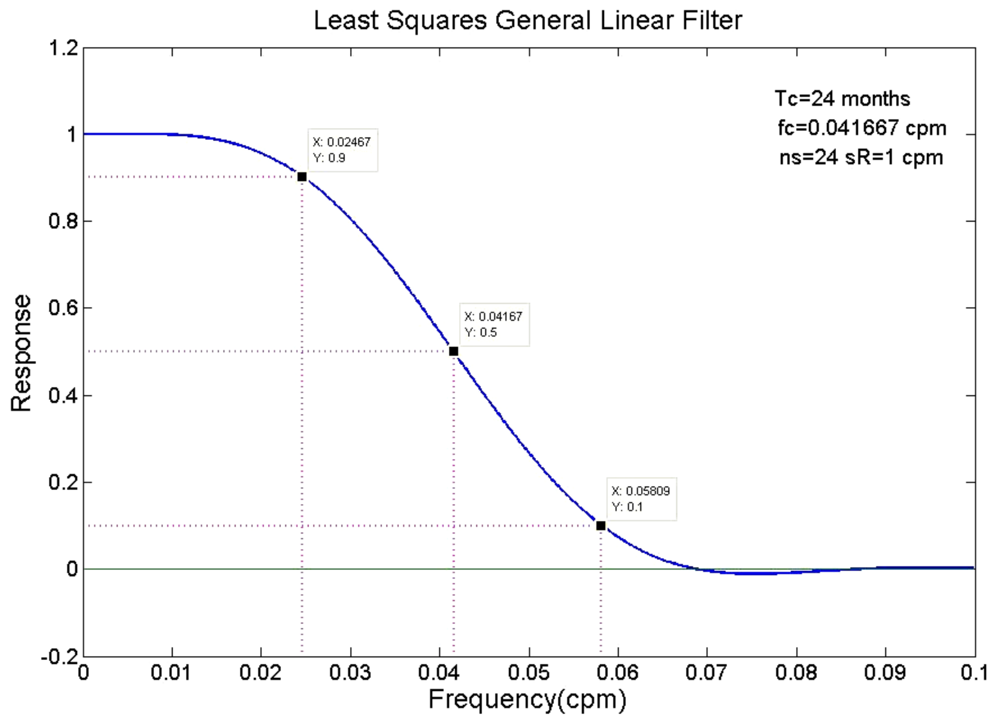

Figure A-1. Frequency response function for filter with Tc=24 months, width *ns*=24 months. Note response is 1.0 at $f \leq 0.01$ and 0.1 at $f = 0.0581$ cpm.

Filter Application – The 24-month filter described above is used with mmsl time series that have had the seasonal cycle removed following least squares harmonic analysis to determine the amplitude and phase of the seasonal constituents, Sa and Ssa (Boon, 2007). Note that these constituents have fixed frequencies of 0.08333 cpm and 0.1666 cpm, respectively, and they have been determined in each case using the maximum available record length through 2009 at the ten NWLON stations shown in Fig. 3 of the main report. After removal of the seasonal cycle, the series is de-meaned and de-trended before applying the filter.

Filtering is done *in place* using the algorithm given below. An output series results that is equal in length to the input series but starting *ns* months *later* than the input series. The decadal signal is then derived using all but the last 2*ns months in the output series and stored for later use.

```
for i=1:N-2*ns
    temp=g(1)*y(i+ns);
      for j=1:ns
          temp=temp+(y(i+ns+j)+y(i+ns-j))*g(j+1)
      end
    y(i)=temp;
end
```

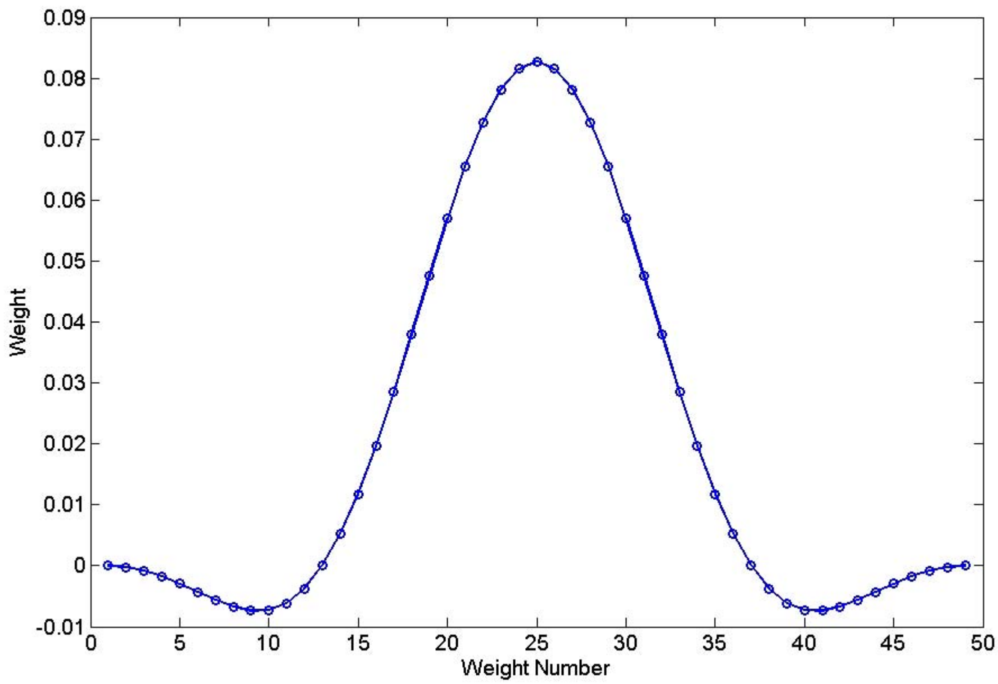

Figure A-2. Filter weights g_u for filter with Tc=24 months, *ns*=24 months. Numeric values for the filter weights are listed below.

g(25-33)	*g*(34-41)	*g*(42-49)
8.2716782e-002	1.9669051e-002	-6.7544848e-003
8.1551215e-002	1.1810802e-002	-5.6297751e-003
7.8125704e-002	5.2029447e-003	-4.2737178e-003
7.2648072e-002	2.0944326e-018	-2.9102775e-003
6.5446053e-002	-3.7561183e-003	-1.7141981e-003
5.6941176e-002	-6.1281256e-003	-8.0209459e-004
4.7615662e-002	-7.2671373e-003	-2.3044945e-004
3.7975375e-002	-7.3902524e-003	-6.7129868e-020
2.8512185e-002		

II-A. EVALUATION OF FILTER OUTPUT

We are interested in the decadal signal in part because of its association with low-frequency forcing derived from ocean-atmosphere processes. The present study does not seek to identify specific relationships but we have noted a degree of association between major highs in the decadal signal, as we have derived it, and major global events such as El Niño (Fig. A-3). Further evidence that the signal is driven by global-scale processes exists in the peak-to-peak similarity among all ten Chesapeake Bay stations (Fig. 9).

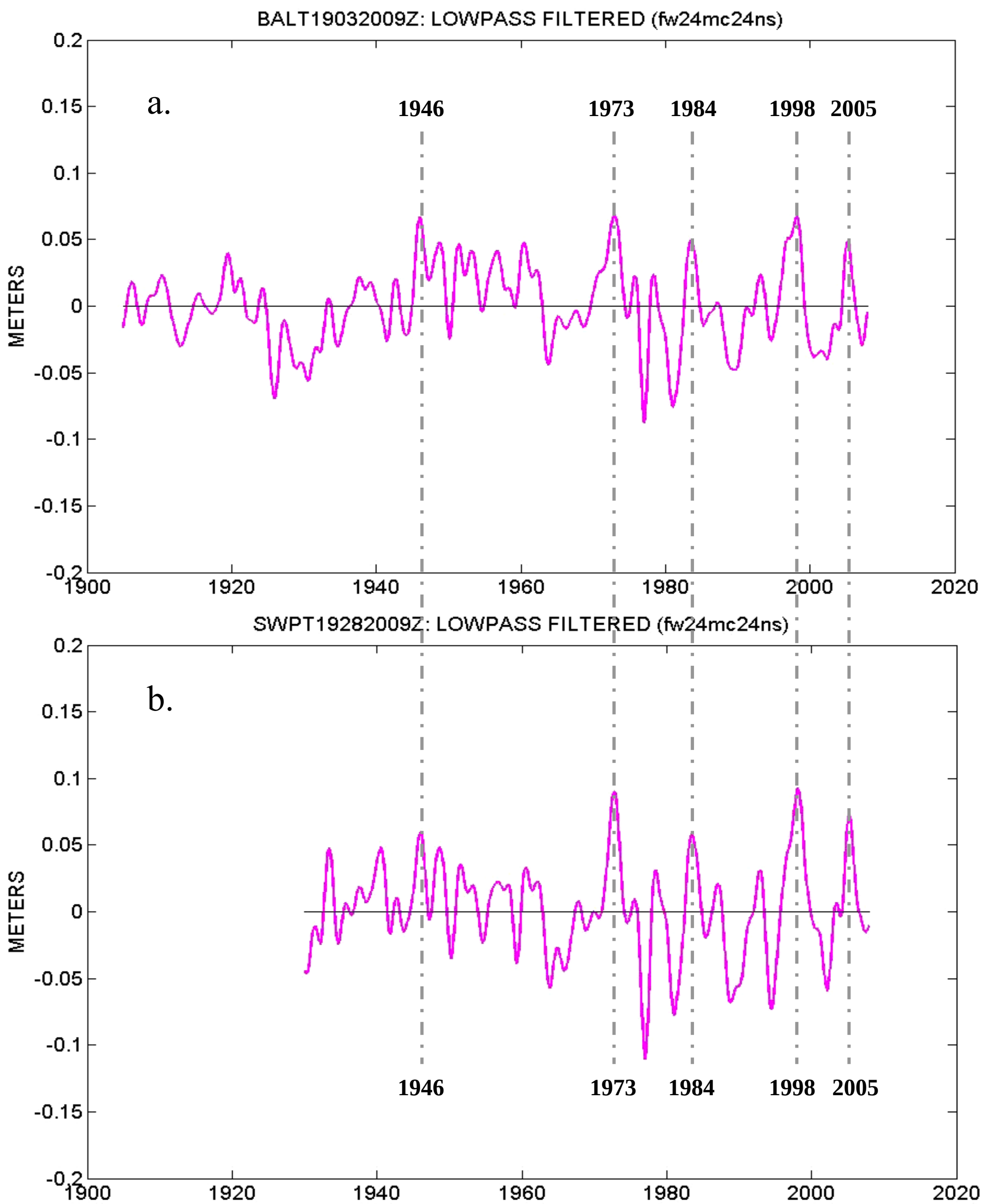

Figure A-3. Decadal signal at a) Baltimore, MD, b) Sewells Point, VA.
Major El Niño events occurred in 1972-73, 1982-83, and 1997-98.

Cross-correlation – The match-up of decadal signal peaks in Fig. A-3 suggests strong correlations at certain times in the decadal signal record. This can be further explored through a cross-correlation analysis using the MATLAB function 'xcorr' with normalization option. This function determines the correlation between two discrete time series at various time lags in one series relative to the other – lags in both directions designated as either positive (lead) or negative (lag). Fig. A-4 (BALT vs. SWPT) illustrates high correlation (0.86) near zero lag and moderate correlation at -156 months (13 yrs) and 155 months (12.9 yrs). Fig. A-5 (SWPT vs. CBBT) shows very high correlation (0.93) at zero lag and moderate correlation at -159 months (13.2 yrs) and 160 months (13.3 yrs).

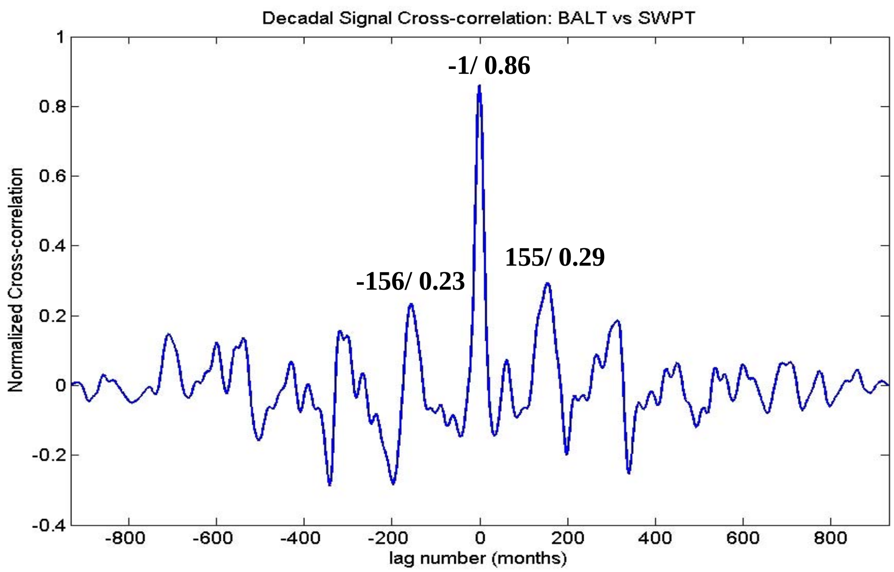

Figure A-4. Cross-correlation between decadal signals at Baltimore, MD, and Sewells Point, VA

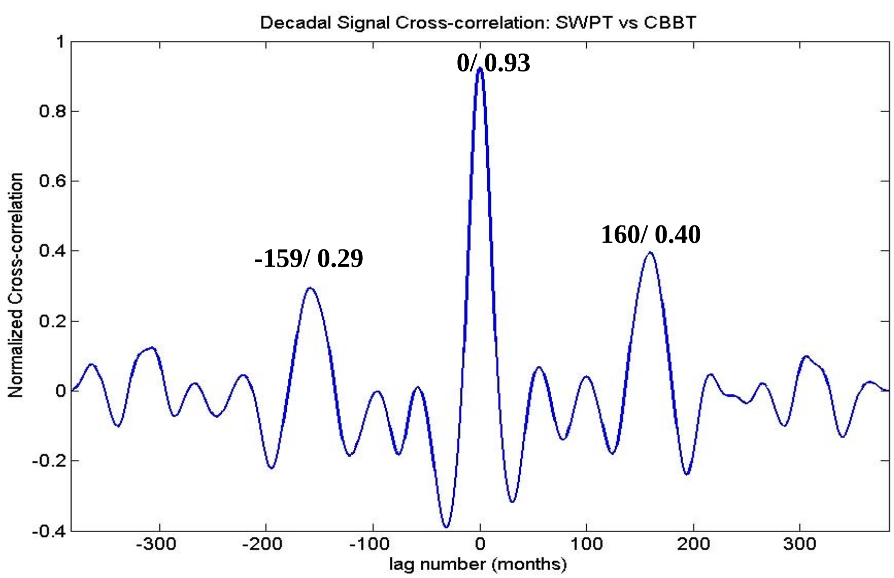

Figure A-5. Cross-correlation between decadal signals at Sewells Point, VA, and the Chesapeake Bay Bridge Tunnel, VA.

Periodograms - Ideally a band-pass filter would be preferable to a low-pass filter in order to extract a signal with periodicity confined to a known range of frequencies. This is not possible when analyzing decadal signals because a second low-pass filter with a very low cutoff frequency would be required to achieve it at the cost of a very large filter width. Using only a single low-pass filter, there is no lower limit to the frequency content that is now part of the decadal signal. The question that arises is whether energy (variance) is present at frequencies so low that only a portion of a cycle is captured and that portion may in fact represent a long-term acceleration or deceleration in sea level trend – information that will be lost if the decadal signal is later removed from the mmsl series (raw series less seasonal cycle). On the other hand, if the frequency content is not exceptionally low, one may argue that the information is an integral part of the decadal variation and not evidence of a separate long-term trend or acceleration in sea level.

To address the above problem, a periodogram displaying energy at the Fourier frequencies may be constructed (Bloomfield, 2000). This has been done for the five NWLON stations that have record lengths of 72 years or more. Two periodograms are presented for each station: the first shows the energy distribution for the unfiltered mmsl series and the second shows the low-pass distribution at frequencies of 0.05 cpm and lower.

It is noticeable in most of the unfiltered series periodograms that the energy levels are fairly flat across the frequency scale until the frequency of 0.05 cpm is reached near the lower end of the scale. The bottom diagram narrows the frequency range and for the low-pass signal we see most of the energy grouped into two bands: 0.01 to 0.02 cpm (~8 years to ~4 years) and 0.001 to 0.01 (~80 years to ~8 years). The peaks seen in the lower of the two bands are coarse estimates due to the restriction in bandwidth (1/T where T = record length in months; i.e., 1/T = 1/(103x12) = 0.0008 cpm). That said, the dominant peak in most instances in the lower band is found at about 0.007 cpm (~12 years); in the upper band the dominant peak occurs around 0.017 cpm (~5 years)

Longer records will yield better estimates of the main frequencies at which energy typically resides in the decadal signal. However, it should be clear at this point that the decadal signal does not simply consist of geophysical "noise" that accumulates at the bottom of the spectrum. There is a fairly high degree of coherence in the signals at Baltimore and Sewells Point at opposite ends of Chesapeake Bay (Fig. A-3) and at the eight stations in between, a result consistent with the expected forcing: ocean-atmosphere exchange on a global scale. In contrast to this, local tidal characteristics such as the tidal range and type of tide (semidiurnal, diurnal, mixed) vary from station to station.

An interesting feature of the decadal variation shown at both stations in Fig. A-3 is the visually apparent shift to lower frequencies and higher amplitudes in the signal oscillations after 1973. It has been reported that a climate shift and a different ENSO evolution began in 1976 (Trenberth et al., 2002).

Baltimore, MD (BALT):

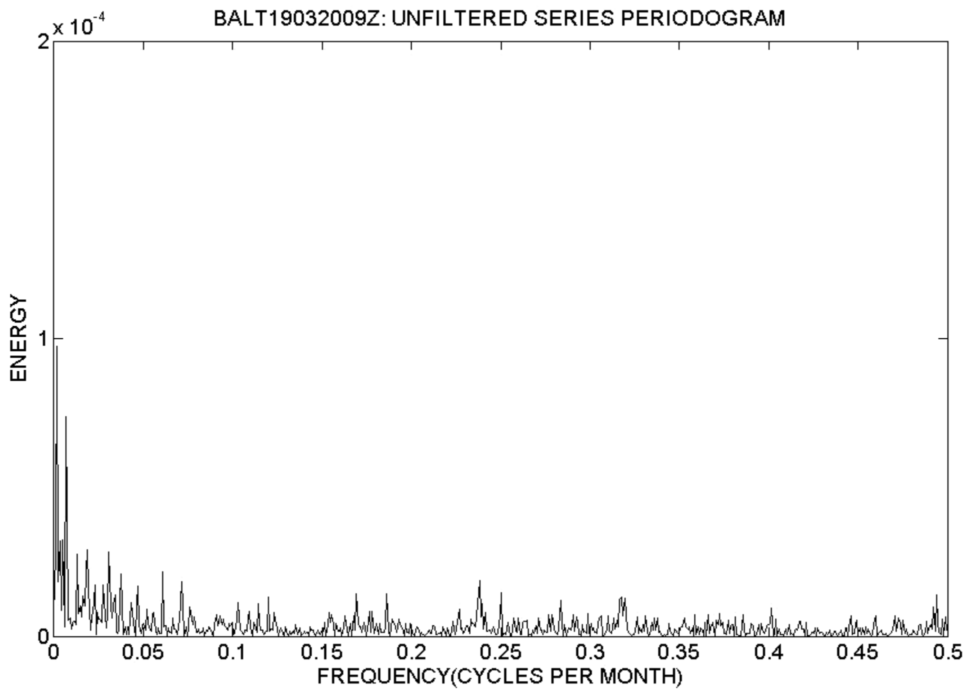

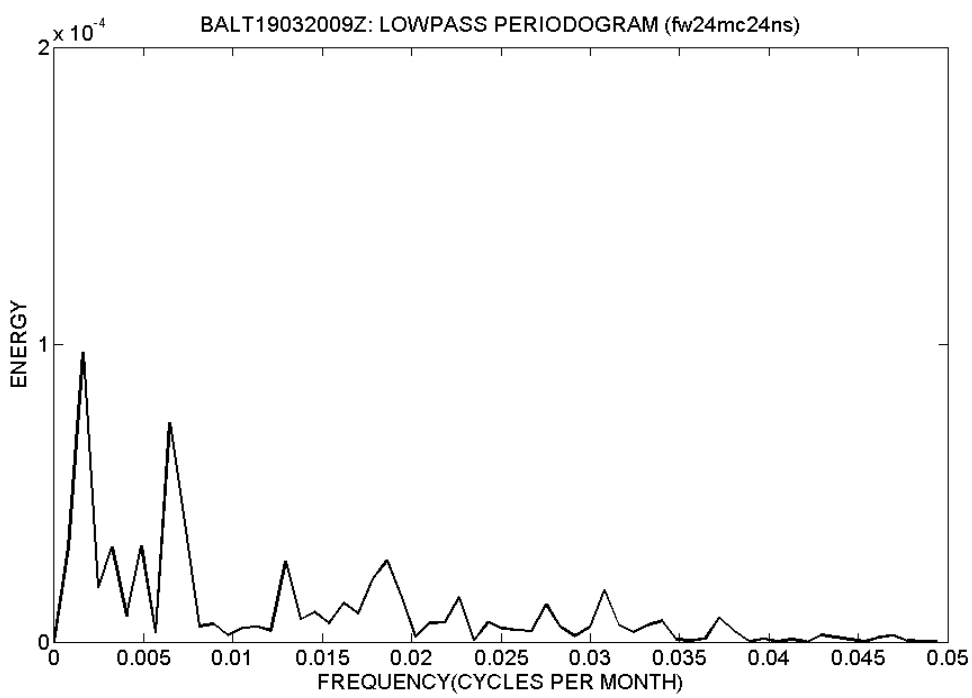

Annapolis, MD (ANNA):

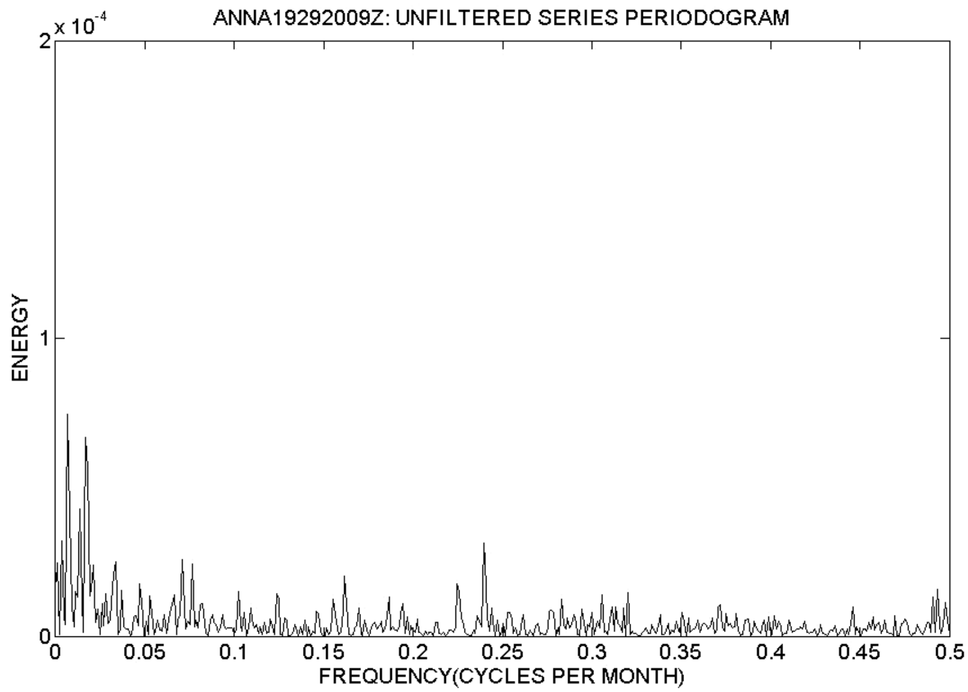

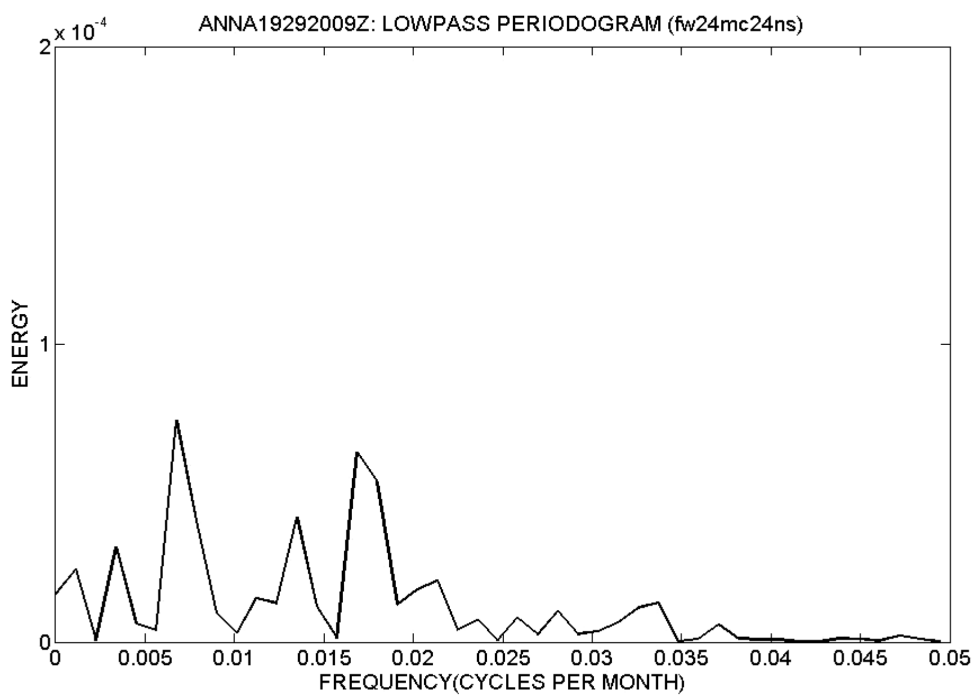

Washington, DC (WASH):

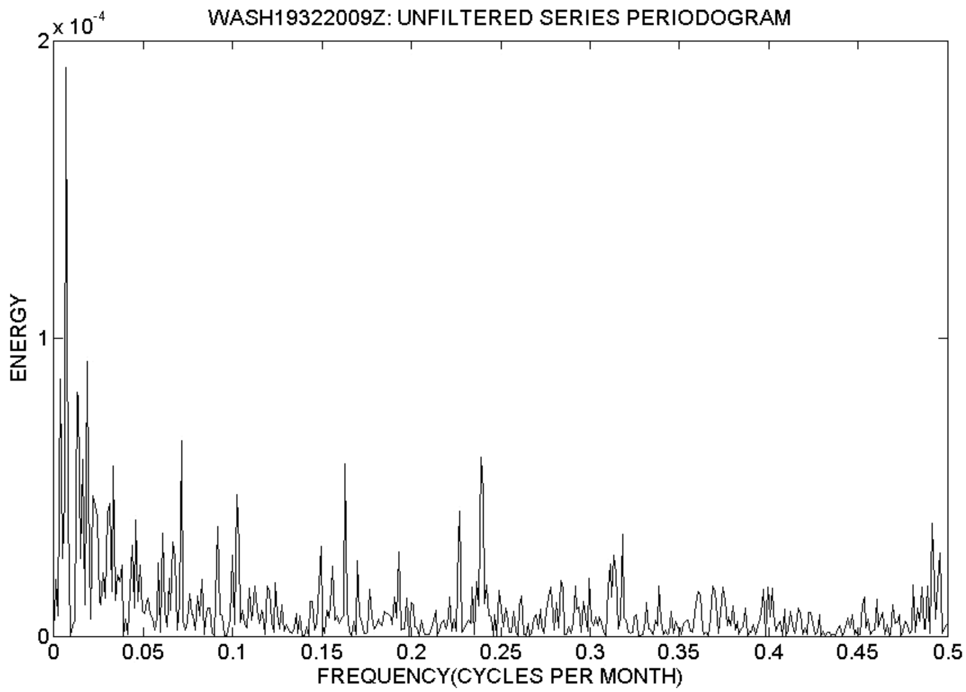

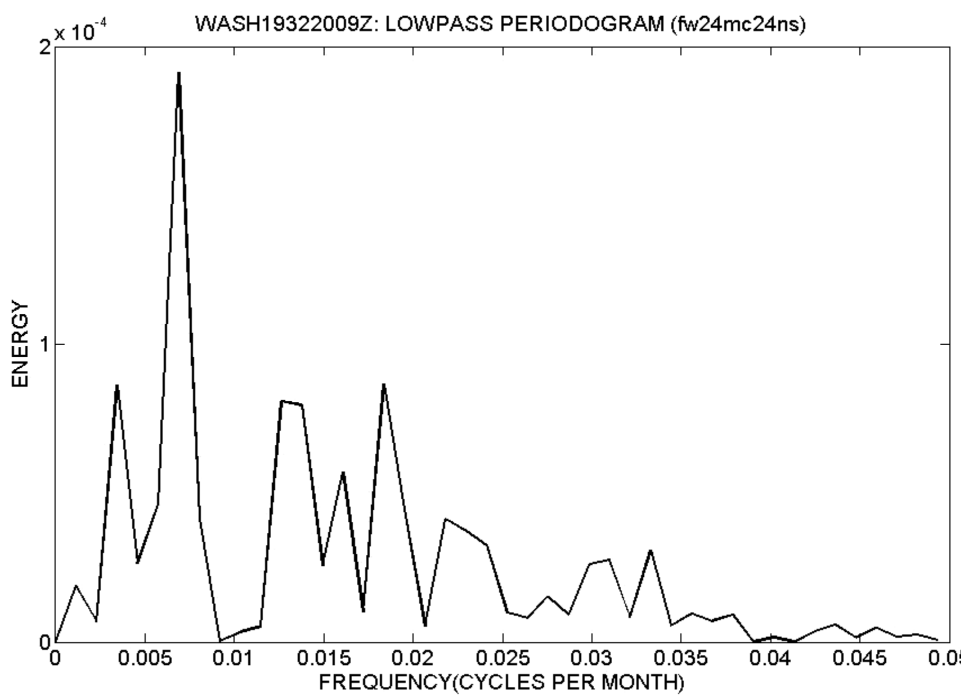

Solomon's Island, MD (SOLI):

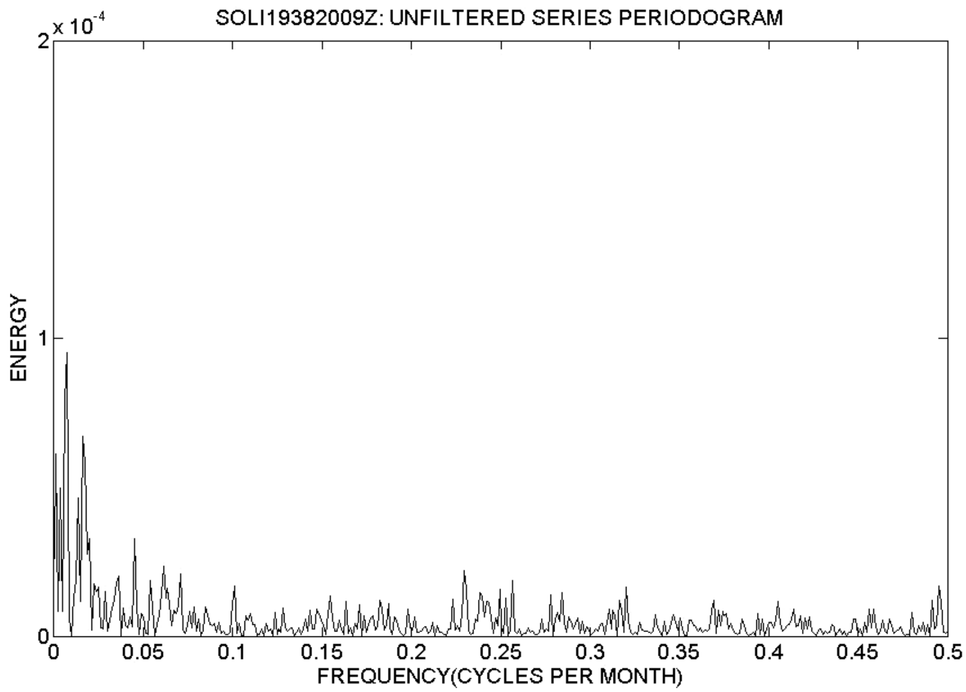

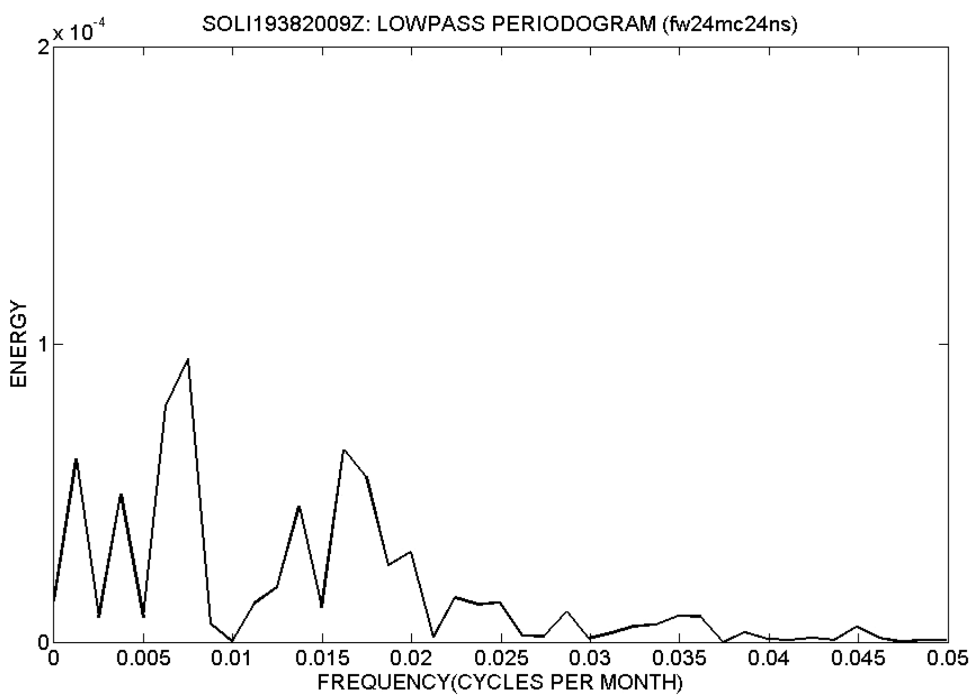

Sewells Point, VA (SWPT)

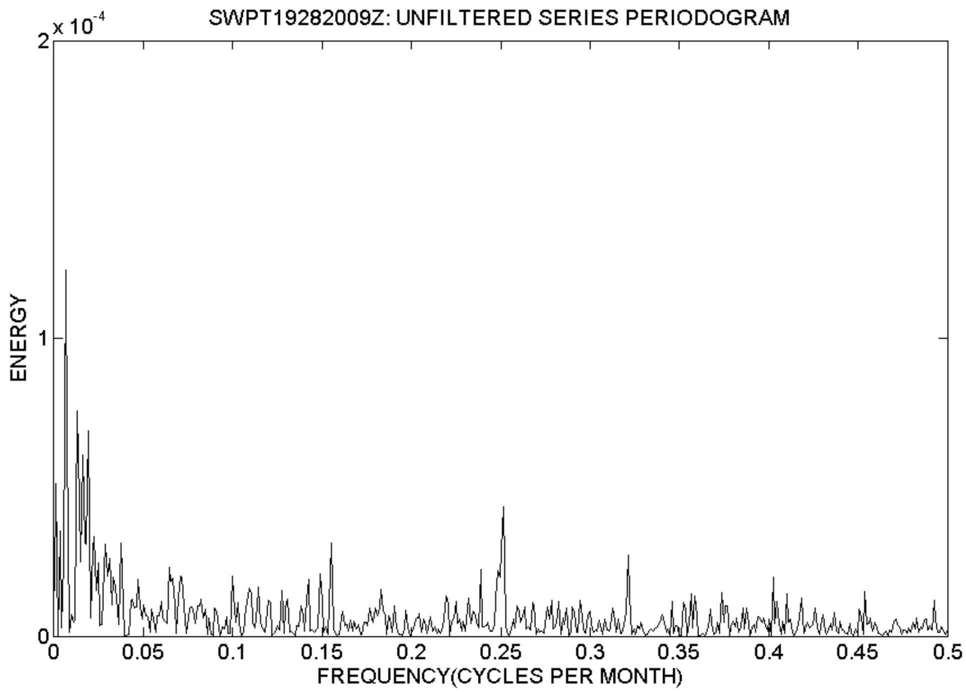

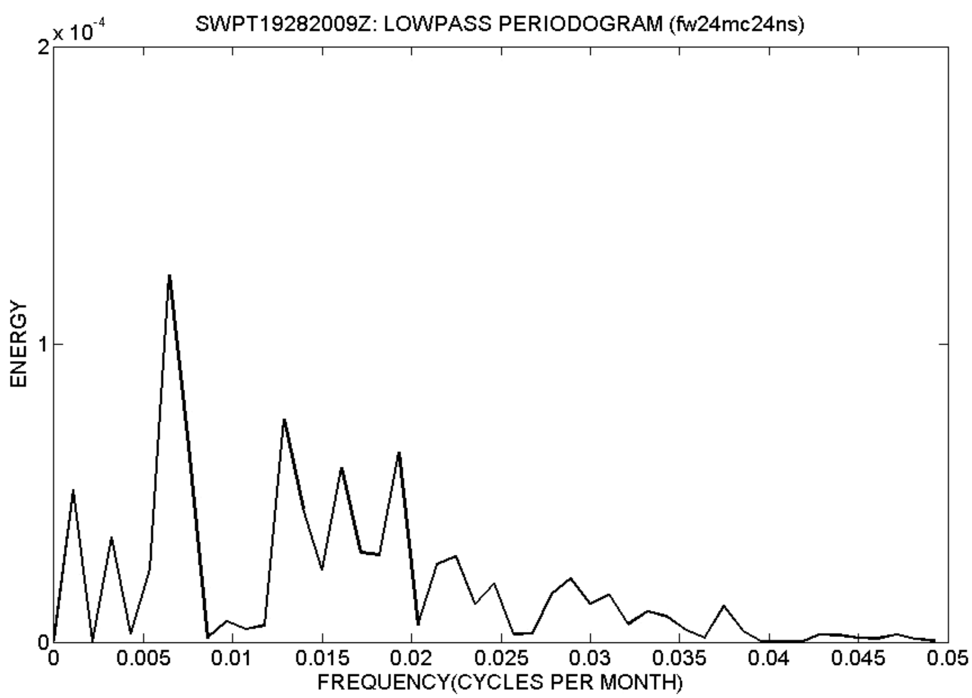

APPENDIX B

DECADAL SIGNAL AND RELATIVE SEA LEVEL TRENDS AT CHESAPEAKE BAY NWLON STATIONS

DECADAL SIGNAL AND RELATIVE SEA LEVEL TRENDS AT CHESAPEAKE BAY NWLON STATIONS

The decadal signal is extracted from each mmsl time series after removal of the seasonal cycle using the methods described in Appendix A. In this Appendix, graphs are presented that show the de-seasoned mmsl series with and without the decadal signal for the periods 1912-1943, 1944-1975 and 1976-2007 at National Water Level Observation Network (NWLON) stations in Chesapeake Bay that have the required amount of data for each period (http://www.tidesandcurrents.noaa.gov/). The linear trend and 95% confidence interval about the trend, as well as significance test results for serial correlation, are shown on each graph. The following stations identified by their NWLON number are included:

BALT	Baltimore, MD	8574680
ANNA	Annapolis, MD	8575512
WASH	Washington, DC	8594900
CAMB	Cambridge, MD	8571892
SOLI	Solomons Is., MD	8577330
LEWI	Lewisetta, VA	8635750
GLPT	Gloucester Pt., VA	8637624
KIPT	Kiptopeke, VA	8632200
CBBT	Ches.Bay Br.Tunnel	8638863
SWPT	Sewells Pt., VA	8638610

NOTE: NWLON stations at Washington, DC, and Gloucester Point, VA, were damaged during Hurricane Isabel in 2003 resulting in several months data loss. The NWLON station at Gloucester Point was discontinued and re-established approximately 2 nautical miles ESE at Yorktown, VA (8637689). The continuing record at Yorktown has been used to extend GLPT through 2009 by referring water levels at both stations to the tidal datum of mean sea level (MSL) for the 1983-2001 National Tidal Datum Epoch. It is estimated that a datum transfer of this type may involve a systematic error of up to 3 cm.

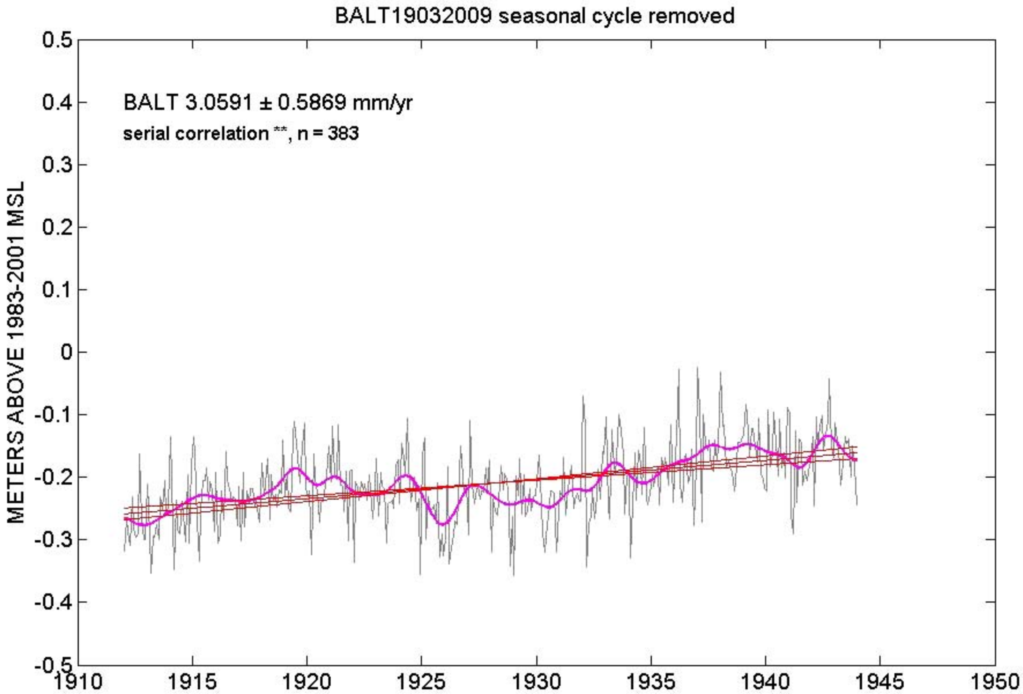

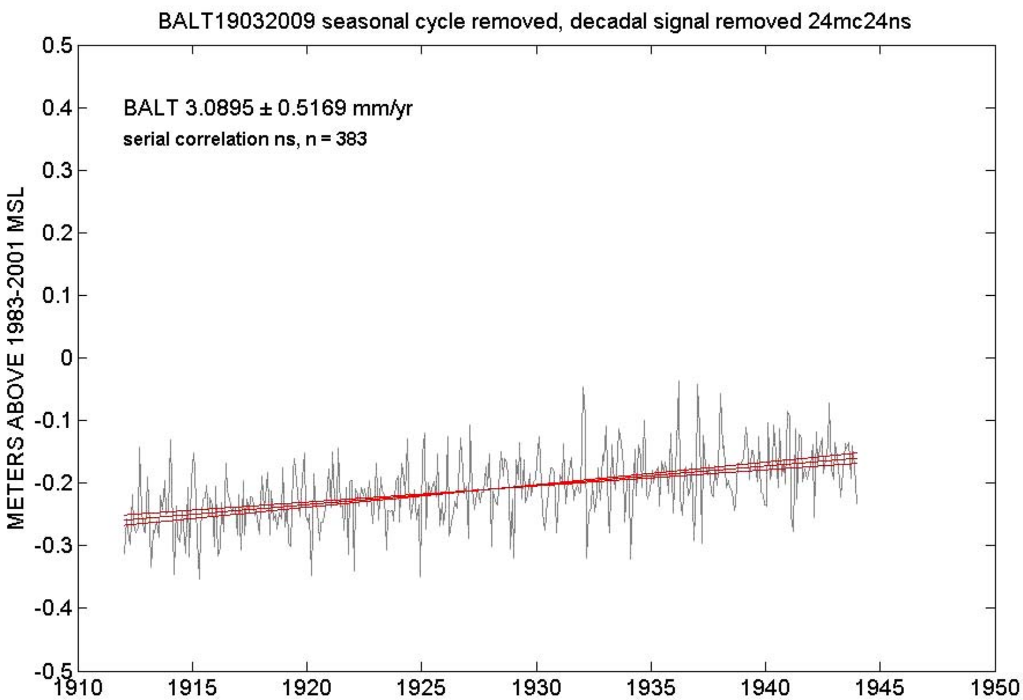

Figure B-1. RSL trends and 95% confidence intervals before (upper) and after (lower) removal of the decadal signal at BALT, 1912-1943 period.

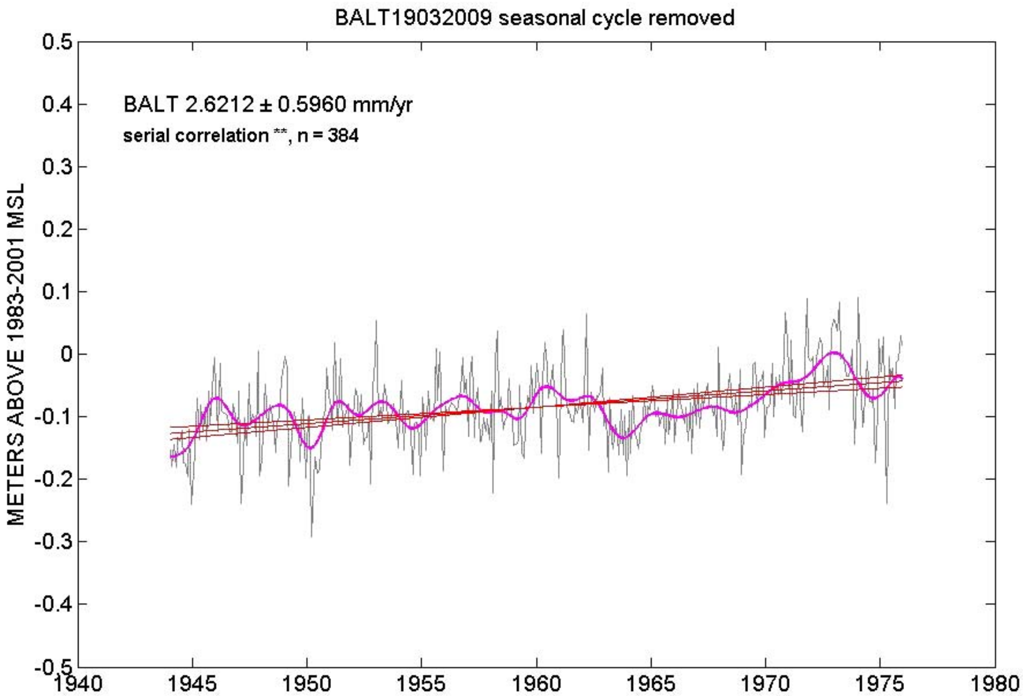

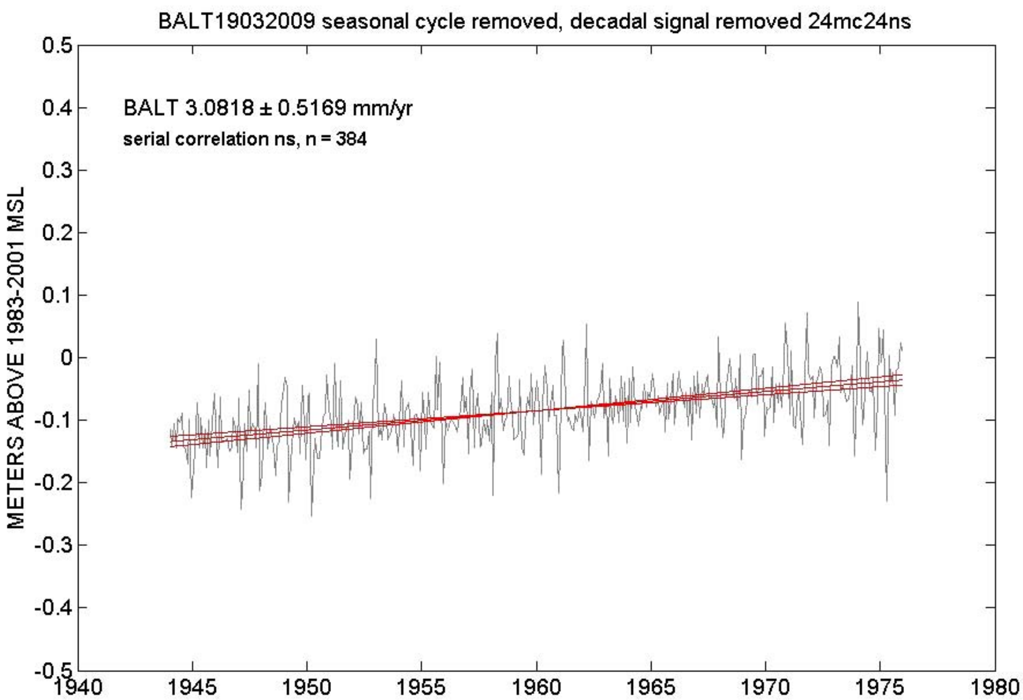

Figure B-2. RSL trends and 95% confidence intervals before (upper) and after (lower) removal of the decadal signal at BALT, 1944-1975 period.

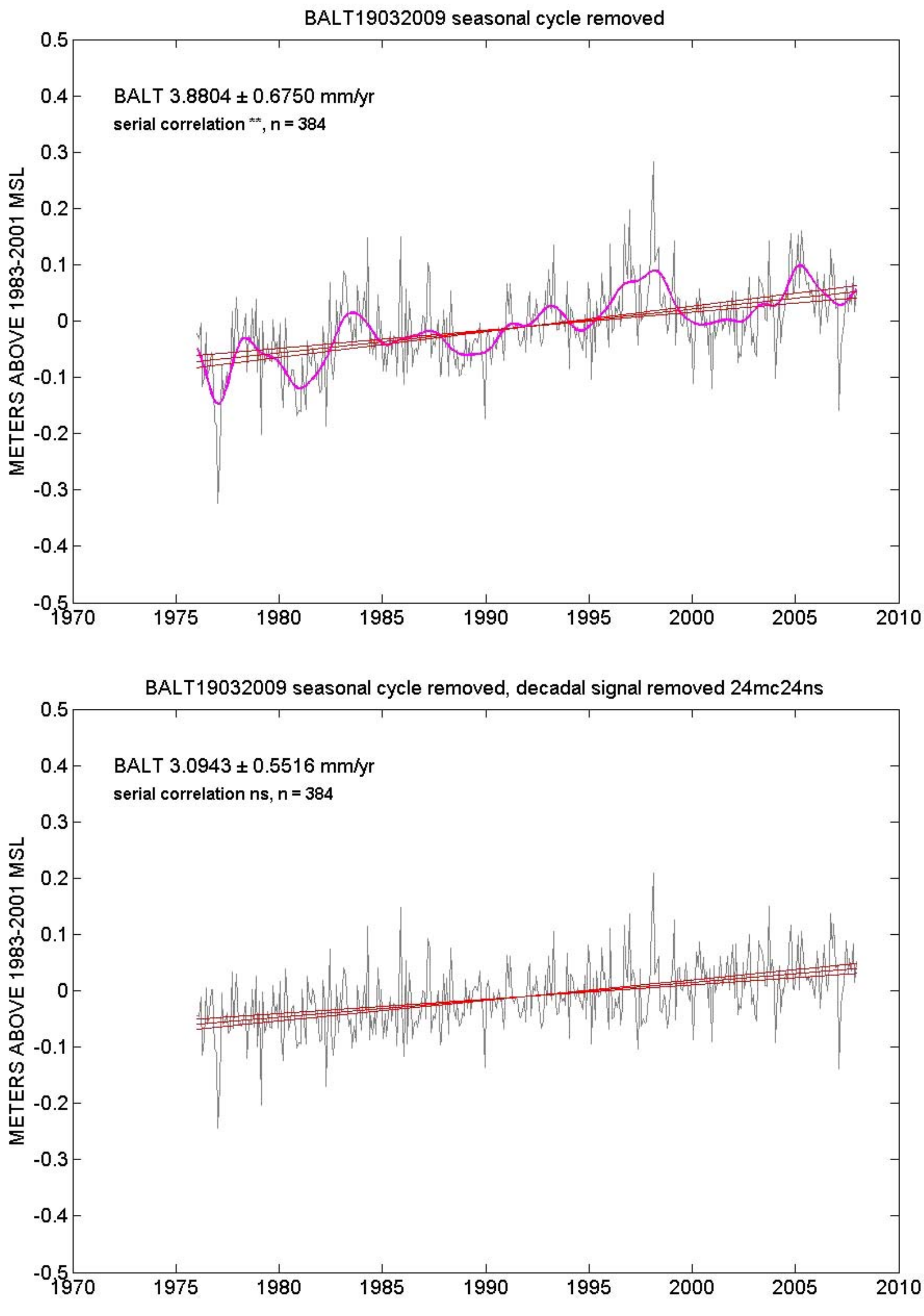

Figure B-3. RSL trends and 95% confidence intervals before (upper) and after (lower) removal of the decadal signal at BALT, 1976-2007 period.

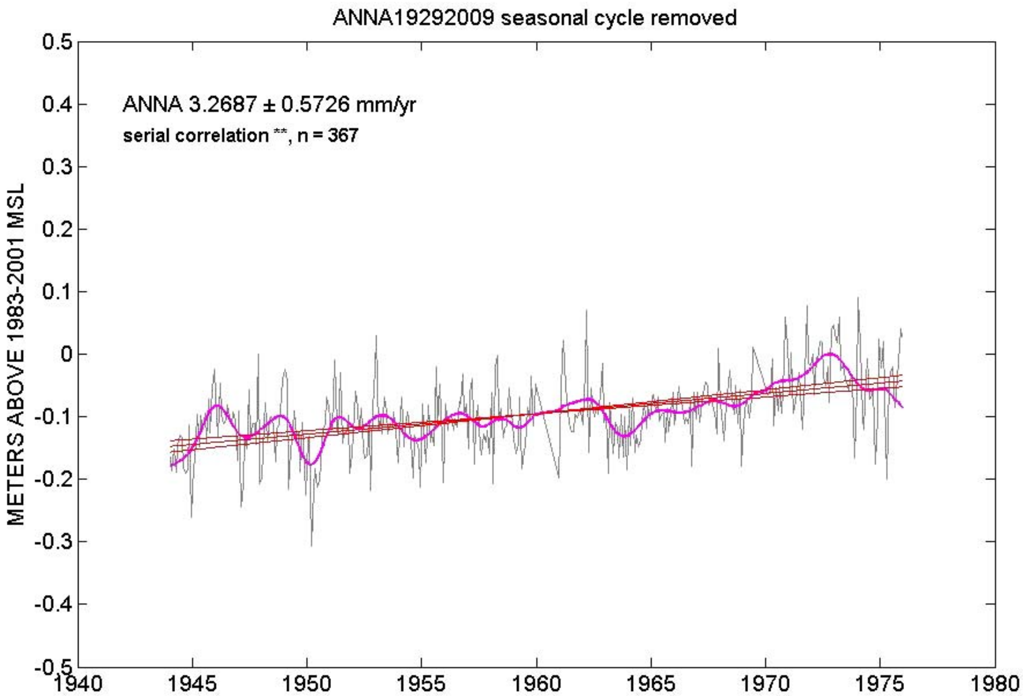

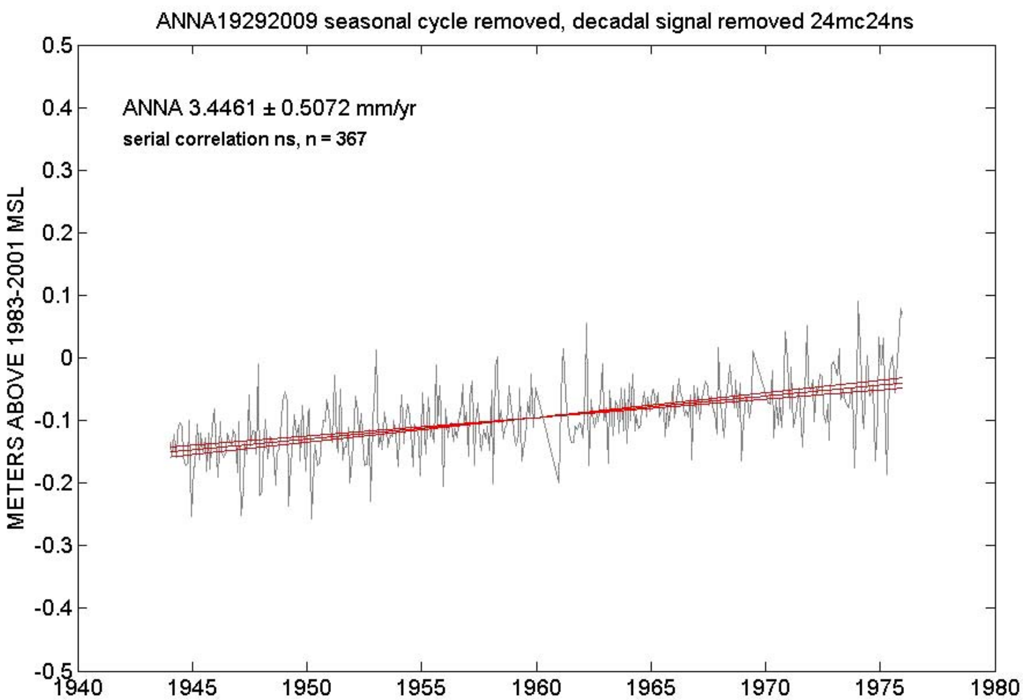

Figure B-4. RSL trends and 95% confidence intervals before (upper) and after (lower) removal of the decadal signal at ANNA, 1944-1975 period.

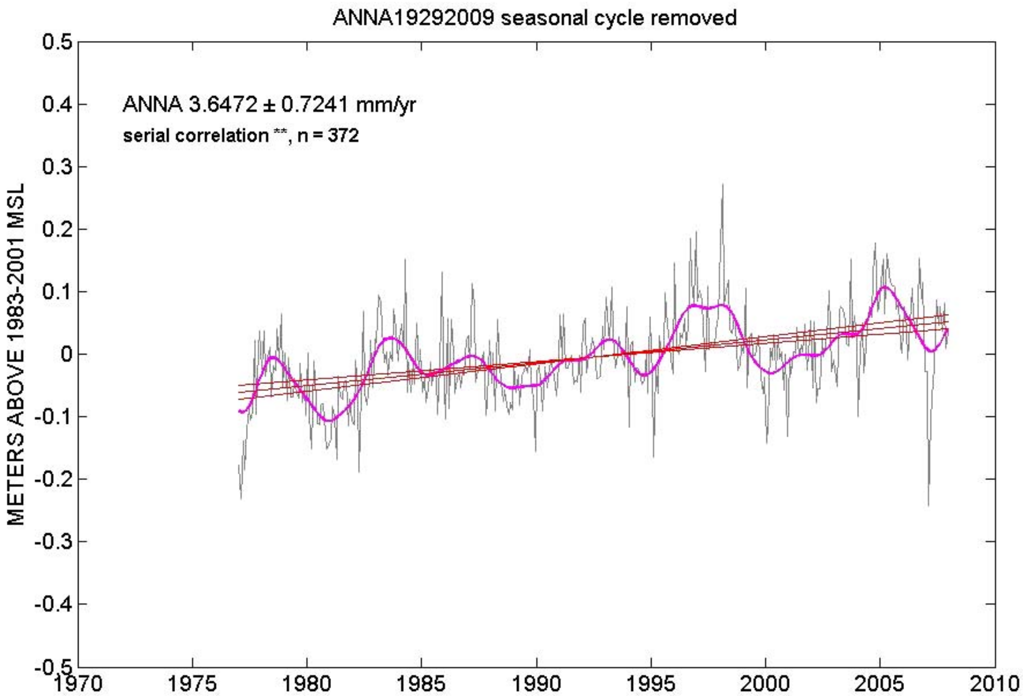

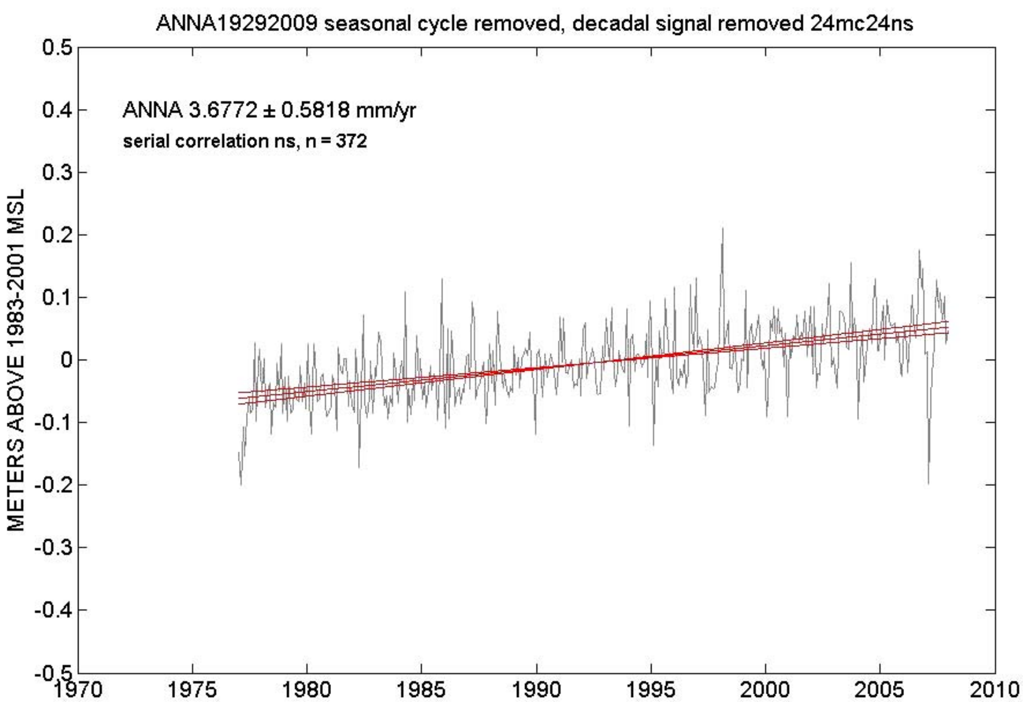

Figure B-5. RSL trends and 95% confidence intervals before (upper) and after (lower) removal of the decadal signal at ANNA, 1976-2007 period.

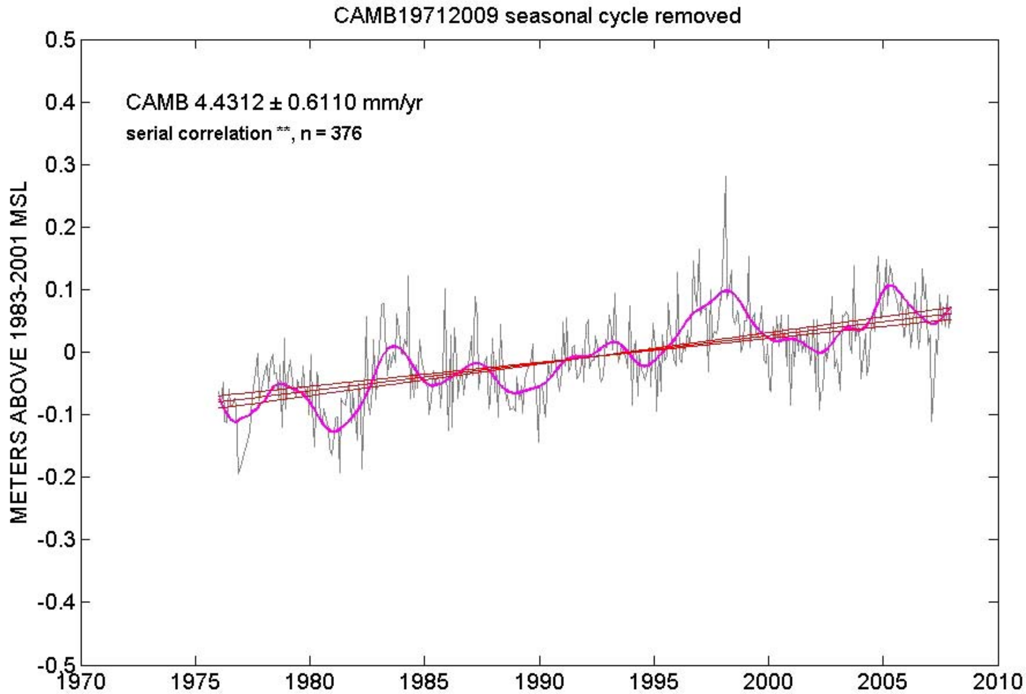

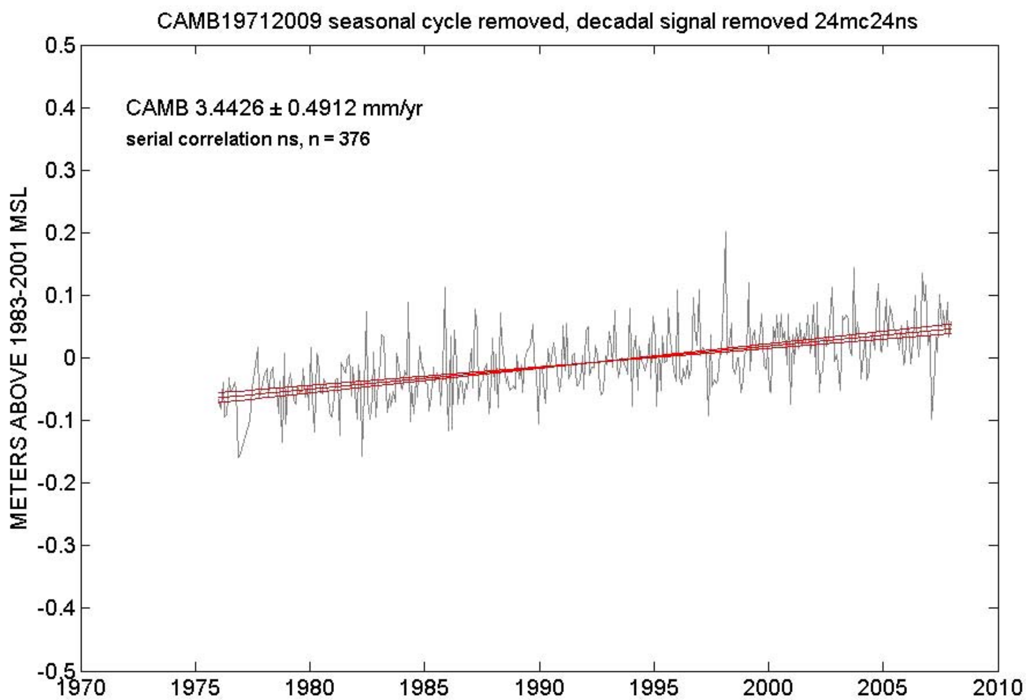

Figure B-6. RSL trends and 95% confidence intervals before (upper) and after (lower) removal of the decadal signal at CAMB, 1976-2007 period.

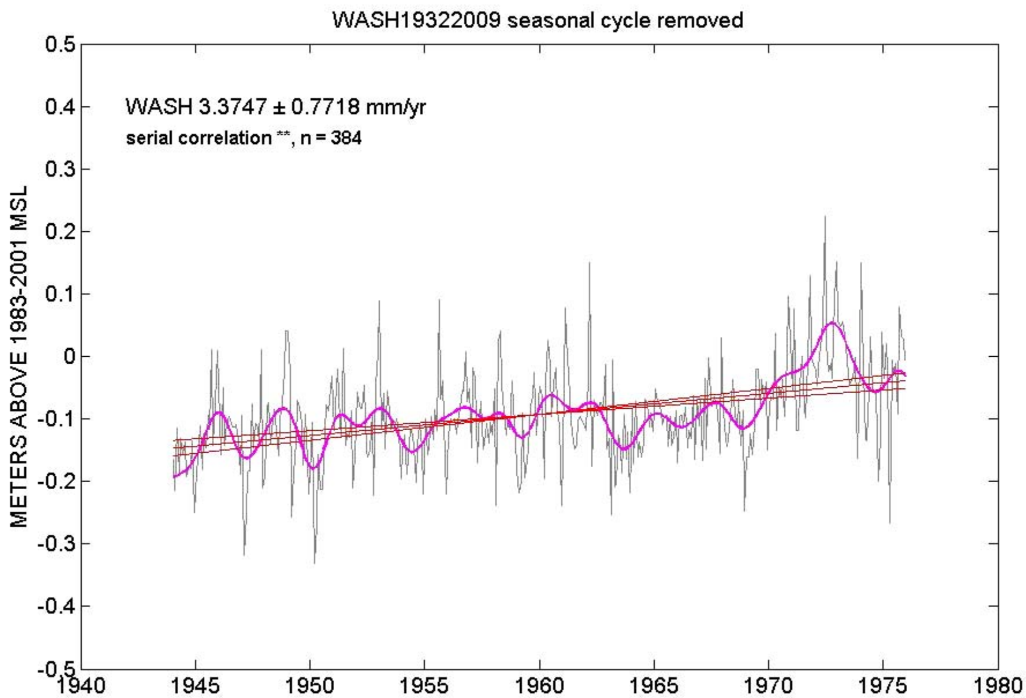

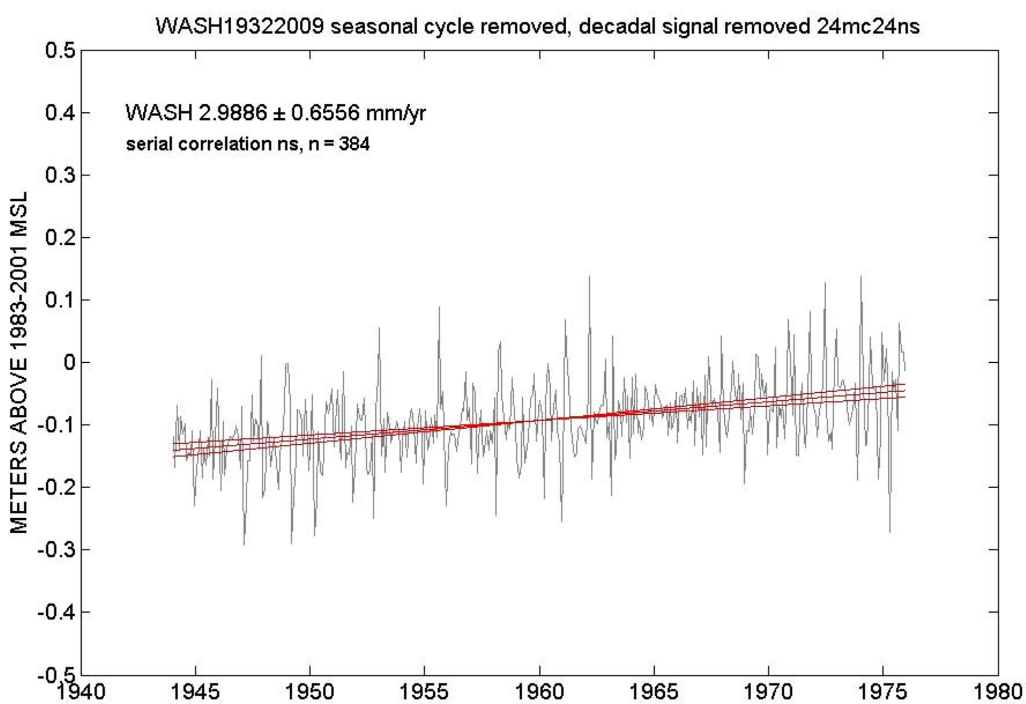

Figure B-7. RSL trends and 95% confidence intervals before (upper) and after (lower) removal of the decadal signal at WASH, 1944-1975 period.

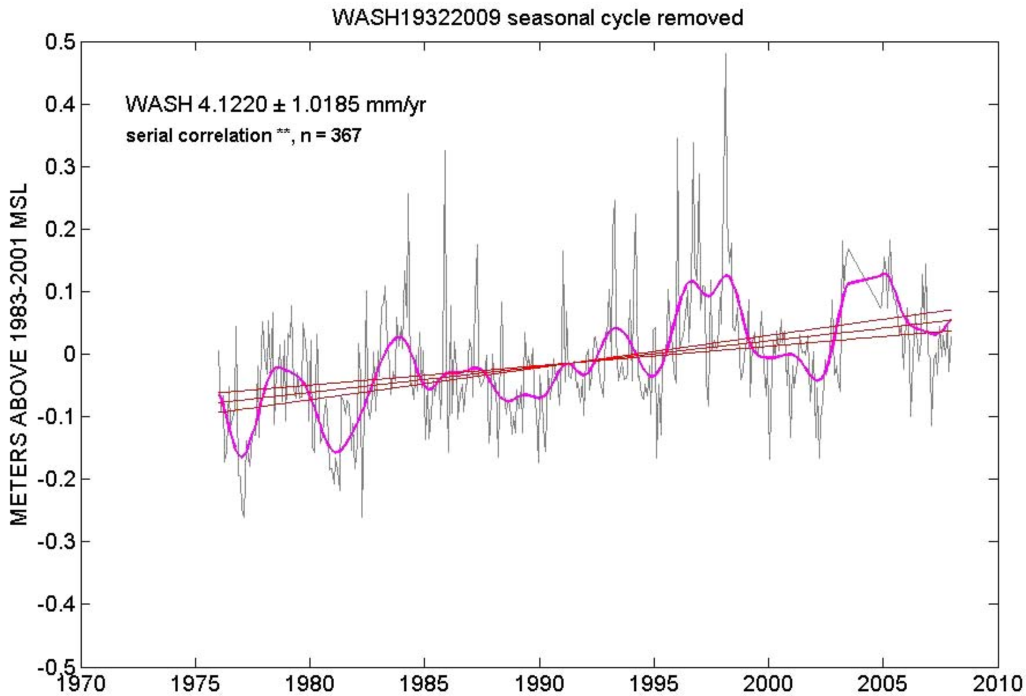

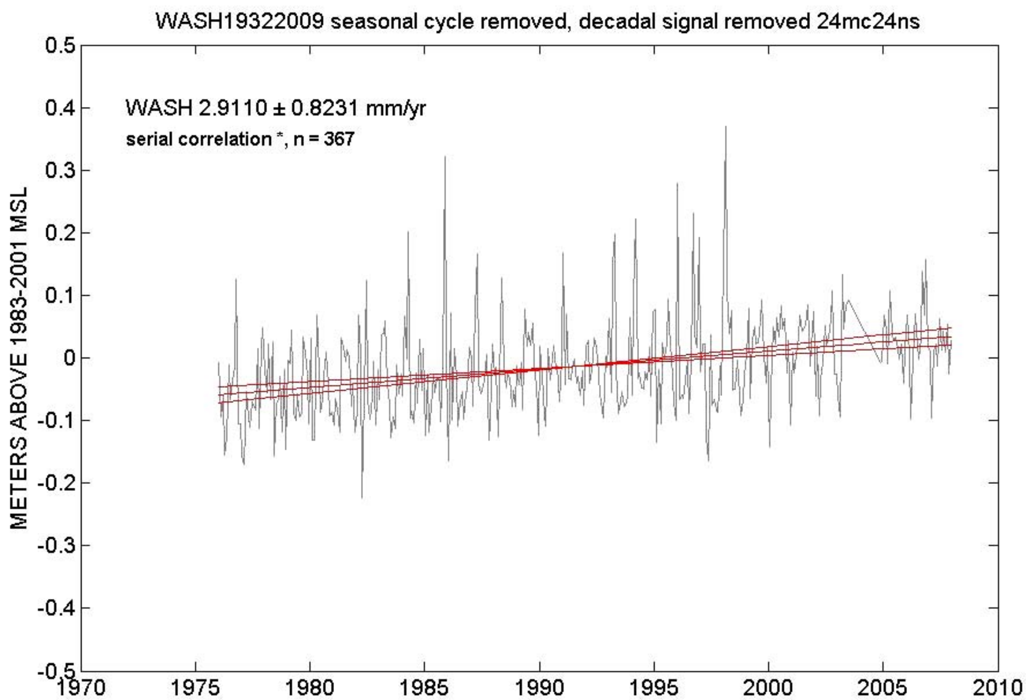

Figure B-8. RSL trends and 95% confidence intervals before (upper) and after (lower) removal of the decadal signal at WASH, 1976-2007 period.

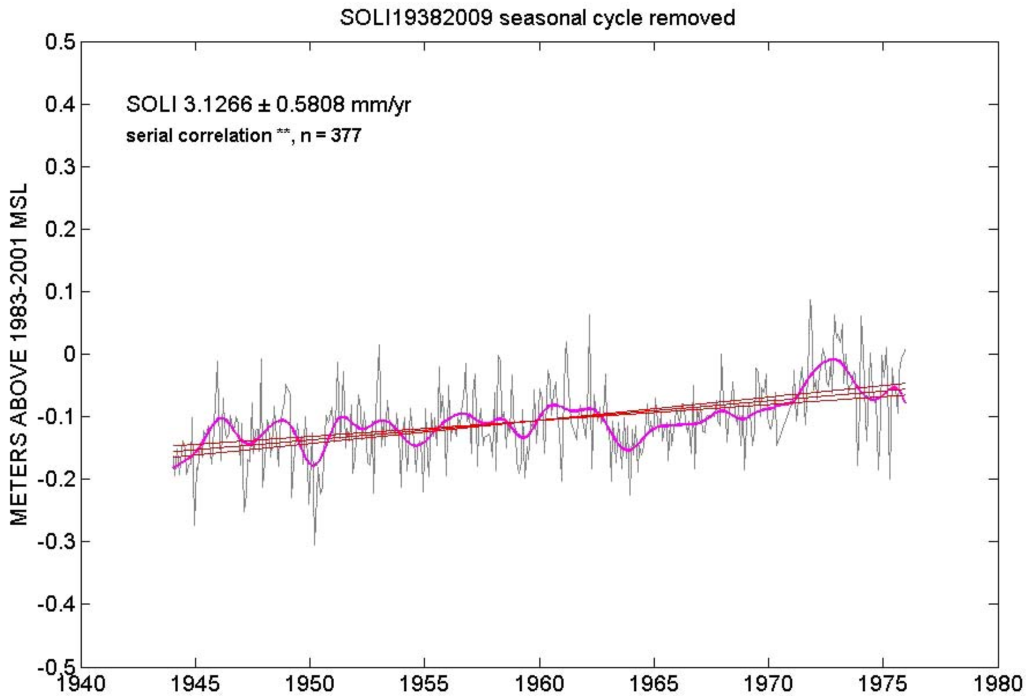

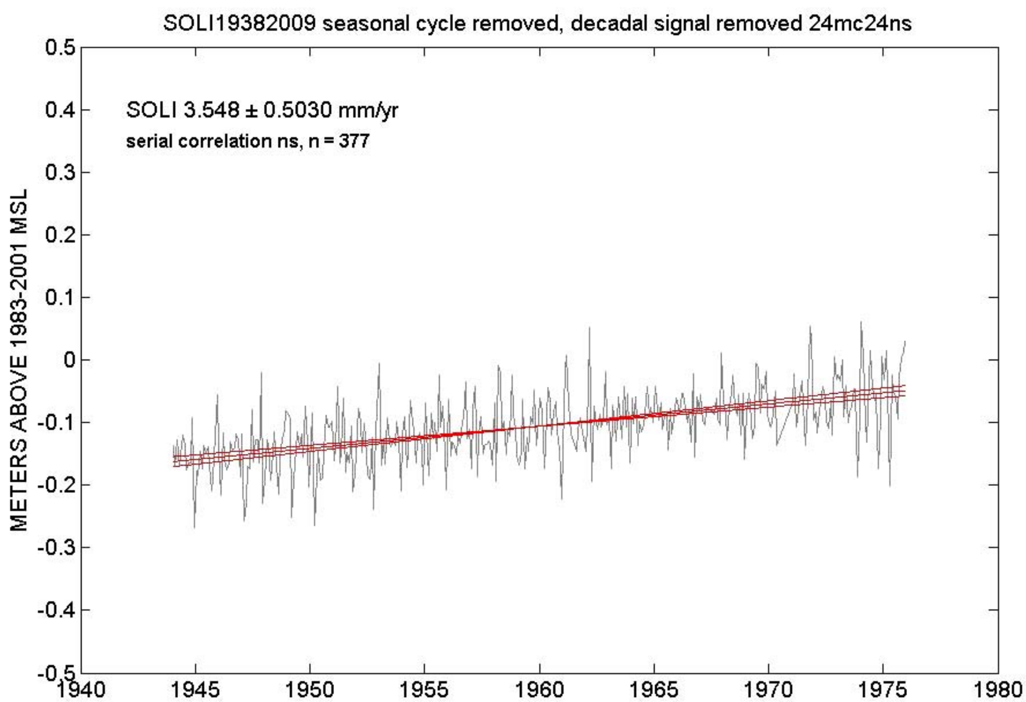

Figure B-9. RSL trends and 95% confidence intervals before (upper) and after (lower) removal of the decadal signal at SOLI, 1944-1975 period.

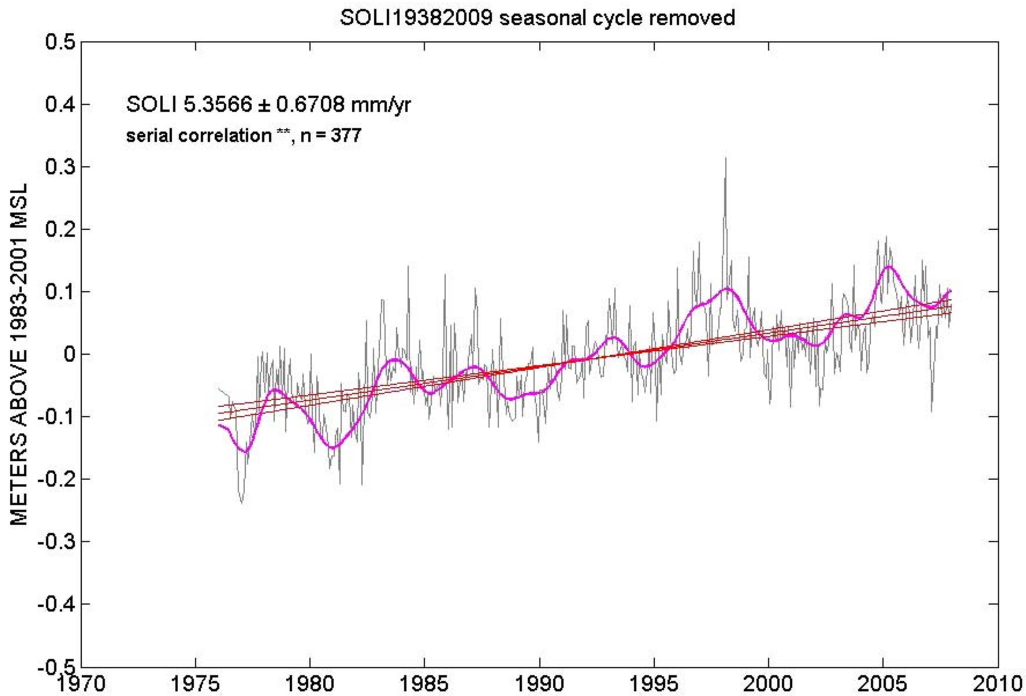

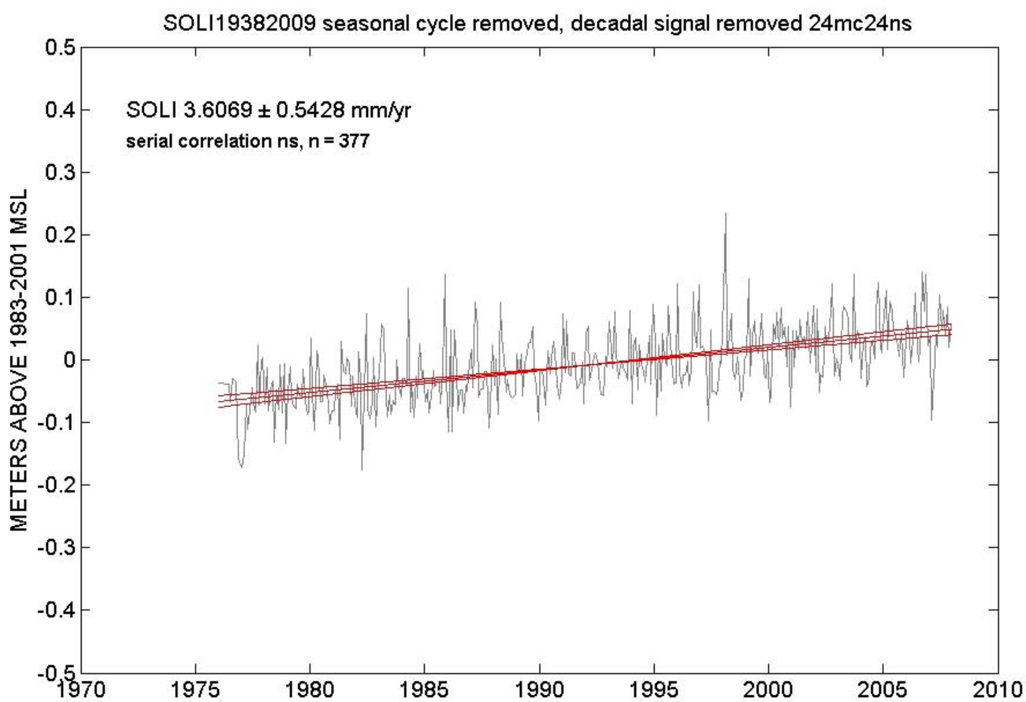

Figure B-10. RSL trends and 95% confidence intervals before (upper) and after (lower) removal of the decadal signal at SOLI, 1976-2007 period.

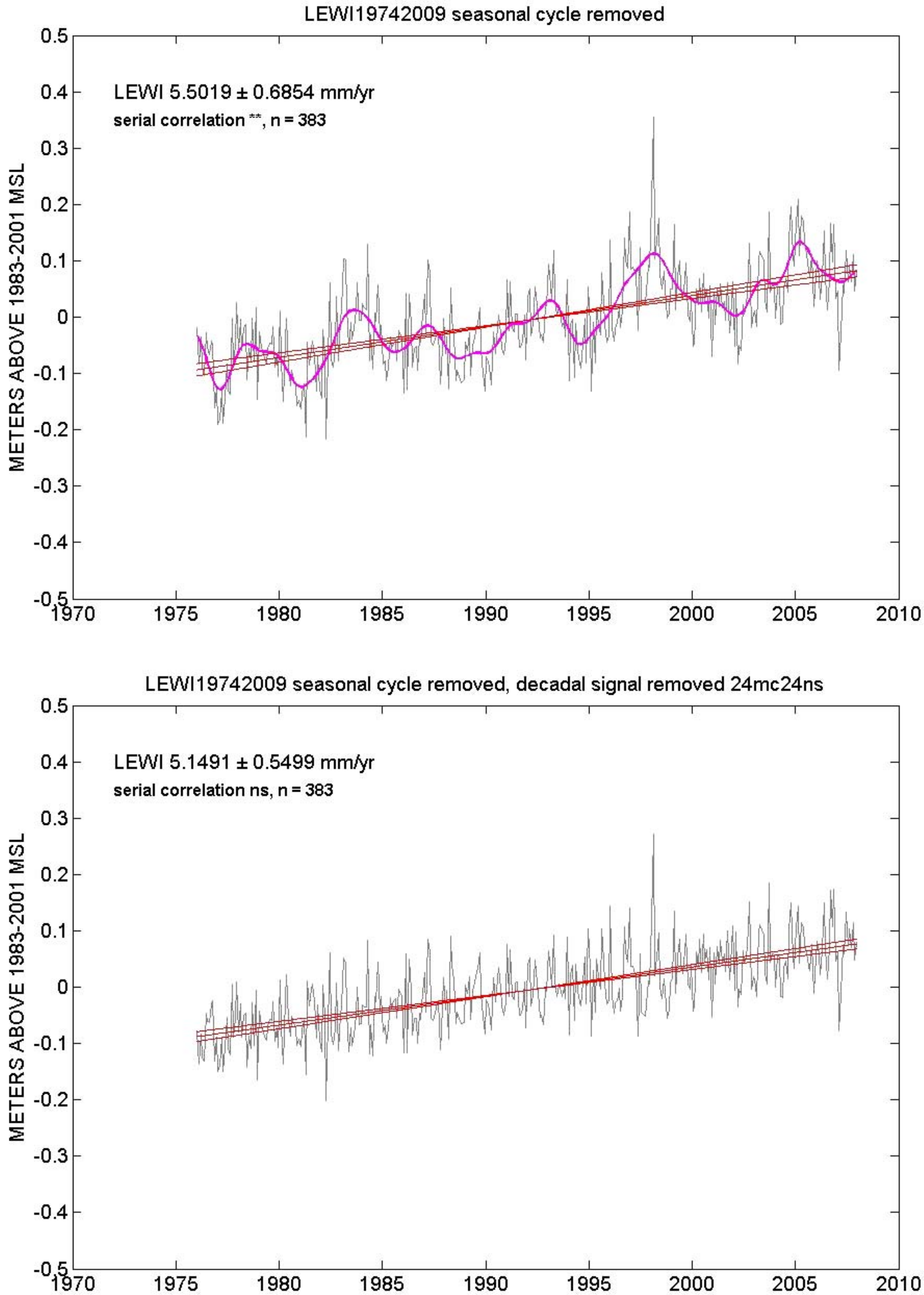

Figure B-11. RSL trends and 95% confidence intervals before (upper) and after (lower) removal of the decadal signal at SOLI, 1976-2007 period.

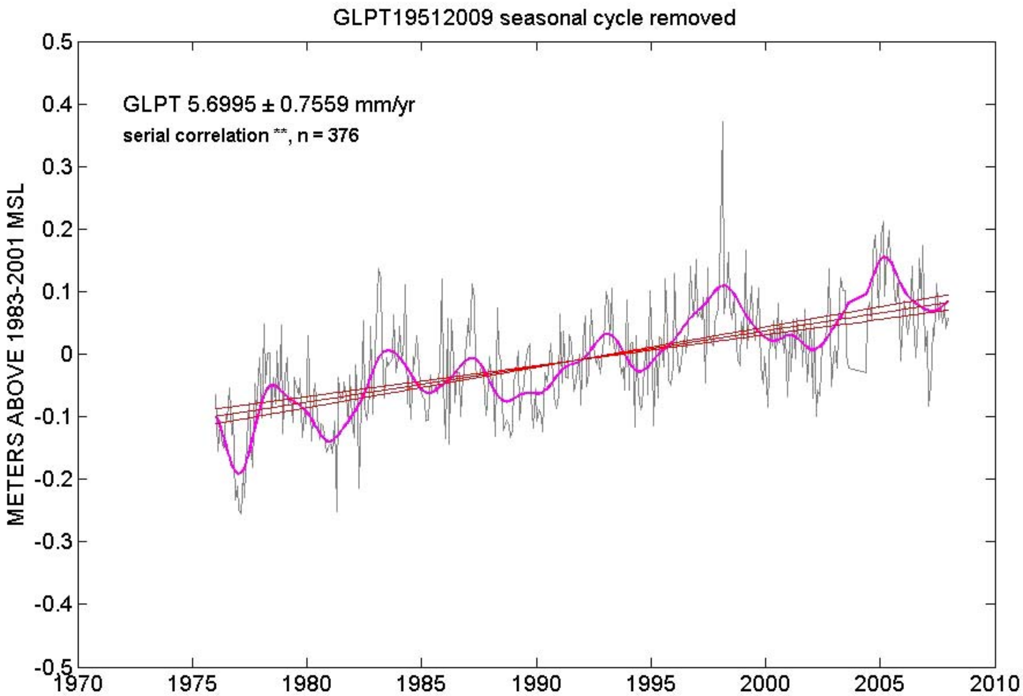

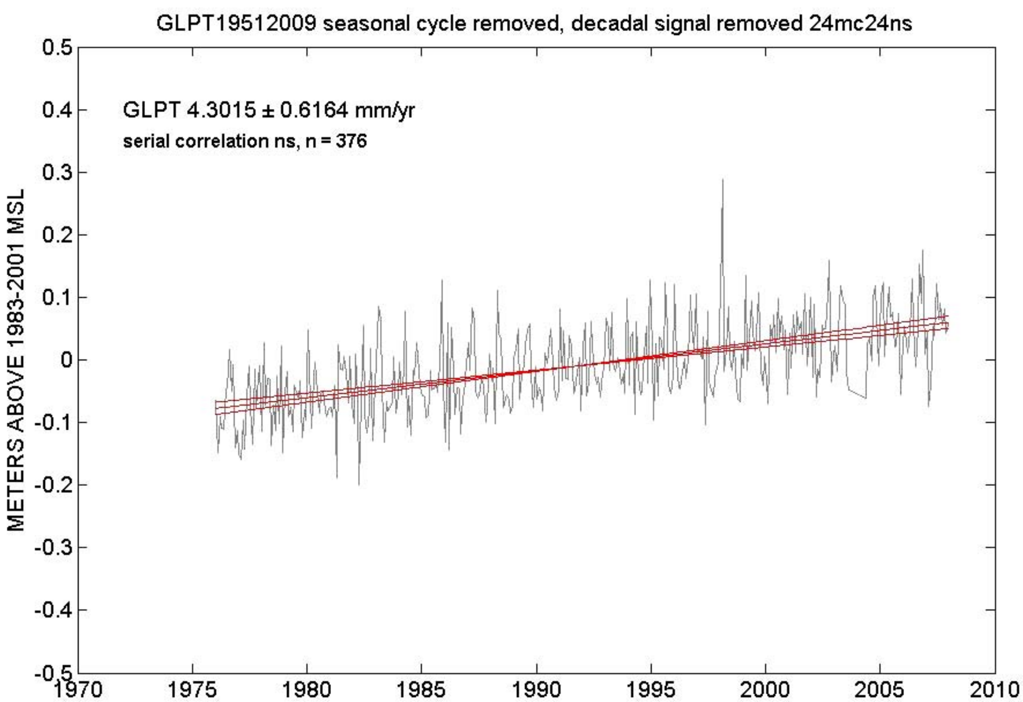

Figure B-12. RSL trends and 95% confidence intervals before (upper) and after (lower) removal of the decadal signal at GLPT, 1976-2007 period.

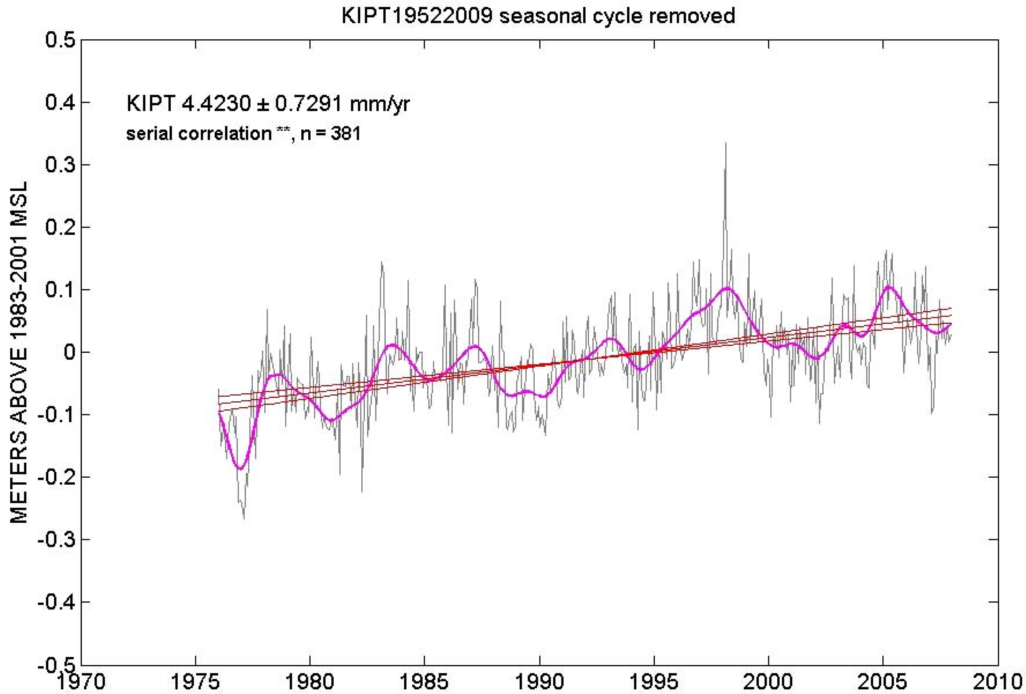

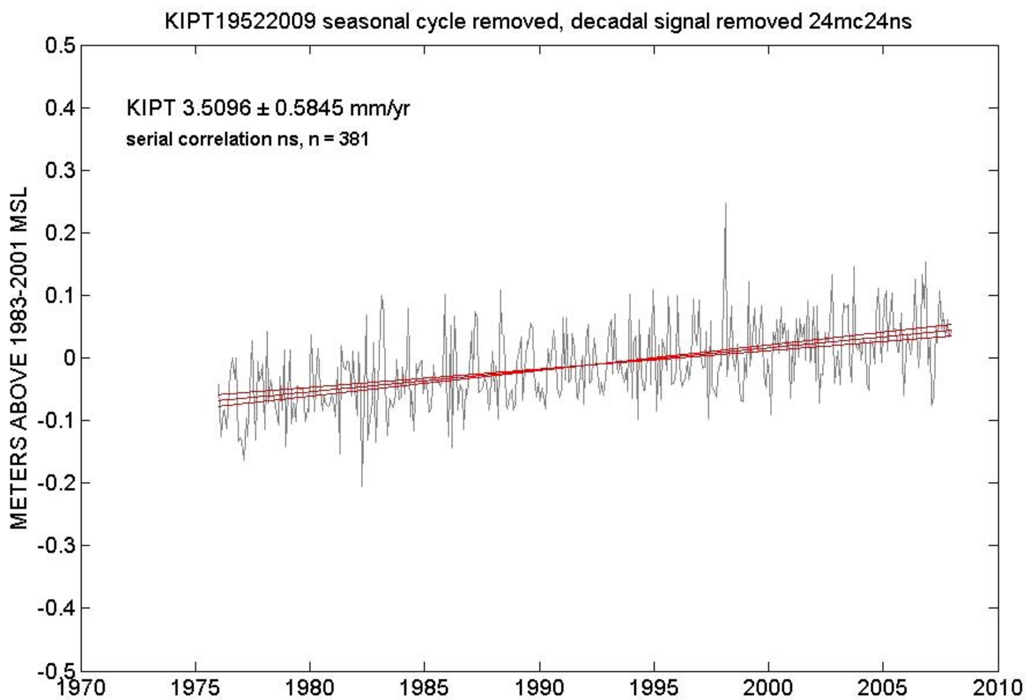

Figure B-13. RSL trends and 95% confidence intervals before (upper) and after (lower) removal of the decadal signal at KIPT, 1976-2007 period.

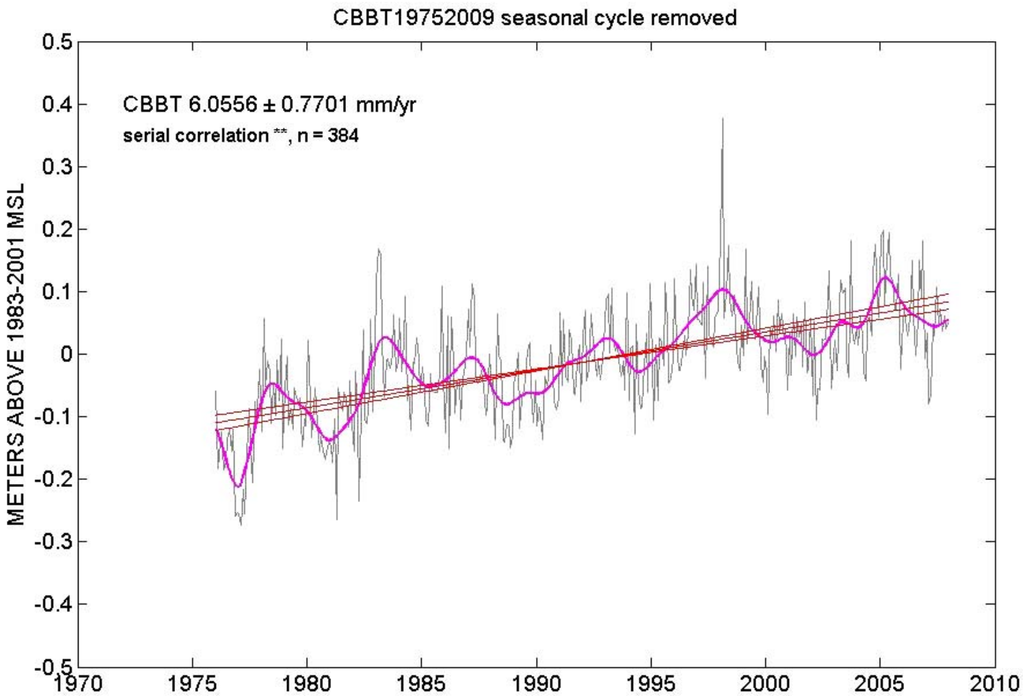

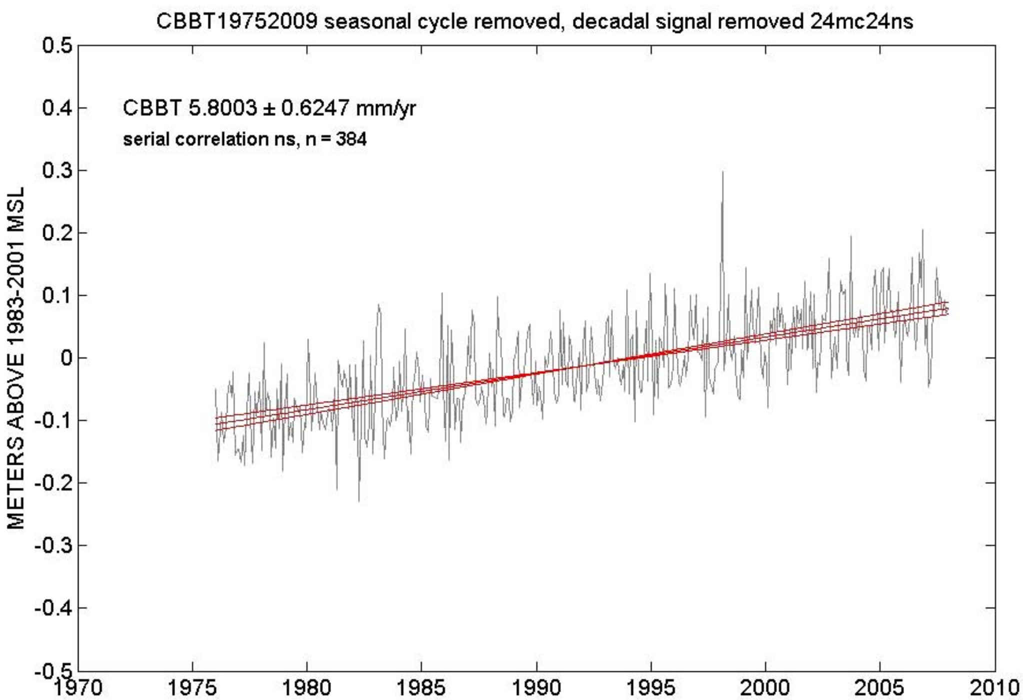

Figure B-14. RSL trends and 95% confidence intervals before (upper) and after (lower) removal of the decadal signal at CBBT, 1976-2007 period.

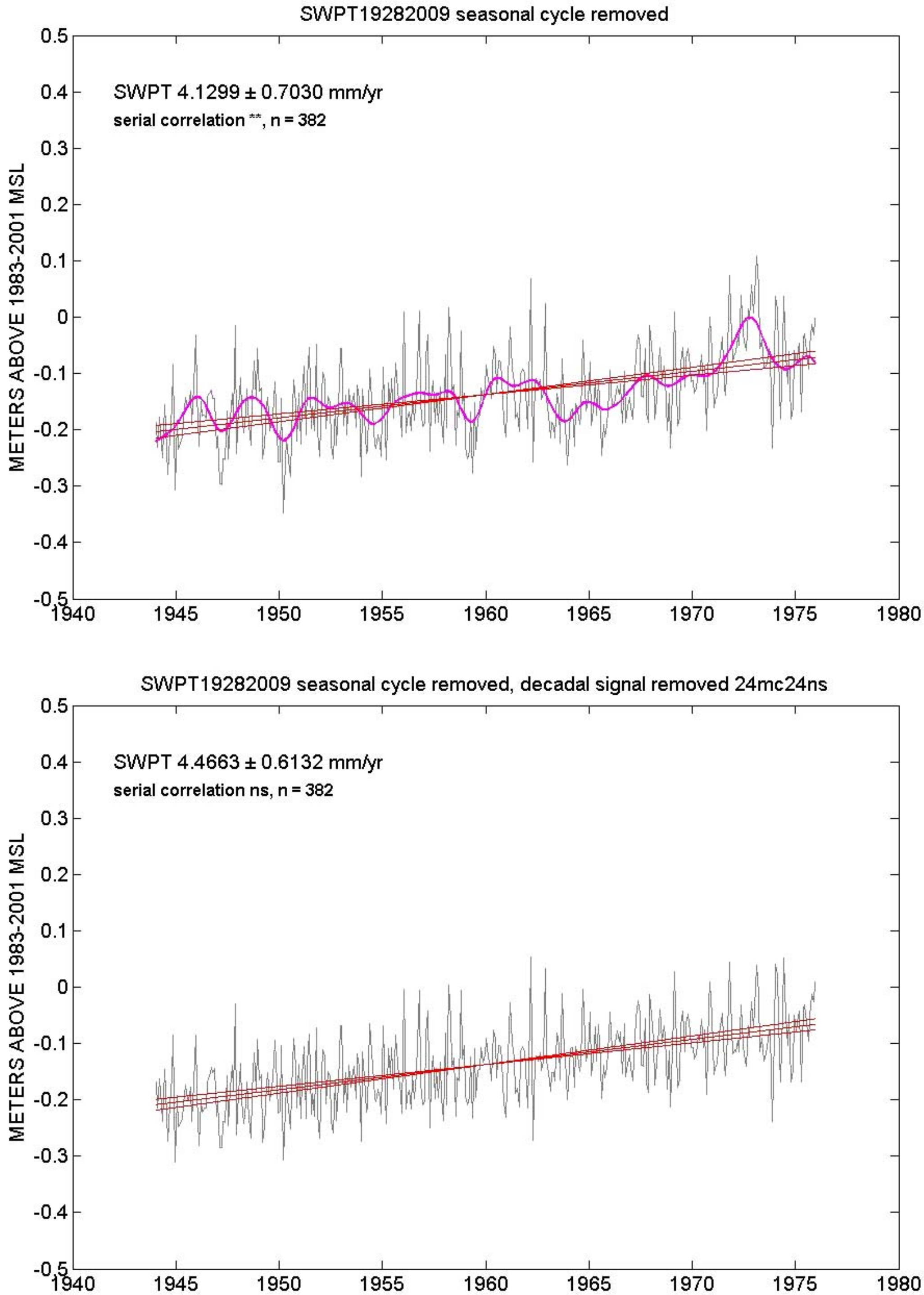

Figure B-15. RSL trends and 95% confidence intervals before (upper) and after (lower) removal of the decadal signal at SWPT, 1944-1975 period.

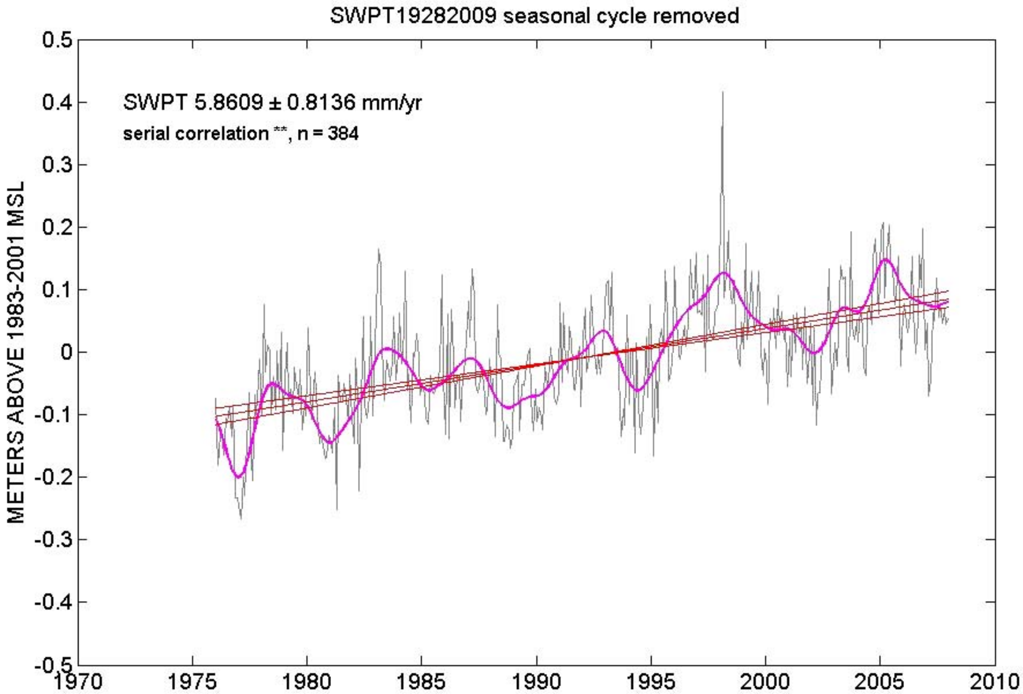

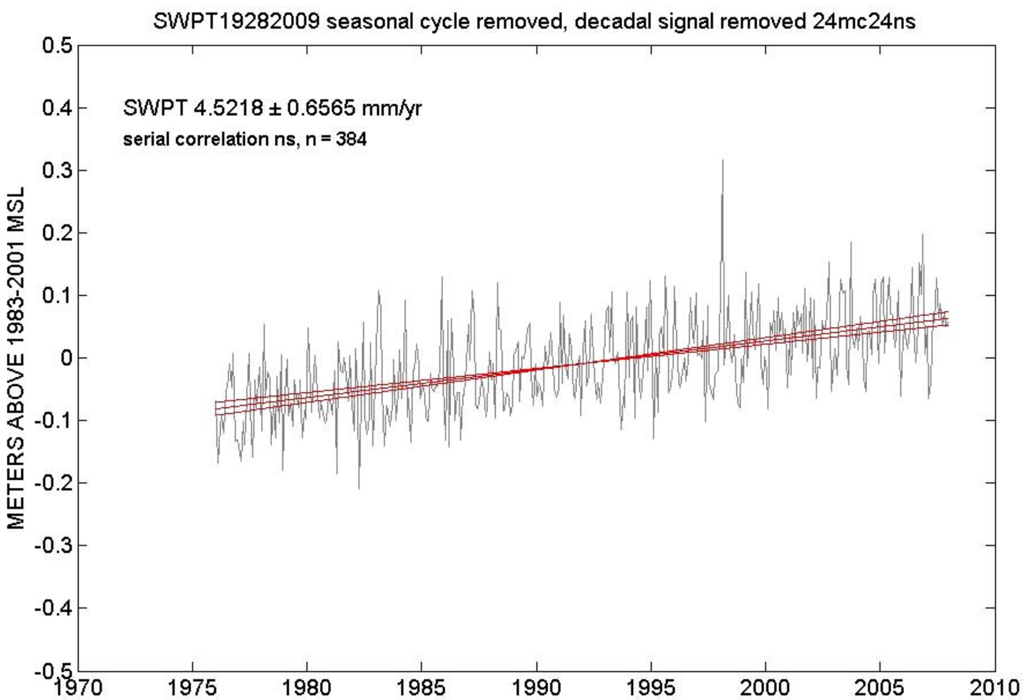

Figure B-16. RSL trends and 95% confidence intervals before (upper) and after (lower) removal of the decadal signal at SWPT, 1976-2007 period.